INFLUENCE OF TEMPERATURE AND PRECIPITATION ON RADIAL GROWTH PROPERTIES OF HYBRID WHITE SPRUCE (*Picea glauca* (Moench) *x engelmannii* (Parry)) IN CENTRAL INTERIOR BRITISH COLUMBIA, CANADA

by

Anastasia Ivanusic

B.S.c., University of British Columbia – Okanagan Campus, 2013

THESIS SUBMITTED IN PARTIAL FULFILLMENT OF
THE REQUIREMENTS FOR THE DEGREE OF
MASTER OF SCIENCE
IN
NATURAL RESOURCE AND ENVIRONMENTAL STUDIES

UNIVERSITY OF NORTHERN BRITISH COLUMBIA

April 2020

© Anastasia Ivanusic, 2020

Abstract

It is prudent to understand how changes in climate will affect tree-ring growth, wood fibre quality, and percent carbon content in natural and planted stands in central interior British Columbia (BC), as BC produces high volumes of wood fibres that are competitive in a global market. Wood properties within natural and planted stands of hybrid white spruce (*Picea glauca* (Moench) *x engelmannii* (Parry)) (percent carbon, ring-width, earlywood and latewood width and wood cell properties of cell wall thickness, density, microfibril angle, radial diameter and coarseness) were assessed to determine if climate variation is a limiting growth factor. Results show precipitation is an important limiting factor in planted stand growth with some indication that increasing temperatures limit growth in natural stands. Relationships between climate and percent carbon indicate that rising winter, spring, and summer temperatures coupled with reduced precipitation strongly limit percent carbon accumulation in most natural and planted stands.

Table of Contents

List of Tables:

List of Figures:

Acknowledgements:

I would first and foremost like to thank my supervisors, Dr. Lisa Wood and Dr. Kathy Lewis, for taking me on as their MSc student and providing me valuable mentorship throughout my time at UNBC. Special thanks to Dr. Wood for putting up with my forestry naiveite, my constant questions (that were almost always answered by a good literature search) and for providing never-ending support and encouragement. Thanks also to my committee member Dr. Paul Bicho for providing valuable guidance during our time working together. Thanks to the Canfor Research staff in Burnaby for assistance with my research analysis. Special thanks to my field assistants, Lisa Wood, Brenden Carswell, Kailee Mackinnon, Izzy Bourque, Dominic Gammon and Jerry Doffe. Thank-you to Aita for making maps for this thesis. I would like to thank several special people from my UNBC graduate cohort for making the hard days bearable with coffee, hiking and music breaks – Victoria, Ilsa, Aita, Luke, and Kailee. I would especially like to thank my mom and dad who have been incredibly encouraging and supportive through my time as a student. I would like to thank my partner Dominic who has always been there to support me even though he sometimes has no idea what I was complaining about. Finally, I would like to share with Lisa that I did not in fact, become a coffee drinker during this degree!

Support and funding for this research was provided by Natural Resource Canada, a UNBC Research Award, and through a collaborative Mitacs grant with Canfor Forest Products Ltd.

Chapter One: Introduction

1.1 CONTEXT

Models presented by the Intergovernmental Panel on Climate Change suggest that mean global temperatures are expected to increase 0.3 to 0.7 °C by the year 2035 with increased precipitation at higher latitudes and decreased precipitation at lower latitudes (IPPC 2013). Extreme temperatures and precipitation events are projected to increase in frequency with more warmer- and colder-than-average days and nights and increased heavy precipitation events (IPPC 2013). The Pacific Northwest is expected to become warmer and wetter annually with increased maximum and minimum temperatures, and decreased depth and water content of snowpack (MWLAP 2002; Lo et al. 2010; Fleming and Whitefield 2010).

British Columbia (BC) is expected to experience increased drought stress and greater changes in temperature and precipitation that will vary across the topographic landscape (Spittlehouse 2007; Lo et al. 2010; Jiang et al. 2016). Boreal forests in central BC, that contain dense areas of several spruce species, are predicted to be one of the most sensitive areas to changing climates within BC (Wang et al. 2012). Tree growth within interior BC has historically been temperature limited with some indication that precipitation variability is becoming a more limiting growth factor in specific locations (Wood and Smith 2015; Cortini et al. 2016). Climate forces may cause BC forests to undergo ecosystem shifts, change boreal tree success, alter carbon accumulation, and trigger degradation of tracheid or wood product quality, including quality of pulp fibre (Wang et al. 2012).

Pulp products originating from BC's forests have been characterized by long, slender, thin-walled fibres that have superior strength, low coarseness and high uniformity (Taylor et al. 1982; Corriveau et al. 1991; Watson and Bradley 2009). BC old-growth hybrid white spruce (*Picea glauca* x *engelmanni*), found in the sub-boreal forests where ranges of white and Engelmann spruce overlap, are a preferred species for pulp and paper-making processes with lower proportions of latewood cells and longer tracheids (Taylor et al. 1982). Large thin-walled xylem cells can easily compress into sheets that provides higher tensile strength due to a greater number of hydrogen bonds (Lenz et al. 2010; Shmulsky and Jones 2011, pg 410-411). Pulp with these characteristics, historically processed from old-growth timber, is considered of high quality with good market value.

Timber harvest in BC will increasingly shift from naturally generated old-growth stands to artificially reforested stands due to decreasing availability of old-growth forests. This shift will result in harvest of younger, faster grown trees with reduced wood fibre quality (Lenz et al. 2010). Changing climates may also affect wood quality differently in old-growth and managed stands. Alterations to wood fibre characteristics, and thus wood quality, could substantially impact the market value of BC wood products.

1.2 BACKGROUND INFORMATION

Tree age can have a major impact on the quality of wood and desired end-product use, especially due to differences between juvenile wood and mature wood. Juvenile wood, formed from the pith is characterized by large radial diameter, thin-walled cells that are shorter and have larger fibril angles with increased variability in comparison to mature wood traits. Younger trees with greater proportions of juvenile wood produce lower quality wood products because of reduced strength with shorter, smaller, and more horizontally orientated microfibril angles compared to mature trees with a greater proportion of mature wood (Zobel and van Buijtenen 1989, pg 19; Kennedy 1995; Barnett and Jeronimidis 2003; Adamopoulos et al. 2006). Age of transition between juvenile wood and mature wood is highly variable and depends on site-specific management practices, genetic differences, site conditions, and sampling height (Cameron et al. 2005; Alteyrac et al. 2006). Research with spruce has suggested that transition age can range between 12 and 31 years (Cameron et al. 2005; Alteyric et al. 2006).

Complex interactions between external factors, such as temperature and precipitation, and internal processes, such stomatal activity and needle elongation, can also affect tree growth and wood quality (Figure 1.1) (Fritts 1976). Climate parameters are often expressed in wood through specific patterns of annual ring-width (RW), earlywood width (EW), latewood width (LW) and earlywood and latewood densities, as evidence by a large, long-term body of literature (Fritts 1976). Annual ring-growth is comprised of EW cells, produced at optimal growth periods, and LW cells, which are produced when growth rates slow in conjunction with reductions in temperature, precipitation, or photoperiod length. EW cells are characterized by thin walls and reduced cell density that reflect high-growth periods while LW cells have thicker cell walls and higher density reflecting periods of slower growth. Additionally, wood cell properties of cell wall thickness (CWT), density (D), cell radial diameter (RD) and microfibril angle (MFA) can reflect temperature and precipitation variation, often with increased sensitivity compared to RW, EW, or LW (Wood and Smith 2015).

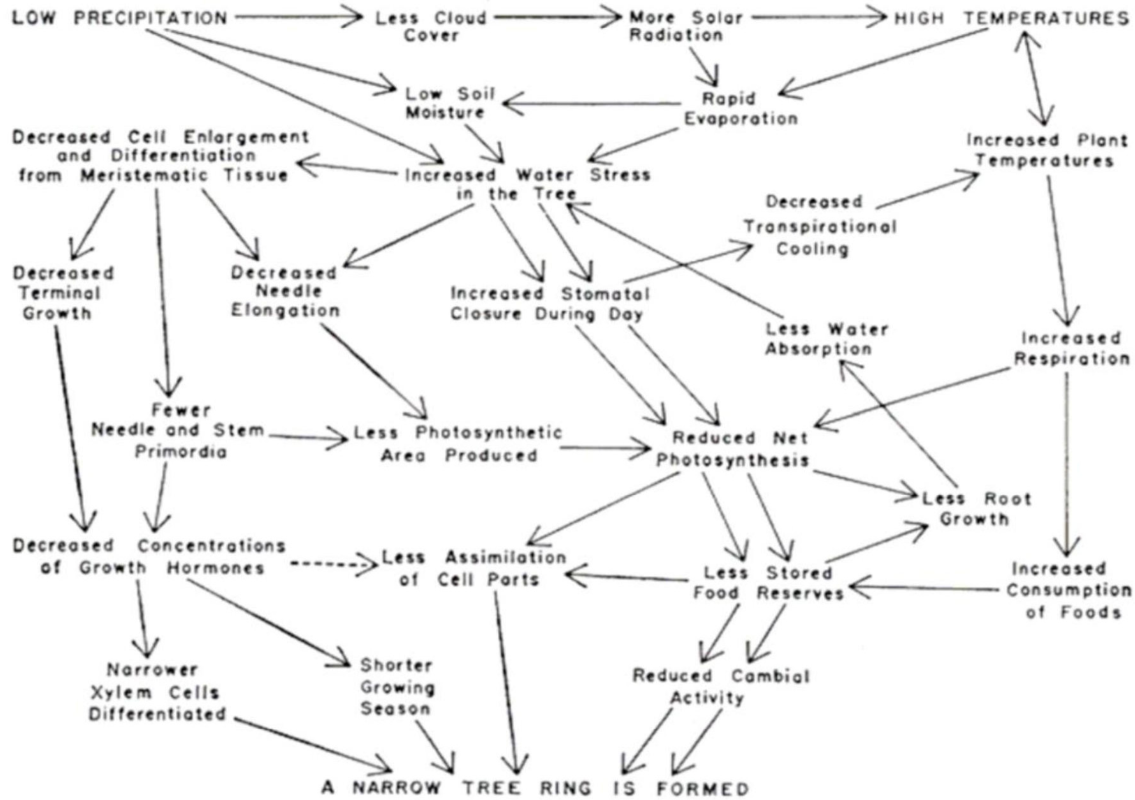

Figure 2.1 Conceptual model by Fritts 1966 depicting complex interactions between climate and production of a narrow ring.

As radial tree growth is strongly affected by changes in climate, it can be inferred that carbon accumulation will also be directly affected. The substantial changes predicted for interior BC climate over the next decade may reduce carbon dioxide uptake and carbon accumulation and potentially push forests beyond sustainability thresholds (Millar and Stephenson 2015). Dendrochronological techniques may be used to enhance understanding of relationships between above ground carbon accumulation and climate (Bouriaud et al. 2005), similar to tree radial growth climate relationships.

Interpreting relationships between radial tree growth and carbon accumulation, including CWT and D, can improve carbon sequestration projections (Weber et al. 2018). Wood D and CWT are suggested to correlate with carbon concentration; thicker, denser xylem cell walls should have greater proportions of cellulose and lignin and thus carbon (Elias and Potvin

2003; Thomas and Malczewski 2007; Lachenbruch and Mcculloh 2014; Weber et al. 2018). Unfortunately, relationships between wood cell properties and carbon are not well understood as past research has focused mainly on biomass instead of direct measurements of carbon (Zabek and Prescott 2006; Castaño-Santamaría and Bravo 2012).

1.3 RESEARCH GAPS

Radial growth changes in RW, EW, LW, and wood cell properties of hybrid white spruce are expected as a result of changes to climate in central interior BC. However, few studies have examined radial growth properties of RW, EW, and LW in central interior BC spruce (Flower and Smith 2011; Wood and Smith 2015). Previous research has mainly focused on RW and density relationships, and not on other properties such as CWT, RD, coarseness, and MFA (Watson and Luckman 2001; Larocque and Smith 2005; Pitman and Smith 2012; Wimmer and Grabner 2000; Wood and Smith 2013; Wood and Smith 2015; Watson and Luckman 2016). Comparisons between carbon measurements and wood cell properties are lacking as literature focuses on biomass as a driving factor in carbon research instead of direct carbon measurements within wood structure (Zabek and Prescott 2006; Castaño-Santamaría and Bravo 2012). Finally, there is a lack of information on the relationship between climate and radial growth characteristics of young plantations in central interior BC compared to older, naturally occurring stands (Sanchez-Salguero et al. 2013).

1.4 THESIS OBJECTIVES

The purpose of this study was to determine how RW, EW, LW, MFA, coarseness, CWT, RD, and D properties of natural and planted stands of hybrid white spruce in central interior BC vary over time and with climate. Additionally, this study aimed to determine how structural percent carbon values within wood related to tracheid features and to climate.

Specific objectives were as follows:

1. Determine annual RW, EW and LW and their variabilities for trees in natural and planted stands over time.
2. Examine the statistical correlation between monthly and seasonal climate variables and growing season length with RW, EW, and LW and visually interpret relationships between climate variables and RW, EW, and LW over time.
3. Determine average annual wood cell properties of D, coarseness, MFA, CWT, and RD, for trees in natural and planted stands and determine i) the variability of wood cell properties over time ii) the statistical correlation between monthly and seasonal climate variables with wood cell properties and iii) visually interpret relationships between wood cell properties modelled from climate data to measured wood cell properties over time.
4. Review existing literature regarding relationships between percent carbon and wood D and/or CWT measurements.
5. Compare values of D and CWT to measured percent carbon values using statistical methods and visual interpretation .
6. Determine relationships between monthly and seasonal climate variables to percent carbon variation over time. Visually interpret relationships between climate variables and percent carbon variation over time.

This thesis contains an introductory chapter, two data chapters that address the above questions, and a concluding chapter where data chapters are synthesized. Chapter 2 explores RW, EW, LW, and wood cell properties in natural and planted stands near Prince George and Fort St. James in relation to climate. Chapter 3 examines relationships between percent carbon and properties of RW, EW, LW, CWT and D. Chapter 3 also determines if the percent carbon between individual stands and regional-level stand aggregates differs and if relationships exist between percent carbon and climate variation over time in natural and planted stands near Prince George and Fort. St. James.

1.5 REFERENCES

Adamopoulos S and Passialis CVE. 2006. Strength properties of juvenile and mature wood in black locust (*Robina Psudoacacia* L .). Wood and Fiber Science. 39(2): 241–249.

Alteyrac J, Cloutier A. & Zhang, ASY. 2006. Characterization of juvenile wood to mature wood transition age in black spruce (*Picea mariana* (Mill.) B.S.P.) at different stand densities and sampling heights. Wood Science & Technology. 40: 124–138. https://doi.org/10.1007/s00226-005-0047-4

Bouriaud O, Bréda N, Dupouey J.L, Granier A. 2005. Is ring width a reliable proxy for stem-biomass increment? A case study in European beech. Canadian Journal of Forest Research. 35(12): 2920–2933. https://doi.org/10.1139/x05-202

Cameron AD, Lee SJ, Livingston AK, Petty JA. 2005. Influence of selective breeding on the development of juvenile wood in Sitka spruce. Canadian Journal of Forest Research. 35(12): 2951–2960. https://doi.org/10.1139/x05-219

Castaño-Santamaría J and Bravo F. 2012. Variation in carbon concentration and basic density along stems of sessile oak (*Quercus petraea* (Matt.) Liebl.) and Pyrenean oak (*Quercus pyrenaica Willd*.) in the Cantabrian Range (NW Spain). Annals of Forest Science. 69(6): 663–672. https://doi.org/10.1007/s13595-012-0183-6

Cook ER. and Peters K. 1981. The smoothing spline: A new approach to standardizing forest interior tree-ring width series for dendroclimatic studies. Tree-Ring Bulletin, 41: 45-53.

Cook ER. and Holmes RI. 1999. Users manual for program ARSTAN. Tucson, AZ.

Conkey LE. 1986. Red spruce tree-ring widths and densities in eastern North America as indicators of past climate. Quaternary Research: 26: 232-243.

Cortini F, MacIsaac DA, Comeau PG. 2016. White spruce growth and wood properties over multiple time periods in relation to current tree and stand attributes. Forests, 7(3). https://doi.org/10.3390/f7030049

Dale MRT, Fortin MJ. 2014. Spatial analysis: a guide for ecologists. Cambridge University Press.

Delong C, Tanner D, Jull MJ. 1993. A field guide for site identification and interpretation for the southwest portion of the Prince George forest region. Province of British Columbia: Ministry of Forests: https://www.for.gov.bc.ca/hfd/pubs/docs/Lmh/Lmh24.pdf.

Douglass AE. 1920. Evidence of climatic effects in the annual rings of trees. Ecology: 1(1).

Flower A and Smith DJ. 2011. A dendroclimatic reconstruction of June-July mean temperature in the northern Canadian Rocky Mountains. Dendrochronologia. 29(1): 55–63. https://doi.org/10.1016/j.dendro.2010.10.001

Fritts HC. 1976. Tree rings and climate. New York (NY): Academic Press Inc.

Grissino-Mayer HD 2003. A manual and tutorial for the proper use of an increment borer. Tree-Ring Research, 59(2): 63-79.

Kozlowski TT, Kramer PJ, Pallardy SG. 1991. The physiological ecology of woody plants. San Diego (CA): Academic Press, Inc.

Lo YH, Blanco JA, Seely B, Welham C, Kimmins JP. 2010. Relationships between climate and tree radial growth in interior British Columbia, Canada. Forest Ecology and Management. 259(5): 932–942. https://doi.org/10.1016/j.foreco.2009.11.033

Millar CI and Stephenson NL. 2015. Temperate forest health in an era of emerging megadisturbance. Science. 349(6250): 823–826. https://doi.org/10.1126/science.aaa9933

O’Neill GA, Wang T, Ukraintez N, Charleson L, Mcauley L, Yankcuhk A, Zedel S. 2017. A proposed climate-based seed transfer system for British Columbia. Prov. B.C., Victoria, B.C. Tech. Rep. 099, 57.

Saranpaa P. 2003. Wood density and growth. In: Barnett JK, Jeronimidis G, editors. Wood quality and its biological basis. Great Britain: Blackwell Publishing & CRC Press, Biological Sciences Series. p. 87-117.

Shmulsky R, Jones PD. 2011. Fundamentals of tree-ring research. Tucson: The University of Arizona Press.

Speer HJ. 2010. Fundamentals of tree-ring research. Tucson: The University of Arizona Press.

Stokes MA. and Smiley TL. 1968. An introduction to tree-ring dating. University of Arizona Press: Tucson.

Tardif J, Camarero JJ, Ribas M. and Guti errez E. (2003) Spatiotemporal variability in tree growth in the Central Pyrenees: climatic and site influences. Ecological Monographs, 73, 241–257.

Weber JC, Sotelo Montes C, Abasse T, Sanquetta CR, Silva DA, Mayer S, Graciela IBM, Garcia RA. 2018. Variation in growth, wood density and carbon concentration in five tree and shrub species in Niger. New Forests. 49(1): 35–51. https://doi.org/10.1007/s11056-017-9603-7

Wimmer R and Grabner M. 2000. A comparison of tree-ring features in Picea abies as correlated with climate. IAWA Journal. 21(4): 403–416. https://doi.org/10.1163/22941932-90000256

Wood LJ and Smith DJ. 2015. Intra-annual dendroclimatic reconstruction for northern British

Columbia, Canada, using wood properties. Trees. 29: 461–474. https://doi.org/10.1007/s00468-014-1124-9

Yamaguchi DK. 1991. A simple method for cross-dating increment cores form living trees. Can. J. For. Res. 21: 414-416.

Zabek LM and Prescott CE. 2006. Biomass equations and carbon content of aboveground leafless biomass of hybrid poplar in coastal British Columbia. Forest Ecology and Management. 223(1–3): 291–302. https://doi.org/10.1016/j.foreco.2005.11.009

Zobel BJ. and Talbert J. 1984. Applied forest tree improvement. John Wiley & songs.

Chapter 2: Relationship between climate and tracheid properties in natural and planted stands of hybrid white spruce *Picea glauca* (Moench) x *engelmannii* (Parry) in central interior British Columbia, Canada.

2.1 ABSTRACT

Understanding how tree growth, in naturally and artificially regenerated trees, is influenced by climate is important for determining forest productivity and wood quality in boreal forests of central interior British Columbia. The focus of this study was to investigate the effects of climate on radial growth (ring-width, earlywood, and latewood) and wood cell properties (cell wall thickness, density, radial diameter, microfibril angle, and coarseness) in natural and planted stands of hybrid white spruce (*Picea glauca* (Moench) x *engelmannii* (Parry)), in regional areas of the John Prince Research Forest (JPRF) and surrounding Prince (PG) George. Results suggest that winter, summer, and autumn climate strongly influence radial growth in planted stands with some variation between regional areas. Natural stands had similar relationships but lacked model verification. However, results indicate natural chronologies truncated to the last 30 years of growth may have increased sensitivity to climate variation compared to full-length natural stand chronologies in both JPRF and PG. Differences in climate sensitivity were found between natural and planted stands and between the JPRF and PG.

2.2 INTRODUCTION

2.2.1 Context

Global temperatures are predicted to increase between 0.3 to 0.7 °C by the year 2035. Prevalence of extreme weather conditions, characterized by more warmer and colder days and nights, and increased heavy precipitation events, are expected to increase (IPPC 2013). The Pacific Northwest of North America is expected to become warmer and wetter annually with increased maximum and minimum temperatures and decreased depth and water content of snowpack that will vary across the topographic landscape (MWLAP 2002; Lo et al. 2010; Fleming and Whitfield 2010). Unfortunately, compared to the global average, British Columbia (BC) is expected to have substantial warming and increased drought stress (Lo et al. 2010; Jiang et al. 2016).

Plastic variation that coordinates to fluctuations in climate can be seen in annual ring-with (RW), earlywood (EW), and latewood (LW) wood properties and wood cell properties of cell wall thickness (CWT), radial diameter (RD), coarseness, microfibril angle (MFA) and density (D). Analysis of average annual wood cell properties can provide greater resolution of the climate-growth relationships compared to analysis of annual RW, EW and LW properties (Chen et al. 2010; Bouriaud et al. 2005; Wood and Smith 2012; Wood and Smith 2015). Previous studies have found age-related and climate-related growth patterns within radial wood properties vary significantly depending location and species (Watson and Luckman 2001; Larocque and Smith 2005; Pitman and Smith 2013; Wood and Smith, 2012; Watson and Luckman 2016).

2.2.2 Background

Climatic conditions have a large influence on photosynthetic capabilities and subsequent tree growth. Tree growth over time may be measured by RW in trees that produce a distinct annual tree ring. In regions that demonstrate seasonality, annual growth rings form thin-walled, large cells during optimal growth periods, called "EW", and thick walled, high density cells, called "LW" when conditions have transitioned to sub-optimal near the end of the growing season (Fritts 1967; Saranpaa 2003; Shumlsky and Jones 2011). EW cell production is initiated by changes in photoperiod length and increases in soil and air temperatures typical of spring-like conditions (Vaganov et al. 1999; Heinrichs et al. 2007). The growth hormone within apical meristems, auxin, becomes active during these optimal environmental conditions. Cambial zone cell division and expansion stimulated through meristematic auxin release and increased turgor pressure produce cells that are large in radial diameter, soft, thin-walled, and non-supportive, which are characteristics of EW (Barnett and Jeronimidis 2003). Initial EW is dependent on the previous growing season's energy reserves before full current-year photosynthetic production occurs. In the northern hemisphere, maximum growth for EW occurs in June and July, which coincide with peak photoperiods (Rossi et al. 2006; Heinrichs et al. 2007). Terminal shoot cessation is initiated by decreases in temperature, precipitation, or a reduction in photoperiod length. These changes will reduce levels of auxin and other plant growth regulators, cytokinin and gibberellin, which will reduce cell production and cause maturation or secondary wall thickening within existing cells (Zobel and van Buijtenen 1989, pg 27; Heinrichs et al. 2007). Secondary wall thickening during this slower-growth maturation period creates thick, hard, structural, multi-layered cell walls with organized microfibril layers held together by hemicellulose and lignin, and are characteristic of LW (Wimmer 2002; Barnett and Jeronimidis 2003). This multi-layered secondary cell wall provides structural support for growth stress. The beginning of LW production in a variety of North American conifers, including spruce, has been found to range from July 1st to August 4th with termination of xylem production between July 20th and September 20th (Heinrichs et al. 2007).

2.2.3 Age Related Growth Characteristics

Trees undergo changes in RW, EW, LW, and wood cell properties as they age from seedling to mature trees. Competition for resources drives young trees to establish dominance with explosive juvenile growth, producing what is known as juvenile wood (JW) for several years. JW will have larger RWs, larger proportions of EW cells and fewer LW cells. Once established, radial growth slows and stabilizes into what is known as mature wood (MW) with smaller RWs and lower proportions of EW (Shmulsky and Jones 2011). The transition from JW to MW within spruce species is not as easily defined as other conifers and has been suggested to be anywhere between 13 and 31 years depending on the species (Cameron et al. 2005; Alteyrac et al. 2006). Age-related growth differences can also be found in wood cell properties such as CWT, D, RD, coarseness, and MFA. Distinct differences have been found between JW and MW; with rapidly decreasing RD combined with increasing D and CWT as the tree matures (Mitchell and Denne 1997; Saranpaa 2003; Zubizarreta-Gerendiain et al. 2012). Cell RD within MW has been shown to gradually increase with cambial age to compensate for increased crown and hydraulic resistance related to increased taller stems (Lindstrom 1997; Mitchell and Denne 1997; Vahey et al. 2007; Lenz et al. 2010; Newton 2016). Coarseness and cell tangential widths have been shown to increase from pith to bark with cambial age combined with decreases in tangential fibre width seen after 40 years (Kienholz 1931; Panshin and deZeeuw 1980; Lindstrom 1997; Muneri and Raymond 2001;

Lundgren 2004; Havimo et al. 2008; Franceschini et al. 2012). However, there is some indication that white spruce can continue increasing tangential cell widths with age (Taylor et al. 1982). MFA, which is the degree of tilt in cellulose microfibrils from the longitudinal axis primarily within the S_2 secondary cell wall layer, decreases pith to bark (Erickson and Arima 1974; Wimmer 2002; Adamopoulos et al. 2007; Kostiainen et al. 2014).

2.2.4 Relationships between RW, EW, LW, and Climate

Growth rate and subsequent EW and LW proportions within an annual ring are directly influenced by photosynthetic capacity. Genotype and environmental factors including humidity, stand density, photoperiod, and changes to air temperature, soil temperature, and water availability can affect the rate of photosynthesis (Fritts 1976; Wimmer, 2002). Photosynthetic capacity within interior BC trees has historically been temperature dependent as heavy rainfall and large snowmelts usually provided adequate precipitation for growth (Watson and Luckman 2007).

Some evidence suggests that higher-than-normal temperatures can negatively affect RW growth by inducing water stress. Water stress can increase respiration and evapotranspiration leading to moisture loss without adequate precipitation inputs (Fritts 1976; Gindl et al. 2000; Chen et al. 2010; Miyamoto et al. 2010; George et al. 2019). On specific sites within southern BC, water stress has been shown to be the largest limiting growth factor in Douglas-fir (*Pseudotsuga menziensii* (Mirb.) Franco var. *glauca*), lodgepole pine (*Pinus contorta* Dougl. var. *latifolia*) and hybrid white spruce (*Picea glauca* x *engelmannii*) (Lo et al. 2010). Additionally, growth rates of coastal BC Douglas-fir (*Pseudotsuga menziesii* (Mirb.) Franco) have direct correlations between increasing soil moisture deficits and reduced RW and EW found in both mature (Robertson et al. 1990) and planted (Bower et al. 2005) stands. Alternatively, warmer-than-normal spring, summer, and autumn temperatures have been shown to positively influence radial growth with adequate precipitation inputs in several conifer species in BC, Canada, including white spruce (Peterson and Peterson 1994; Ettl and Peterson 1995; Larocque and Smith 2005; Miyamoto et al. 2010). In these conditions spring bud burst can occur earlier and trees can grow bigger. Trees may have a longer time to accumulate and store nutrients in autumn months when typical dormancy would ensue.

2.2.5 Climate-related Growth Trends in Wood Cell Properties

Temperature and precipitation events can also affect growth rates in wood cell properties. Favorable conditions during the growing season can allow for increased cell production, increased cell widths, increased CWT, and increased tracheid length (Kienholz 1931). MFA has been shown to be positively correlated with average summer temperatures in northern interior BC Douglas-fir (Wood et al. 2016). Precipitation increases coupled with adequate temperatures, have been shown to increase tracheid production and RDs (Kienholz 1931). However, higher-than-normal summer temperatures have been shown to correlate with decreases in spruce radial growth and decreased cell RD, CWTs, lumens, and D throughout an annual ring (Chen et al. 2010). Additionally, water stress and lower-than-normal temperatures have also been shown to negatively influence CWT (DeSoto et al. 2011).

2.2.6 Wood Quality in Natural and Artificially Regenerated Stands

Pulp products originating from BC's forests have been characterized by long, slender, thin-walled fibres that have superior strength, low coarseness, and high uniformity (Taylor et al. 1982; Corriveau et al. 1991; Watson and Bradley 2009). Large thin-walled EW cells can easily compress into sheet formation (Lenz et al. 2010; Shmulsky and Jones 2011, pg 410-411) while having high tensile strength due to high proportions of hydrogen bonds. Pulp with these characteristics was historically processed from old mature timber and is considered high quality with high marketability, with spruce as a preferred species (Taylor et al. 1982). Timber harvest in BC will increasingly shift from naturally generated old-growth stands to artificially reforested stands due to decreasing availability of old-growth forests, which may affect wood quality. Shifting from naturally-regenerated old-growth forests to planted forests will result in harvest of younger, fast-grown trees with potentially larger proportions of juvenile wood (Lenz et al. 2010). Additionally, previous research has suggested that several characteristics of planted stands may make them more vulnerable to projected changes in climate that include age effects, stand density and canopy structure, and lower biological diversity and inferior local adaptation of seeds, that could negatively affect wood quality (Sanchez-Salguero et al. 2013).

2.2.7 Research Gaps

Changes to wood cell properties and subsequent wood quality within central interior BC hybrid white spruce are almost certain with projected changes in climate. Although there is considerable research on the influence of climate on radial spruce growth, most of these studies have focused only on RW, EW, and LW (Gou et al. 2005; Chen et al. 2010; Miyamoto et al. 2010; Flower and Smith 2011; Trindade et al. 2011; Wood and Smith 2015; Strong 2017) with wood cell research largely limited to relationships between RW and ring D (Watson and Luckman 2001; Larocque and Smith 2005; Pitman and Smith 2012; Wood and Smith 2013; Wood and Smith 2015; Watson and Luckman 2016). Additionally, there have been few studies on spruce growth in areas of north-central BC (Flower and Smith 2011;

Wood and Smith 2015) and limited studies focused on direct comparisons of climate-related growth changes in both naturally and artificially regenerated stands (Sánchez-Salguero et al 2012; Sánchez-Salguero et al. 2013).

2.2.8 Objectives

This study aims to investigate variations in wood quality of hybrid white spruce (*Picea glauca* x *engelmannii*) in natural and planted stands over time, and how these variations correspond with changes in temperature and precipitation in central interior BC. The objectives of this research were to i) determine annual radial growth profiles of RW, EW, LW , D, RD, CWT, coarseness, and MFA angle at annual scales, ii) determine the variability of radial growth and tracheid properties over time, iii) examine the statistical correlation between monthly and seasonal climate variables and tracheid properties, and iv) visually investigate the effects of climate variables on tracheid properties over time.

2.3 METHODS

2.3.1 Site selection

Hybrid white spruce trees were selected from six natural (N1-N6) stands between 60 and 125 years old, and six planted (P1-P6) stands between 25 and 40 years old from areas in central interior BC (Figure 2.1; Table 2.1). One group of six stands (N1-N3; P1-P3) was selected from the John Prince Research Forest (JPRF), where each stand was within 5km of one another. The second group of six stands (N4-N6; P4-P6) were within a 200km range of Prince George (PG). Biogeoclimatic variant of each site was determined with review of site characteristics and Biogeoclimatic Ecosystem Classification land management handbooks (Table 2.1) (Delong et al. 1993). PG stands were in the willow-wet-cool (wk1) and very-wet-cool (vk1) variants, classified with high precipitation and cooler temperatures. JPRF stands were in the Stuart-dry-warm (dw3) variant that is characterized by lower snow packs and warmer temperatures.

2.3.2 Sample Collection

Twenty dominant trees at each stand were selected for sampling. Sampling occurred at 5m minimum intervals to avoid concerns of spatial autocorrelation (Dale and Fortin 2014). Trees with scars, fire or insect damage, split tops and abnormal growth patterns were avoided. Areas near roads or with open canopies were also avoided to alleviate influences on growth that would reduce the ability to obtain a stand-level climatic growth signal (Fritts 1976). Two 5mm cores at 90 degree spacing from each tree were collected at breast height (and at 30cm aboveground for smaller trees) that was parallel with contours (Grissino-Mayer 2003). An additional 12mm core from each tree was collected at JPRF sites for SilviScan fibre analysis. Surrounding vegetation, slope, elevation, flowing or standing water, diameter-at-breast-height and GPS site and tree location were recorded.

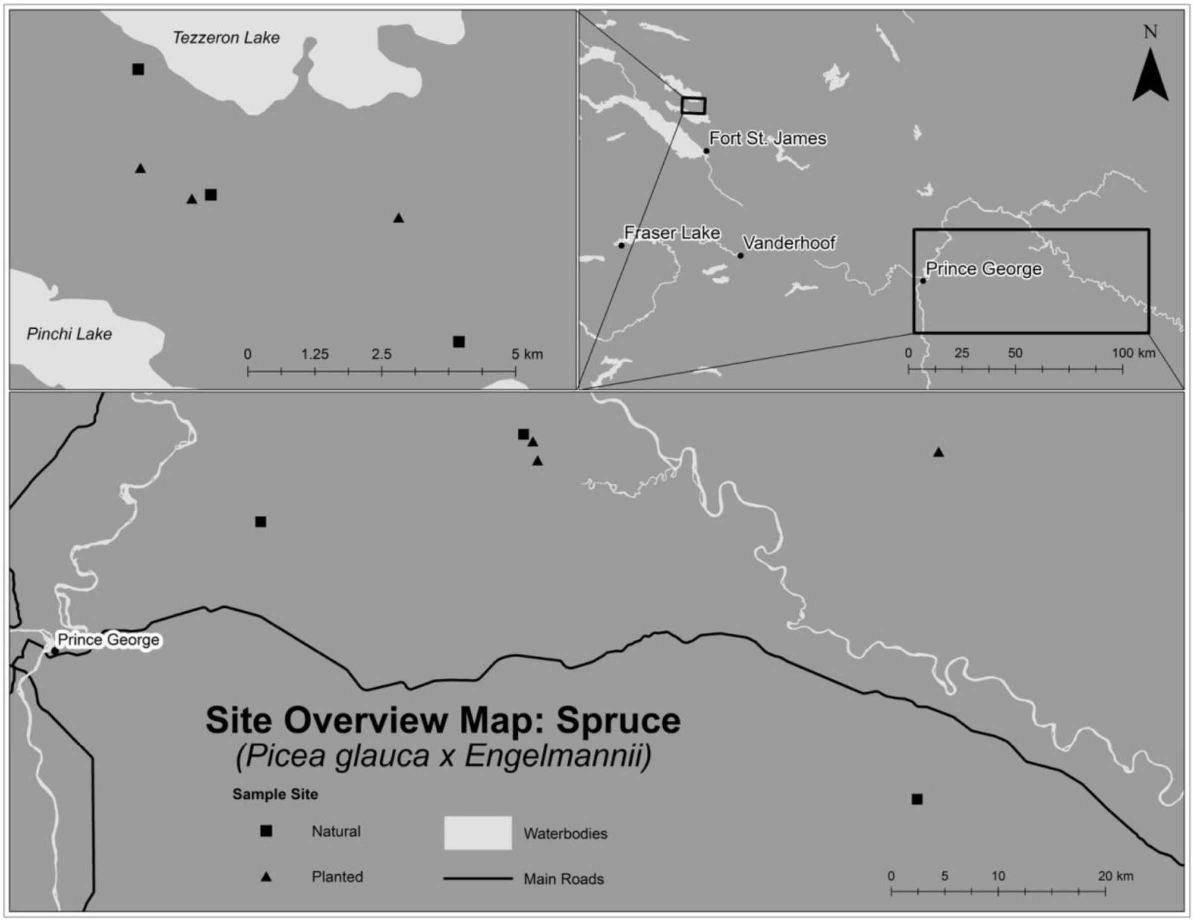

Figure 2.1 Overview map of natural (squares) and planted (triangles) stands sampled near Prince George and Fort St. James.

Table 2.2 Site and stand characteristics of natural (N1-N6) and planted (P1-P6) spruce research sample sites from areas surrounding John Prince Research Forest (JPRF) and Prince George (PG) collected from 2016-2017.

	Geographic Information							Tree Characteristics		
	Site	**Latitude**	**Longitude**	**Elevation (m)**	**BEC zone**	**BEC Subzone**	**BEC Variant**	**Mean Age (years)**	**# of Tree Cores**	**Mean DBH (cm)**
JPRF	N1	54 38'50.8	124 23'35.1	768	SBS	dw	3	101	40	26.5
	N2	54 39'46.6	124 24'36.6	833	SBS	dw	3	119	35	38.3
	N3	54 36'58.21	124 19'05.5	727	SBS	dw	3	52	34	30.5
	P1	54 38'47.5	124 23'68.2	801	SBS	dw	3	40	40	17.8
	P2	54 38'48.0	124 24'34.5	866	SBS	dw	3	40	40	22.3
	P3	54 38'14.17	124 20'05.5	802	SBS	dw	3	25	36	18.9
PG	N4	54 04'58.9	122 01'32.3	730	SBS	wk	1	93	40	40.9
	N5	54 46'33.9	121 29'14.6	1113	SBS	vk	1	145	40	48.2
	N6	54 01'01.0	122 24'54.5	707	SBS	wk	1	154	40	32.4
	P4	54 04'05.9	121 26'48.8	843	SBS	vk	1	30	40	26.1
	P5	54 05'19.9	122 01'31.8	713	SBS	wk	1	30	40	28.2
	P6	54 04'01.1	122 01'09.7	689	SBS	wk	1	33	40	22.9

2.3.3 Sample Preparation of 5mm Cores

Increment cores from JPRF and PG were dried, glued, mounted, labelled, and sanded with progressively finer grit in preparation for cross-dating; 1200 grit sandpaper was used to identify especially narrow rings. A dotting system was used to cross-date. Cores were labeled with a single dot every ten years, two dots every half-century, and three dots every century (Stokes and Smiley 1968). The Yamaguchi (1991) list method was implemented to determine significant marker years. Groups of 18-20 5mm increment cores were scanned using an Epson 1640XL flatbed scanner at 1,200 DPIs for visual assessment of RW, EW and LW widths with WinDendro image analysis. Each core was reviewed to determine accuracy of WinDendro RW, EW and LW auto-measurements, and corrections were performed manually (Speer 2010; Arenas-Castro et al. 2015).

2.3.4 Sample Preparation of 12mm Cores

Of the 120-12mm cores sampled at JPRF, 89 undamaged cores were selected for SilviScan analysis. Resins were removed from selected cores via 12-hour Soxhlet acetone extraction. After extraction, cores were conditioned at 40% relative humidity and 20°C to obtain an 8% moisture content equilibrium. Once at 8% moisture content, cores were cut into 2mm X 7mm radial pith-to-bark strips (tangentially x longitudinally) with a twin-blade saw and sanded. SilviScan analysis was then performed which included 1) image analysis of radial and tangential cell dimensions using optical microscopy, 2) x-ray densitometry to provide measurements of wood density every 25 microns along the wood samples, and 3) x-ray diffractometry yielding measurements of microfibril angle at 5-mm increments (Evans and Ilic 2001).

2.3.5 Creating Master Chronologies

Mean annual characteristic values of density (MD), microfibril angle (MMFA), radial diameter (MRD), coarseness (MCO), and cell wall thickness (MCWT) were cross-dated for each stand using end-dates obtained from SilviScan. Visual cross-dating of 5mm cores with WinDendro and cross-dating of 12mm cores with end-dates were verified using COFECHA (Grissino-Mayer 2001). Cores (series) with unique variation not representative of the stand were eliminated from the chronology for each growth property that allowed for the common stand-level variation to be captured. Inter-series correlation, or stand-level signals, were only accepted for further analysis if the correlation coefficient was greater than 0.3 for natural stands and 0.4 for planted stands, representing the 99% one-tailed confidence level (Grissino 2001). Shorter segment lengths required higher inter-series correlations for accuracy. Average mean sensitivities, which indicate the variability in a master chronology from year to year that ranges from least sensitive (0) to most sensitive (1), were also observed and not accepted for further analysis if less than 0.150 (Table 2.2 and Table 2.3) (Speer 2010; Arenas-castro et al. 2015).

Following analysis using COFECHA, ARSTAN software was used to detrend and index (standardize) series, remove variance, and transform RW, EW, LW, MD, MCO, MRD, and MMFA from ratio values into dimensionless (index) values (Cook and Holmes 1999). This detrending was performed to remove growth-frequency variation attributed to tree geometry and normal rapid growth of young trees (Cook and Peters 1981; Meko and Baisan 2001). Stabilization of RW, EW, and LW was achieved through application of a negative exponential curve or straight line fit followed by a smoothing spline (frequency-response cut-off of -67) (Cook and Peters 1981; Meko and Baisan 2001). A smoothing spline was applied to remove low-frequency variation for MD and MCWT series, and a linear, least squares regression line was applied through MRD data. MMFA and MCO chronologies had unacceptable inter-series correlations and were not used for further analysis. Each series was transformed and averaged to create a master site chronology for all wood characteristics using an rbar (inter-series correlation) running window of 20 years with an overlap of 10 years for mature stands, and a running window of 10 years with an overlap of 5 years for planted stands (Cook and Holmes 1999). Rbar and EPS (expressed population signal) were used to determine when chronologies had low sample size near the beginning of a series and the accuracy of sample representation of the population. Sites <80% EPS were discarded to ensure an adequate representation of population signal (Wigley et al. 1984).

2.3.6 Comparisons of Chronologies with Climate

Climate Data

Historical climate information was obtained from the Adjusted Historical Canadian Climate Data website (https://www.canada.ca/en/environment-climate-change/services/climate-change/modelling-projections-analysis/adjusted-homogenized-canadian-data.html) for PG (Station #1096439, Lat 53°88, Long -122°67, 680m elevation) and Fort St. James (Station #1092970, Lat 54°45, Long -124°25, 686m elevation) weather stations. Climate variables included monthly mean temperature, total monthly precipitation, and winter (previous December and current January, February), spring (current March, April, May), summer (current June, July, August) and autumn (previous September, November, December) seasonal averages. Random missing values within climate data were calculated by averaging four surrounding data points (two from prior and two after the missing value) or filled with modeled climate data from Climate BC (http://cfcg.forestry.ubc.ca/projects/climate-data/climatebcwna/).

Correlation & Regression to climate

RW, EW, LW, MD, MRD, and MCWT of planted and natural stands were tested for normality using skewness and kurtosis values prior to correlation and regression analysis; Shapiro-Wilk was used to validate normality for sites with small sample sizes (Table 2.4 and Table 2.5). Site data failing one test was assessed using histograms to determine severity of skew. Site data failing all tests were assumed non-normal and transformed where possible. Data that were unable to be normalized were removed from further analysis.

Before correlation and regression analysis, a one-way independent t-test and/or analysis of variance (ANOVA) test, with Bonferroni post-hoc test (alpha=0.05), was conducted to determine significant differences in growth of RW, EW, LW and wood cell properties by site in order to group stands together as a regional average (Table 2.6 and Table 2.7). Correlation statistics were calculated for stand-level and regionally averaged data. Annual values of RW, EW, LW, MD, MRD, and MCWT were correlated to mean previous year monthly May-December and mean year current monthly January-September, winter (previous December, current January and February), spring (current March, April, May), summer (current June, July, August), and autumn (previous September, October, November) temperature and precipitation values using a Pearson's correlation coefficient (R) or Spearman's Rank coefficient for non-parametric data that could not be normalized (Figure 2.4 – 2.19). In addition, correlation statistics were determined for data from natural stands that were truncated to the last 30 years of growth (N(X)trunc) (Figure 2.4-2.19). Truncated natural stand data was used to provide an opportunity for comparisons of recent natural stand growth to full-length chronologies and to compare natural and planted datasets within the same climate interval. Partial correlation was used to determine spurious correlations when relationships between radial growth variables were found to both temperature and precipitation within the same months/seasons.

2.3.7 Regression Analysis and Comparison of Measured and Modelled Values

Regression analysis was completed where significant Pearson's correlation coefficients were detected (Tables 2.8-2.10). Significant R^2 values were only accepted where R^2 >0.25 (Wood and Smith 2011; Blanchette et al. 2015). Modelled values were correlated back to measured values to verify model accuracy (Tables 2.8-2.10). Models with significant correlation coefficients and acceptable R^2 values were visually assessed against measured values to determine model accuracy over time (Figures 2.20-2.24).

2.4 RESULTS

2.4.1 Changes in Climate

Climate conditions recorded at Fort St. James and PG weather stations have changed over the last 100 years (Figures 2.2-2.5). Figures 2.2-2.5 depict mean annual temperature and total annual precipitation of autumn (previous September, November, December), winter (previous December, current January and February), spring (current March, April, May) and summer (current June, July, August) for Fort St. James and PG with a 10-year moving average. Historical climate records indicate mean annual precipitation has ranged from 282-770 mm in Fort St. James and 368-934 mm in PG. Average annual precipitation and annual average temperatures have been recorded as 465 mm and 2.8 ˚C for Fort St. James and 633 mm and 3.7˚C for PG. Mean average temperatures have increased 1.2 ˚C and 0.4 ˚C for Fort St James and PG respectively since 1920. Total annual precipitation has generally decreased Fort St. James and increased in PG since 1920. However, recent reductions in precipitation are seen in Fort St. James in the last 30 years.

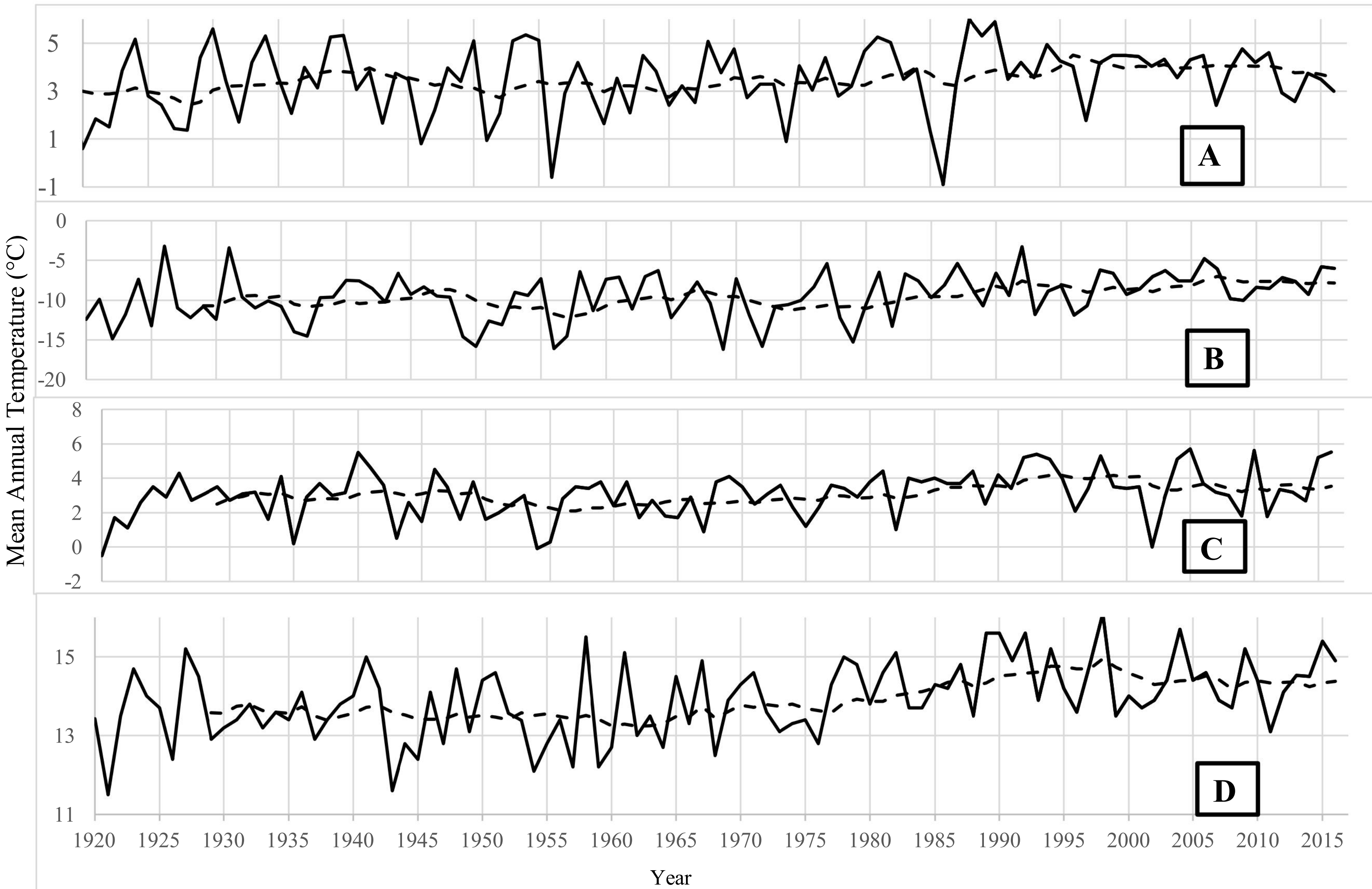

Figure 3.2 Mean annual temperature from Fort St. James climate station from 1920-2016. A= previous autumn; B=winter; C=spring; D=summer. The dashed trendline represents a 10-year moving trend line in temperature variation; moving averages cannot be calculated for the first 10 years because of lack of data before 1920. Note not all y-axis are the same.

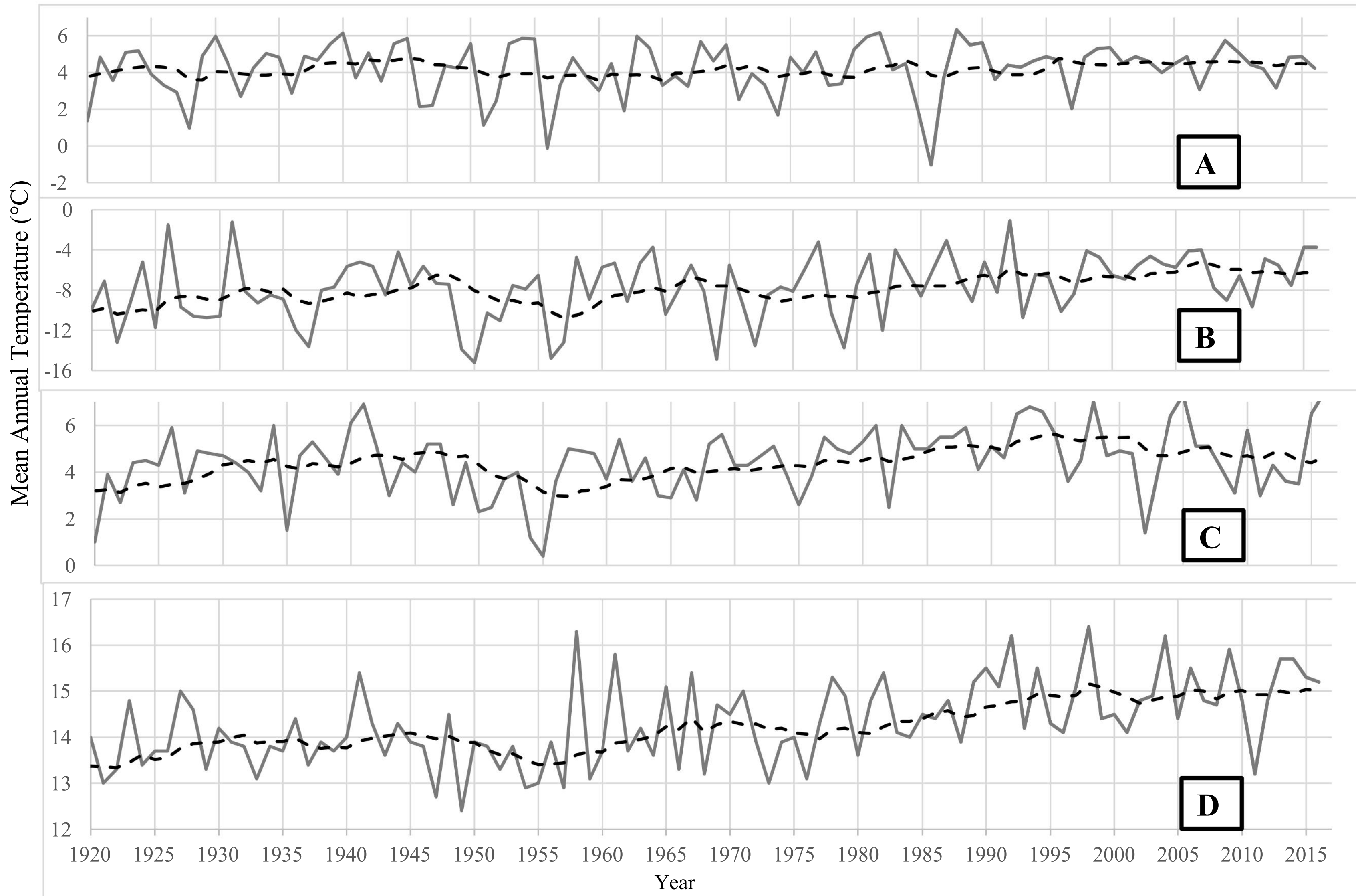

Figure 4.3 Mean annual temperature from Prince George climate station from 1920-2016. A= previous autumn; B=winter; C=spring; D=summer. The dashed trendline represents a 10-year moving trend line in temperature variation. Note not all y-axis are the same.

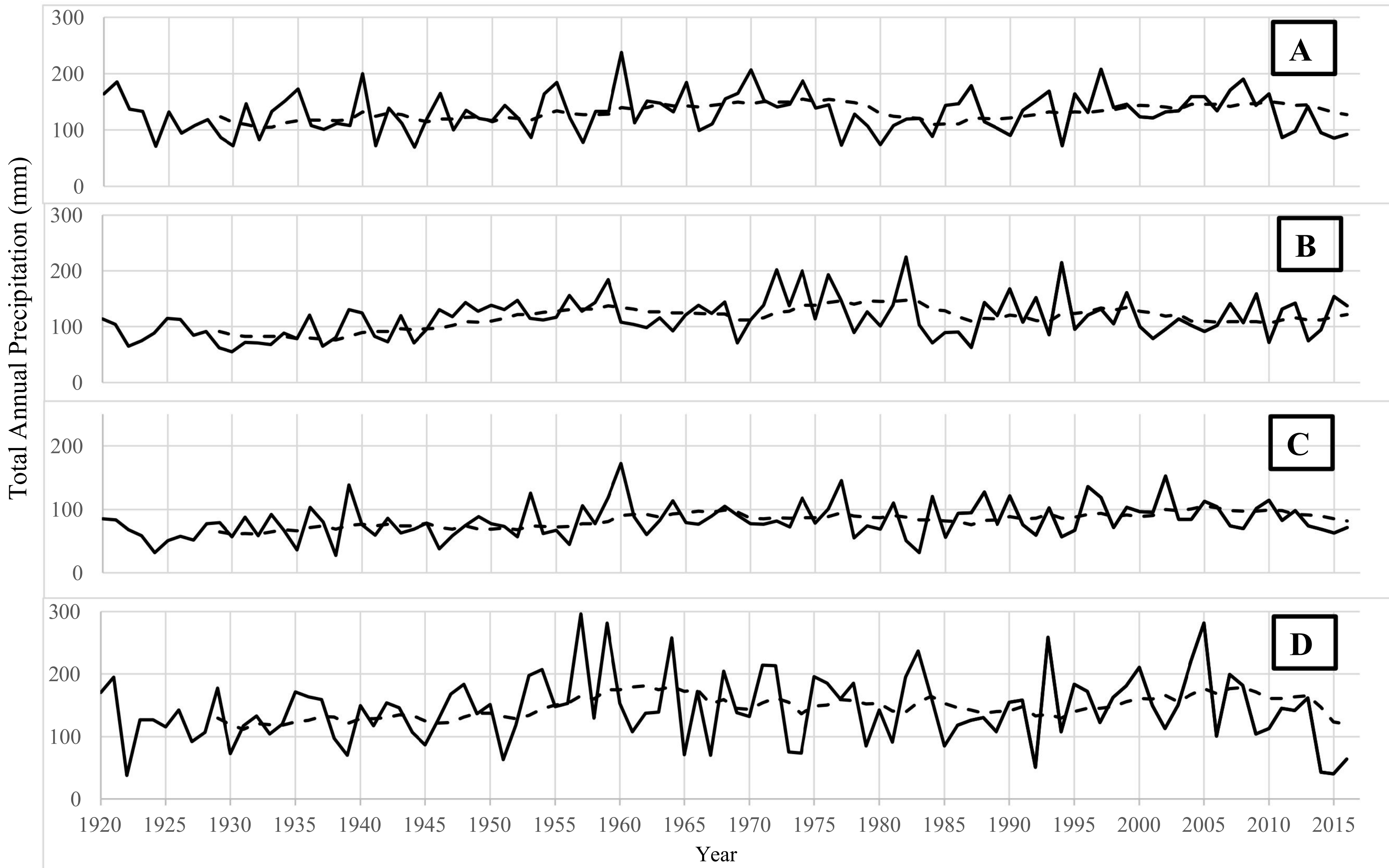

Figure 5.4 Total annual precipitation from Fort St. James climate station from 1920-2016. A= previous autumn; B=winter; C=spring; D=summer. The dashed trendline represents a 10-year moving trend line in temperature variation; moving averages cannot be calculated for the first 10 years because of lack of data before 1920. Note not all y-axis are the same.

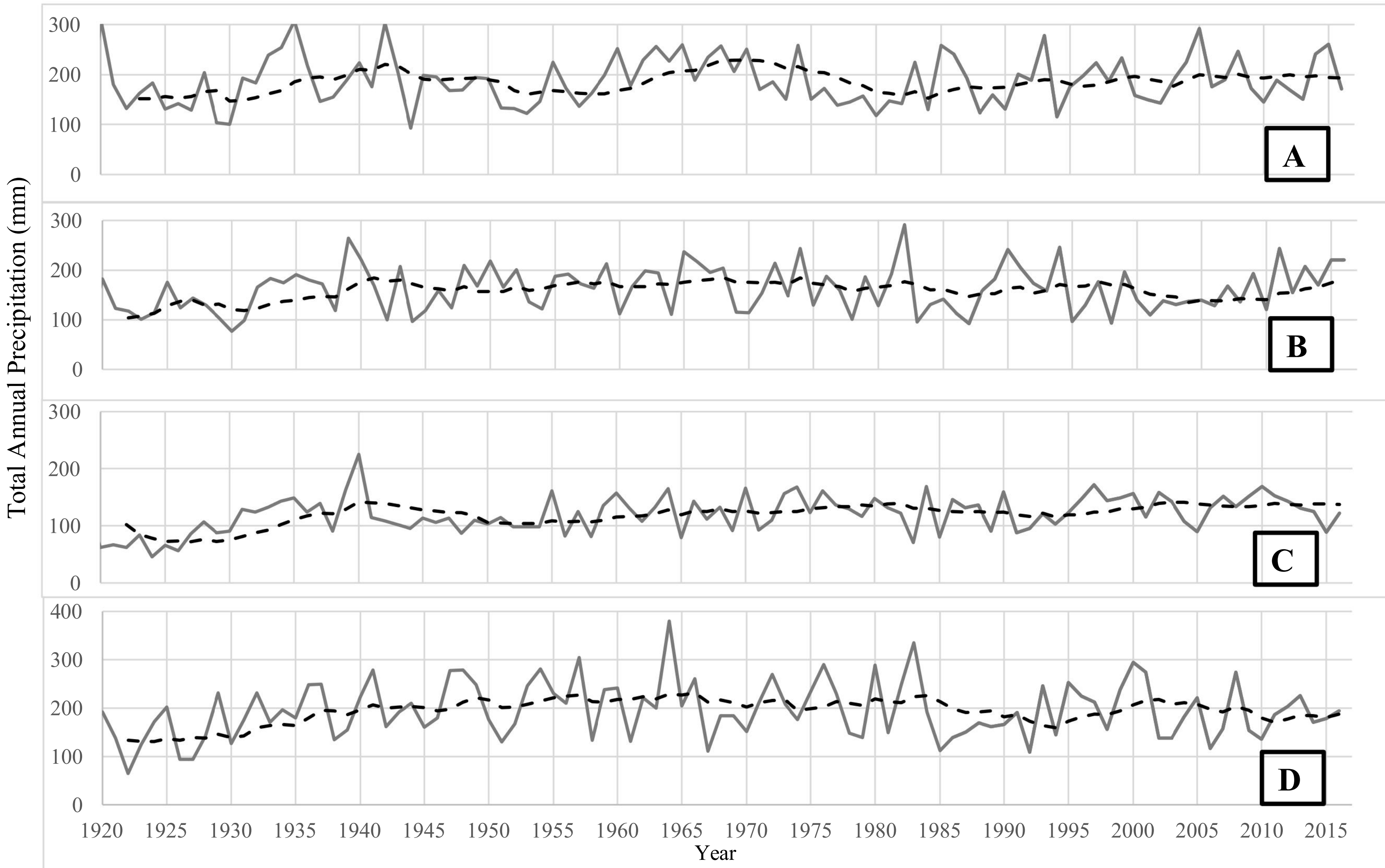

Figure 6.5 Total annual precipitation from Prince George climate station from 1920-2016. A= previous autumn; B=winter; C=spring; D=summer. The dashed trendline represents a 10-year moving trend line in temperature variation. Note not all y-axis are the same.

2.4.2 Chronologies

Chronology lengths for planted stands were between 31-41 years for PG and 29-35 for JPRF. Natural stand chronology lengths were between 144-168 years for PG and 62-113 years for JPRF (Table 2.2). The year of residual EPS cut-off was variable for radial growth characteristics (Table 2.3). Most inter-series and mean sensitivity values were acceptable, >0.3 and >0.15 respectively, excluding all MCO and MMFA that were disregarded from further analysis (Table 2.2 and Table 2.3). Normality testing of RW, EW, LW and wood cell properties chronologies determined most data as normal with the exception of N5trunc-EW, P5-LW and N6-LW; N6-LW was normalized using a log transformation but N5trunc and P5 chronologies could not be normalized (Table 2.4 and Table 2.5).

2.4.3 Climate Correlations

Several significant correlations ($p > 0.05$) were found between tracheid characteristics and the previous and current monthly and seasonal weather record of Fort St. James and PG (Figures 2.6-2.21).

Temperature

PG & JPRF: RW, EW, and LW

RW, EW, and LW chronologies from planted stands in PG and JPRF were significantly negatively correlated with previous autumn and summer and current summer and winter mean monthly temperatures (Figure 2.6 and Figure 2.9). Significant positive correlations were only found between LW in JPRF planted stands and previous year June monthly temperatures. JPRF and PG natural stand RW, EW and LW chronologies had fewer significant correlations with temperature than planted stand chronologies (Figure 2.7 and Figure 2.10). RW, EW, and LW in JPRF and PG natural stands were significantly negatively correlated with previous autumn and current spring and summer monthly temperatures. RW, EW, and LW chronologies from PG natural stands were significantly positively correlated with previous winter and autumn and current year summer temperatures; few positive correlations were found with JPRF natural stands. Several truncated natural stand chronologies were more strongly correlated to climate parameters than full-length chronologies (Figure 2.8 and Figure 2.11). Truncated RW, EW, and LW chronologies from PG natural stands were significantly negatively correlated with previous year spring/summer monthly temperatures and significantly positively correlated with previous year November and current year August monthly temperatures (Figure 2.8). Truncated RW, EW and LW chronologies from JPRF natural stands were significantly negatively correlated to previous June and September and current year winter and July monthly temperatures; no positive correlations were found in JPRF (Figure 2.10).

JPRF: Cell Properties of MCWT, MRD and MD

Very few significant correlations were found between cell property chronologies of planted stands in JPRF and mean monthly temperature. MCWT, MRD, and MD chronologies from JPRF planted stands were significantly correlated to previous year June and August and current year autumn and August mean monthly temperatures (Figure 2.20). Natural stand cell property chronologies from JPRF had more numerous correlations to mean monthly temperature than JPRF planted stands (Figure 2.21). The truncated natural stand chronologies from JPRF were more strongly correlated to temperature than full-length chronologies in most cases (Figure 2.21). MRD and MRDtrunc chronologies from natural stands were significantly negatively correlated with previous year winter and current year winter, spring, summer, and autumn mean monthly temperatures; no positive correlations were found between temperature and MRD or MRDtrunc chronologies. MD chronologies from natural stands were significantly positively correlated with previous and current year summer, September, and current year spring mean monthly temperatures.

Precipitation

PG & JPRF: RW, EW, and LW

Planted stand and truncated natural stand chronologies significant correlations were more numerous and were more strongly correlated to precipitation than full-length natural stand chronologies (Figures 2.12- 2.17). RW, EW and LW chronologies from PG stands were significantly positively correlated to previous and current spring and summer precipitation and negatively correlated with winter and previous autumn precipitation (Figures 2.12 – 2.13). RW, EW and LW chronologies from JPRF planted and natural stands were significantly positively correlated with previous summer and autumn and current year winter, spring and summer precipitation, and significantly negatively correlated with total previous autumn and winter and current winter precipitation (Figures 2.15-2.17).

JPRF: Cell Properties of MCWT, MRD, and MD

Planted stand wood cell property chronologies were more significantly correlated with precipitation than with temperature (Figure 2.18 and Figure 2.19). MCWT chronologies from JPRF planted stands were significantly negatively correlated to total previous July and current spring, summer and September annual precipitation (Figure 2.18); all MCWT chronologies from JPRF natural stands had unacceptable EPS values. MRD chronologies from JPRF planted stands were significantly positively correlated to previous or current spring, summer or and autumn total precipitation and significant negative correlations were found to previous December total precipitation (Figure 2.18). MRD truncated and full-length chronologies had fewer correlations than planted stand chronologies; truncated chronologies had more numerous and stronger correlations than full-length chronologies (Figure 2.19).

MRD full-length chronologies from JPRF natural stands were significantly correlated to previous year August and October and current year June, and September monthly precipitation (Figure 2.19). Truncated MRD chronologies from JPRF were significantly correlated to current year May and summer monthly precipitation (Figure 2.19). MD chronologies from JPRF planted stands were significantly correlated to current year winter and September total precipitation (Figure 2.18). MD full-length chronologies from JPRF natural stands had very few, weak correlations between previous year June December and current year average autumn monthly total precipitation (Figure 2.19). Truncated MD chronologies from JPRF natural stands had no correlations with precipitation (Figure 2.19).

Table 2.2. Master chronology statistics for planted and natural stands in the John Prince Research Forest (JPRF) and Prince George areas within central interior British Columbia. Statistics shown include chronology length, inter-series correlations (ISC), mean sensitivity and EPS cut off and values for RW ring-width, EW earlywood and LW latewood. Note that P3 LW chronology was too short to analyze.

			RW				EW				LW			
	Site	**Chronology Length**	**ISC**	**Mean Sensitivity**	**EPS value**	**EPS cutoff**	**ISC**	**Mean Sensitivity**	**EPS value**	**EPS cutoff**	**ISC**	**Mean Sensitivity**	**EPS value**	**EPS cutoff**
JPRF	N1	1903-2016	0.588	0.168	>0.85	1910	0.560	0.188	> 0.85	1916	0.388	0.250	> 0.80	1917
	N2	1870-2016	0.525	0.174	>0.85	1896	0.518	0.193	> 0.85	1903	0.392	0.258	> 0.80	1920
	N3	1954-2016	0.528	0.169	>0.90	1960	0.517	0.184	> 0.85	1967	0.436	0.300	> 0.80	1970
	P1	1981-2016	0.578	0.203	>0.90	1987	0.569	0.221	> 0.85	1990	0.460	0.395	> 0.80	1992
	P2	1987-2016	0.664	0.227	>0.90	1983	0.646	0.247	> 0.85	1986	0.463	0.386	> 0.80	1988
	P3	1987-2016	0.582	0.185	>0.90	1990	0.568	0.206	> 0.85	1994	0.516	0.384	> 0.80	2005
Prince George	N4	1872-2016	0.485	0.251	>0.90	1973	0.470	0.272	> 0.85	1973	0.348	0.354	< 0.80	-
	N5	1831-2016	0.628	0.170	>0.85	1842	0.567	0.202	> 0.80	1870	0.406	0.299	> 0.80	1870
	N6	1848-2016	0.558	0.182	>0.80	1855	0.541	0.220	> 0.80	1862	0.342	0.282	> 0.80	1970
	P4	1985-2016	0.561	0.255	>0.90	1986	0.611	0.229	> 0.85	1988	0.450	0.375	> 0.80	1989
	P5	1980-2016	0.554	0.193	>0.90	1983	0.532	0.213	> 0.85	1984	0.460	0.355	> 0.85	1989
	P6	1975-2016	0.553	0.207	>0.90	1985	0.556	0.215	> 0.80	1986	0.346	0.381	< 0.80	-

Table 2.3. Master chronology statistics for planted (P1, P2, P3) and natural stands (N1, N2, N3) within the John Prince Research Forest in interior British Columbia. MCO mean coarseness, MD mean density, MMFA mean microfibril angle, MRD mean radial diameter, MCWT mean cell wall thickness.

Site Name	**Chronology Type**	**Chronology Length**	**Interseries correlation**	**Mean sensitivity**	**EPS value**	**EPS cutoff**
N1	MCO	1899-2017	0.402	0.062	<0.8	-
	MD	"	0.487	0.060	>0.8	1930
	MMFA	"	0.080	0.032	-	-
	MRD	"	0.541	0.038	>0.8	1920
	MCWT	"	0.442	0.061	<0.8	-
N2	MCO	1891-2017	0.347	0.062	<0.8	-
	MD	"	0.467	0.062	<0.8	-
	MMFA	"	0.063	0.033	-	-
	MRD	"	0.452	0.033	<0.8	-
	MCWT	"	0.404	0.062	<0.8	-
N3	MCO	1957-2017	0.322	0.066	<0.8	-
	MD	"	0.584	0.065	-	-
	MMFA	"	0.058	0.039	-	-
	MRD	"	0.541	0.033	>0.8	1970
	MCWT	"	0.483	0.065	<0.8	-
P1	MCO	1983-2017	0.443	0.081	<0.8	-
	MD	"	0.683	0.080	>0.9	1991
	MMFA	"	0.070	0.055	-	-
	MRD	"	0.666	0.041	>0.9	1991
	MCWT	"	0.624	0.077	>0.85	1992
P2	MCO	1980-2017	0.303	0.080	<0.8	-
	MD	"	0.608	0.079	>0.9	1989
	MMFA	"	0.139	0.039	-	-
	MRD	"	0.558	0.048	>0.9	1989
	MCWT	"	0.459	0.076	>0.8	1996
P3	MCO	1982-2017	0.492	0.085	<0.8	-
	MD	"	0.642	0.080	>0.8	1992
	MMFA	"	-0.023	0.094	-	-
	MRD	"	0.602	0.048	>0.9	1992
	MCWT	"	0.548	0.079	>0.85	1990

Table 2.4. Normality statistics for ring width (RW), earlywood (EW), latewood (LW) in the John Prince Research Forest and Prince George sites including Skewness and Kurtosis values; Shapiro-Wilk test was used to validate normality of sites with small sample sizes. Skewness > +3 or < -1 was not accepted as normal data. Kurtosis >+1 or <-1 was not accepted as normal data. Grey shading indicates normality values for mature chronologies that were truncated at 30 years. Areas with "-" indicate chronologies tested for normality because of unacceptable EPS values. Shapiro-Wilk normality test confirmed P3-EW & N5trunc-RW are normal data (*); unable to normalize N5trunc-EW & P5- LW (+); N6-LW normalized with log transformation (t).

		RW		EW		LW	
	Site	Skewness	Kurtosis	Skewness	Kurtosis	Skewness	Kurtosis
John Prince Research Forest	N1	0.035	0.045	-0.151	0.394	0.542	0.962
	N1	0.316	-0.387	0.254	-0.459	0.118	-0.170
	N2	0.397	0.299	0.296	0.315	0.245	0.340
	N2	0.451	-0.322	0.553	-0.372	0.134	0.927
	N3	0.423	-0.081	0.472	0.122	0.347	-0.754
	N3	0.644	0.755	-0.048	-0.980	0.605	0.002
	P1	0.404	0.754	0.811	0.406	0.464	-0.419
	P2	0.135	-0.859	0.166	-0.774	0.434	0.881
	P3	-0.351	-0.879	-0.148	-1.228*	-	-
Prince George	N4	0.245	0.702	0.303	-0.109	-	-
	N4	0.329	0.061	0.352	-0.023	-	-
	N5	0.058	0.469	0.091	-0.682	0.049	-0.765
	N5	0.136*	-1.174*	0.018+	-1.275+	0.062	-0.481
	N6	0.370	0.469	0.27	0.411	0.693	-0.006
	N6	0.714	0.403	0.687	0.269	0.515t	0.128t
	P4	-0.018	0.821	0.008	0.205	0.025	-0.060
	P5	0.058	0.788	-0.223	0.061	0.719+	1.636+
	P6	-0.392	0.809	-0.179	-0.198	-	-

Table 2.5. Normality statistics for the John Prince Research Forest sites including Skewness and Kurtosis values. Skewness > 4 + or < -1 was not accepted as normal data. Kurtosis >+1 or <-1 was not accepted as normal data; P3-MRD accepted as normal because very close to cut off value. *MCWT* mean cell wall thickness; *MRD* mean radial diameter; *MD* mean diameter. Grey indicates mature chronologies truncated at 30 years; areas with "-" indicates chronologies that were not used for correlation statistics due to unacceptable EPS values.

	MCWT		MRD		MD	
Site	Skewness	Kurtosis	Skewness	Kurtosis	Skewness	Kurtosis
N1	-	-	0.366	-0.395	-0.264	0.808
N1	-	-	0.471	-0.600	-0.707	0.823
N2	-	-	-	-	-	-
N2	-	-	-	-	-	-
N3	-	-	-0.370	-0.534	-	-
N3	-	-	-0.192	-0.758	-	-
P1	0.587	0.787	-0.188	-0.521	0.234	0.880
P2	0.462	-0.530	-0.191	-0.577	0.391	-0.661
P3	0.699	-0.520	-0.063	-1.006	-0.264	0.808

Table 2.5. ANOVA and t-test statistics for natural (N1, N2, N3) and planted (P1, P2, P3) stands surrounding the John Prince Research Forest. Statistics presented show mean total ring-width (RW), earlywood (EW), latewood (LW), cell wall thickness (CWT), radial diameter (RD), density (D) and standard deviations (SD) per stand. Natural stand data truncated to the last 30 growth are indicated with NXtrunc. Within a column, numbers indicate mean and standard deviation within brackets. Anova test results are presented with letters; similar letters indicate groups that have no significant difference, different letters indicate groups that have a significant difference. Bonferroni(*) post hoc shown for the ANOVA statistical tests; t-test$_{(t)}$.

	RW* (SD)	**RWtrunc* (SD)**	**EW* (SD)**	**Ewtrunc* (SD)**	**LW* (SD)**	**LWtrunc* (SD)**	**MRD (SD)$_{(t)}$**
N1	0.9908 **a** (0.11970)	0.9824 **a** (0.11168)	0.9886 **a** (0.13022)	0.9860 **a** (0.11744)	0.9791 **a** (0.11690)	0.9758 **a** (0.09022)	0.9830 **a** (0.01913)
N2	0.9825 **a** (0.13152	0.9785 **a** (0.15458)	0.9941 **a** (0.14717)	0.9764 **a** (0.16288)	0.9845 **a** (0.12805)	0.9701 **a** (0.12714)	-
N3	0.9988 **a** (0.12412)	0.9814 **a** (0.12752)	0.9935 **a** (0.12162)	0.9819 **a** (0.13281)	0.9888 **a** (0.15280)	0.9776 **a** (0.12758)	0.9988 **a** (0.03900)

	RW* (SD)	**EW* (SD)**	**LW (SD)$_{(t)}$**	**MCWT* (SD)**	**MRD* (SD)**	**MD (SD)***
P1	0.9840 **a** (0.13211)	0.9987 **a** (0.13020)	0.9841 **a** (0.17635)	1.0123 **a** (0.02620)	1.0079 **a** (0.05829)	1.0032 **a** (0.03237)
P2	0.9979 **a** (0.16320)	0.9946 **a** (0.16608)	0.9857 **a** (0.17829)	1.0065 **a** (0.03662)	1.0106 **a** (0.03578)	1.0024 **a** (0.04327)
P3	1.0499 **a** (0.01430)	0.9994 **a** (0.10880)	-	0.9682 **a** (0.11555)	0.9995 **a** (0.04775)	1.0028 **a** (0.03956)

Table 2.6. ANOVA and t-test statistics for natural (N4, N5, N6) and planted (P4, P5, P6) stands surrounding Prince George. Statistics presented show mean total ring-width (RW), earlywood (EW), latewood (LW), cell wall thickness (CWT), radial diameter (RD), density (D) and standard deviations (SD) per stand. Natural stand data truncated to the last 30 growth are indicated with NXtrunc. Within a column, numbers indicate mean and standard deviation within brackets. Anova test results are presented with letters; similar letters indicate groups that have no significant difference, different letters indicate groups that have a significant difference. Bonferroni* post hoc shown for the ANOVA statistical tests; t-test have no "*".

	RW (SD)*	**Rwtrunc (SD)***	**EW* (SD)**	**Ewtrunc(t) (SD)**	**LW(t) (SD)**	**Lwtrunc (SD)**
N4	0.9697 **a** (0.26135)	0.9973 **a** (0.11381)	0.9886 **a** (0.12474)	0.9948 **a** (0.11755)	-	-
N5	0.9858 **a** (0.16724)	1.0090 **a** (0.16176)	0.9929 **a** (0.17653)	-	0.9831 **a** (0.16948)	0.9840 **a** (0.13172)
N6	0.9667 **a** (0.17698)	0.9389 **a** (0.21538)	0.9601 **a** (0.19342)	0.9303 **a** (0.23723)	0.9792 **a** (0.18930)	0.9792 **a** (0.18930)

	RW* (SD)	**EW* (SD)**	**LW**
P4	0.9875 **a** (0.12352)	1.0004 **a** (0.12965)	-
P5	0.9697 **a** 0.26135	0.9904 **a** (0.19133)	-
P6	0.9895 **a** (0.12147)	0.9904 **a** (0.19133)	-

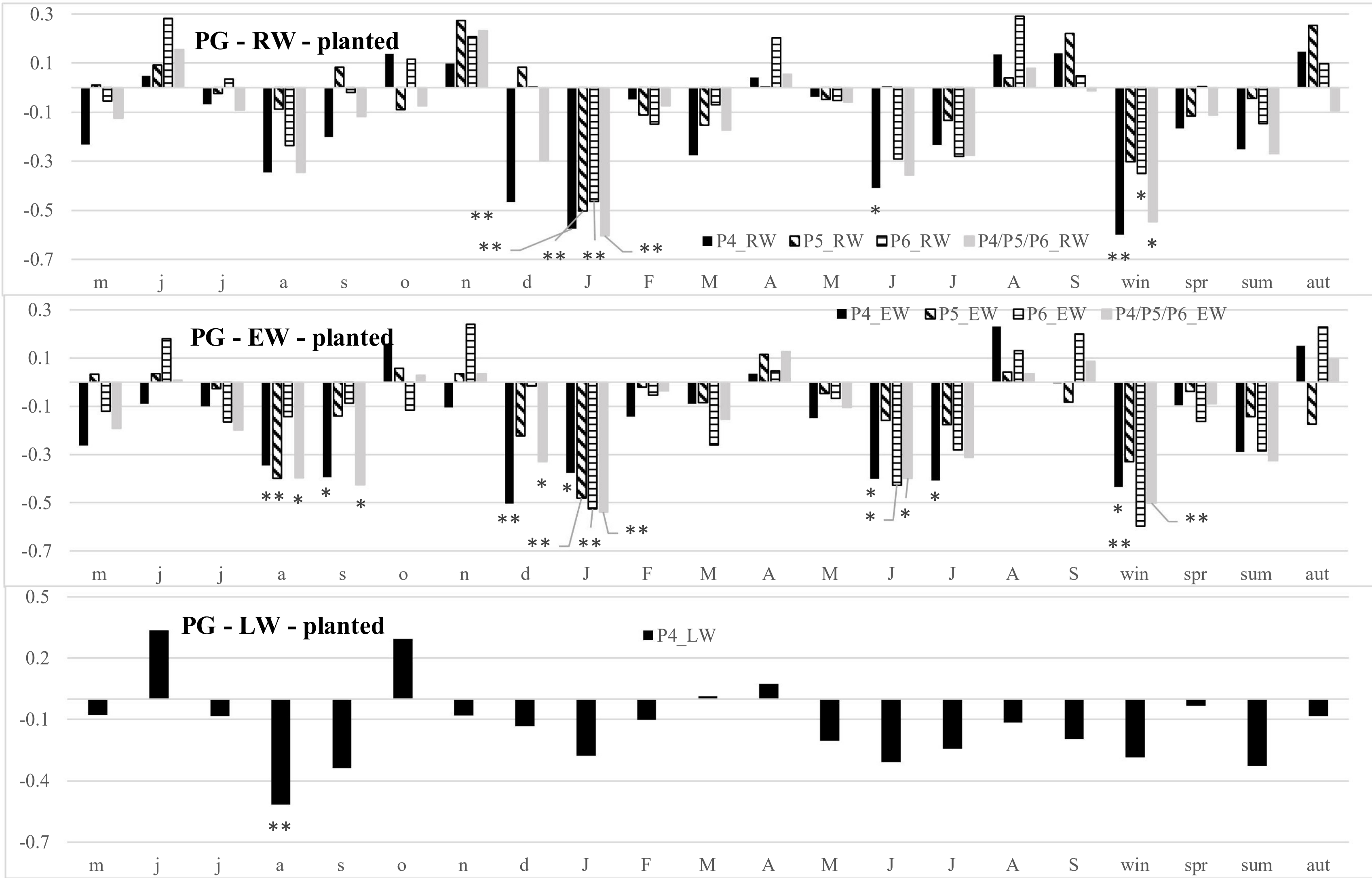

Figure 7.6 Pearson's correlation coefficients for average monthly temperature (°C) and ring-width RW, earlywood EW and latewood LW from planted (P4, P5, P6) stands surrounding Prince George. Significant correlations are represented as ** p = 0.01; * = 0.05 level. Months are represented by lower and upper case letters, respectively; win = winter, spr = spring, sum= summer, aut = autumn.

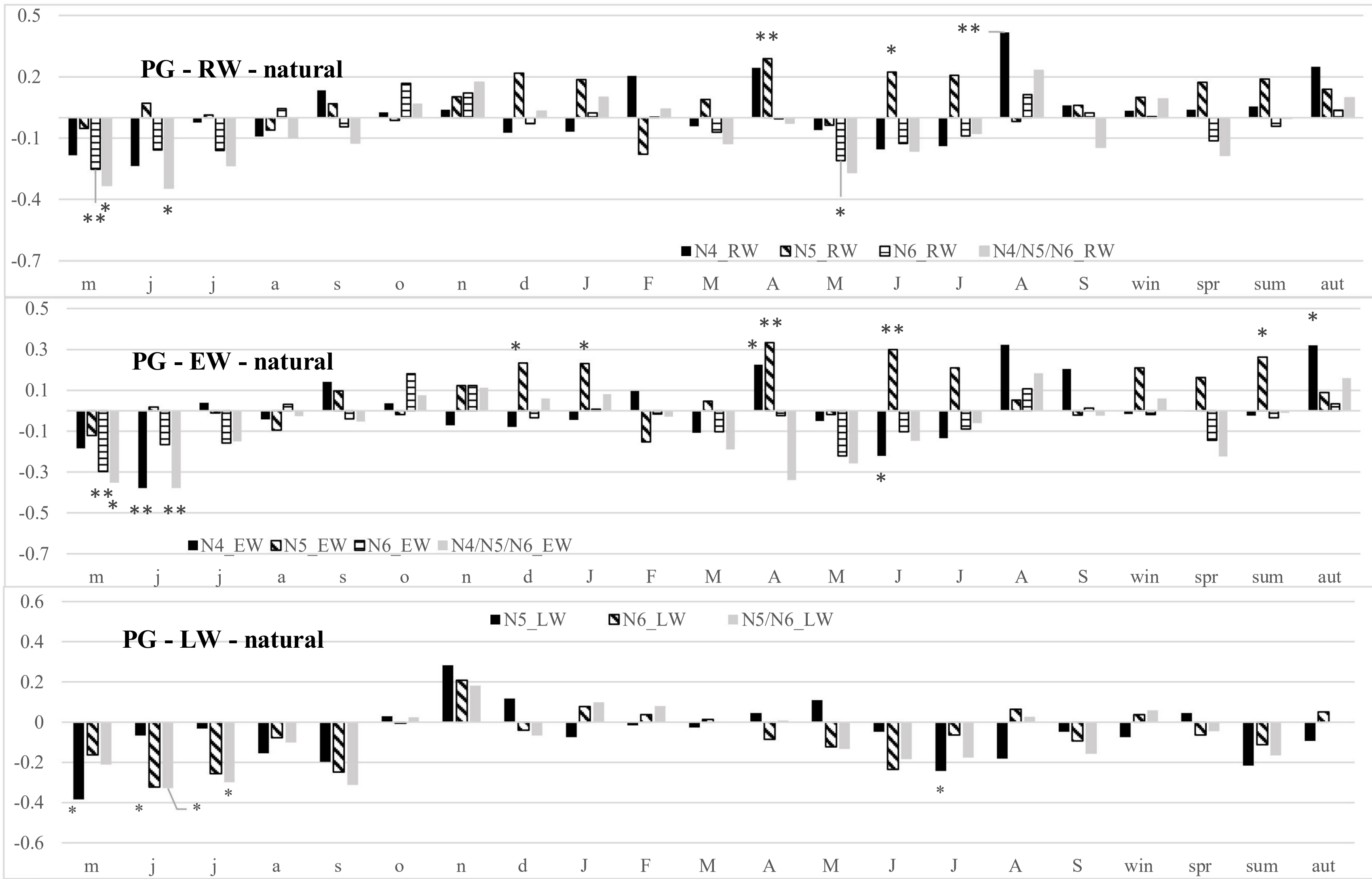

Figure 8.7. Pearson's correlation coefficients for average monthly temperature (°C) and ring-width *RW*, earlywood *EW* and latewood *LW* from natural (N4, N5, N6) stands surrounding Prince George. Significant correlations are represented as_** p = 0.01; * = 0.05 level. Months are represented by lower and upper case letters, respectively; win = winter, spr = spring, sum= summer, aut = autumn.

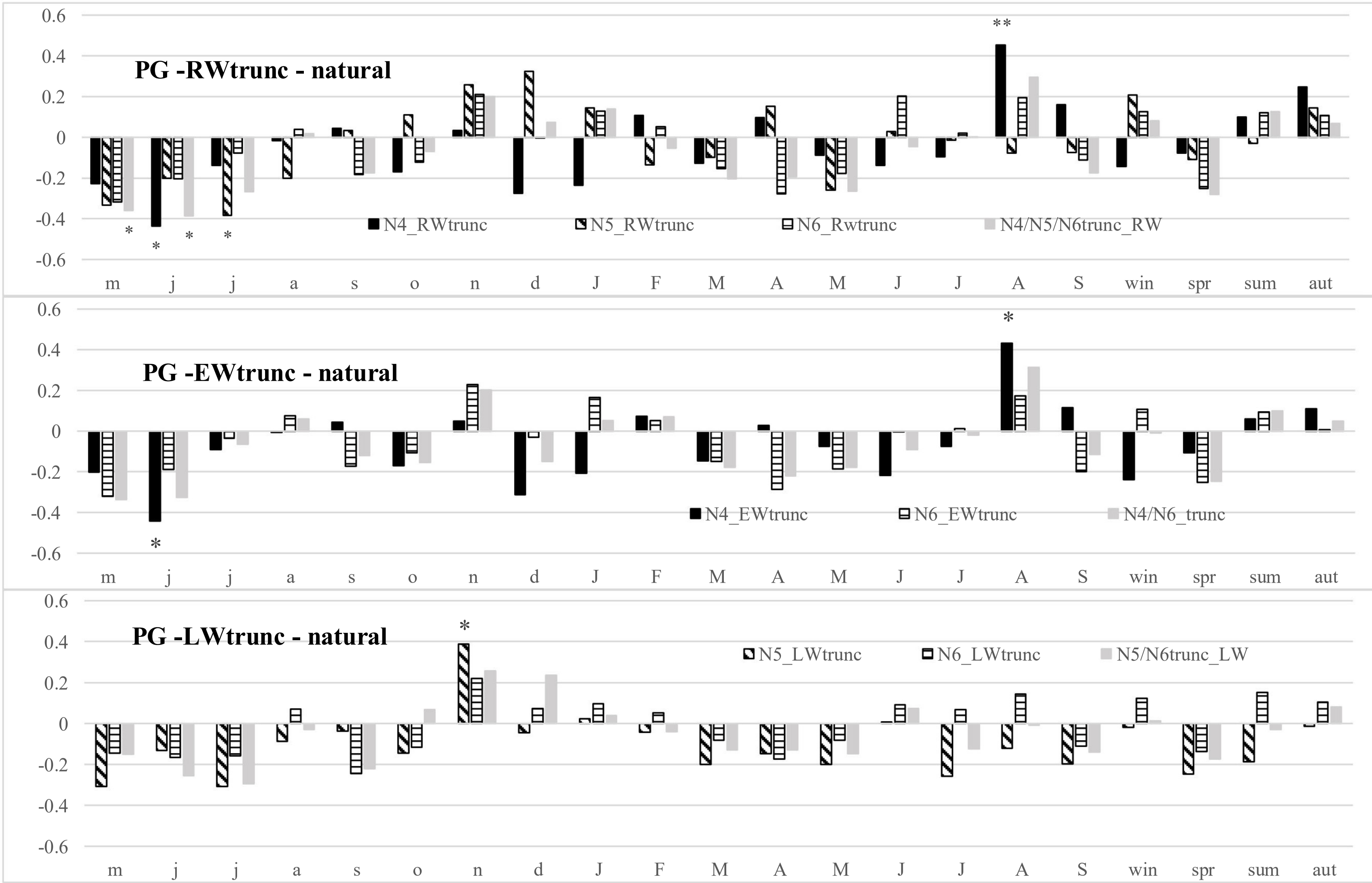

Figure 9.8. Pearson's correlation coefficient for average monthly temperature (°C) and ring-width *RW*, earlywood *EW* and latewood *LW* from natural (N4, N5, N6) truncated to the last 30-years of growth, NXtrunc, surrounding Prince George. Significant correlations are represented as ** p = 0.01; * = 0.05 level. Months are represented by lower and upper case letters, respectively; win = winter, spr = spring, sum= summer, aut = autumn.

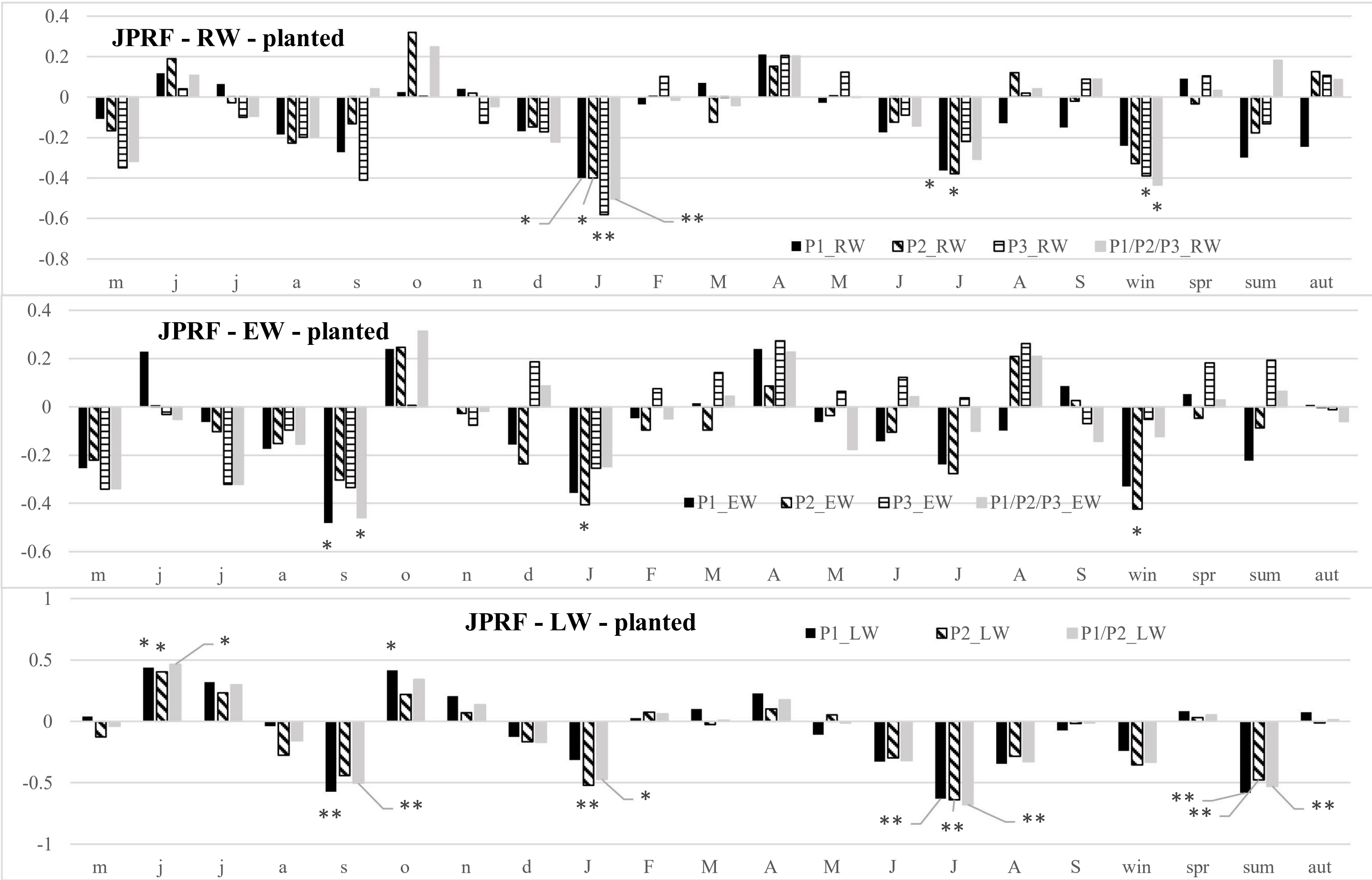

Figure 10.9. Pearson's correlation coefficient for average monthly temperature (°C) and ring-width *RW*, earlywood *EW* and latewood *LW* from planted (P1, P2, P3) stands surrounding the John Prince Research Forest. Significant correlations are represented with ** p = 0.01; * = 0.05 level. Months are represented by lower and upper case letters, respectively; win = winter, spr = spring, sum= summer, aut = autumn.

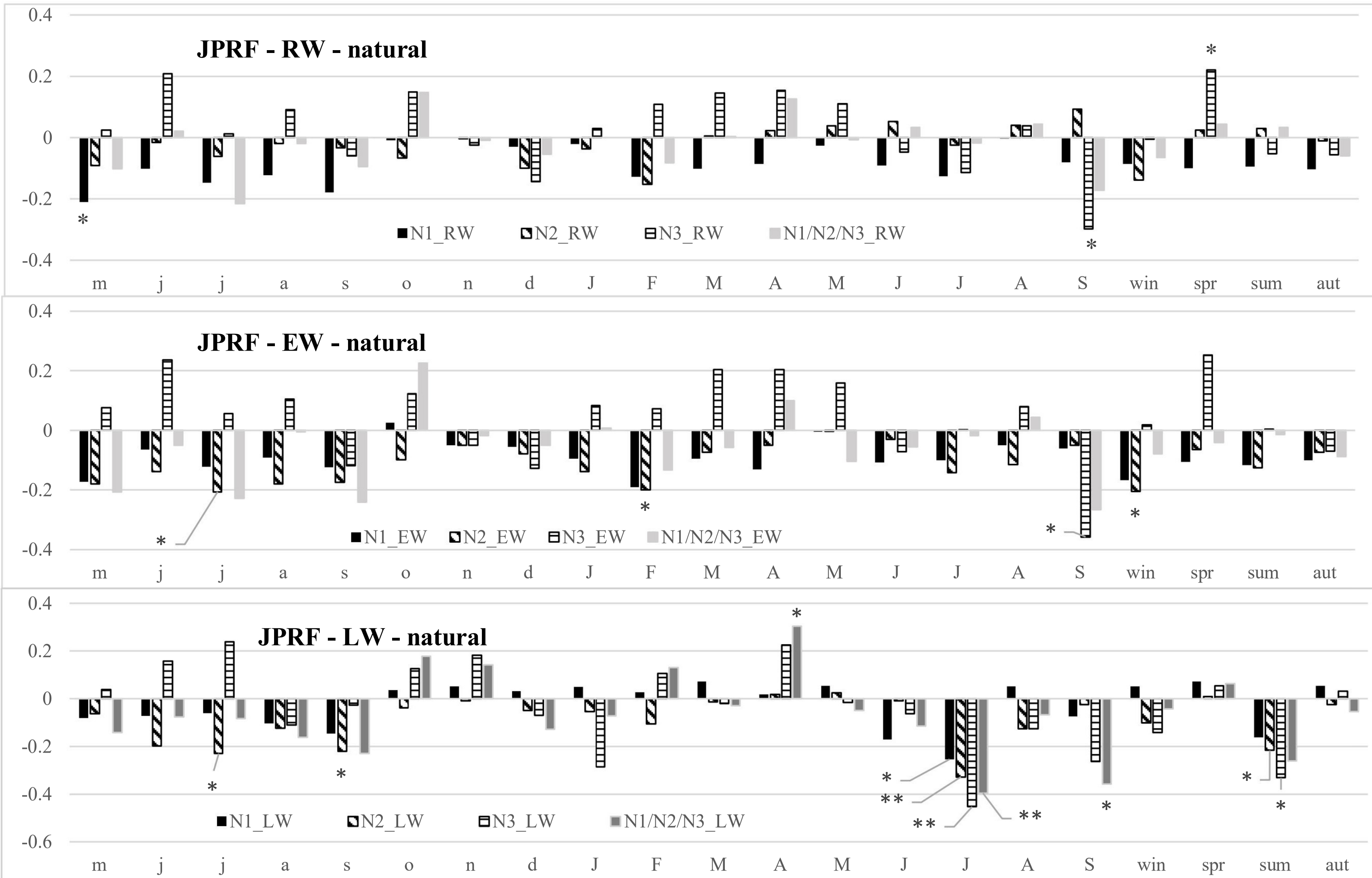

Figure 11.10. Pearson's correlation coefficient for average monthly temperature (°C) and ring-width *RW*, earlywood *EW* and latewood *LW* from natural (N1, N2, N3) stands surrounding the John Prince Research Forest (JPRF). Significant correlations are represented with ** p = 0.01; * = 0.05 level. Months are represented by lower and upper case letters, respectively; win = winter, spr = spring, sum= summer, aut = autumn.

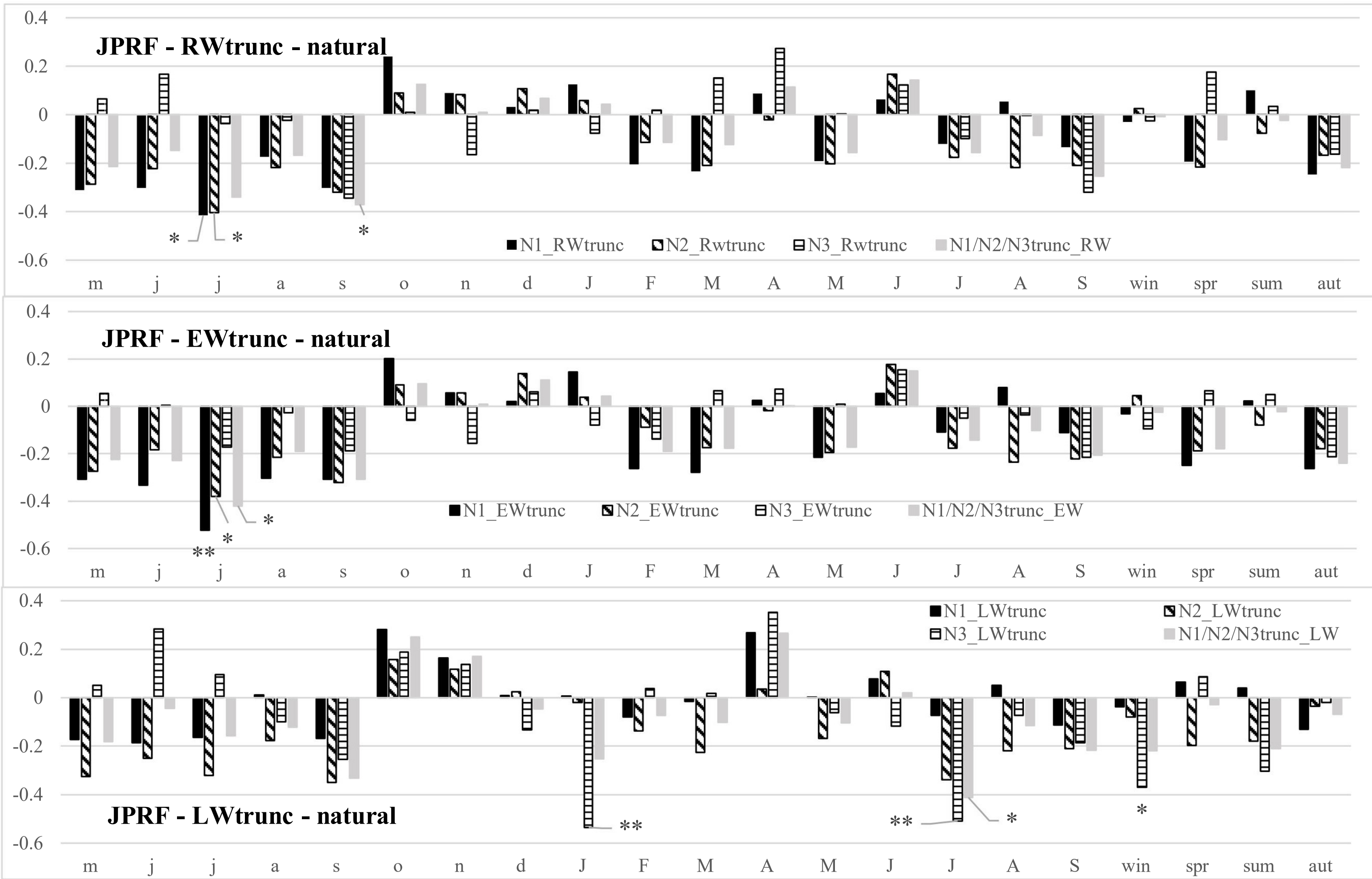

Figure 1213.11. Pearson's correlation coefficient for average monthly temperature (°C) and ring-width *RW*, earlywood *EW* and latewood *LW* from natural (N1, N2, N3) stands truncated to the last 30 years of growth (NXtrunc) surrounding the John Prince Research Forest (JPRF). Significant correlations are represented with ** p = 0.01; * = 0.05 level. Months are represented by lower and upper case letters, respectively; win = winter, spr = spring, sum= summer, aut = autumn.

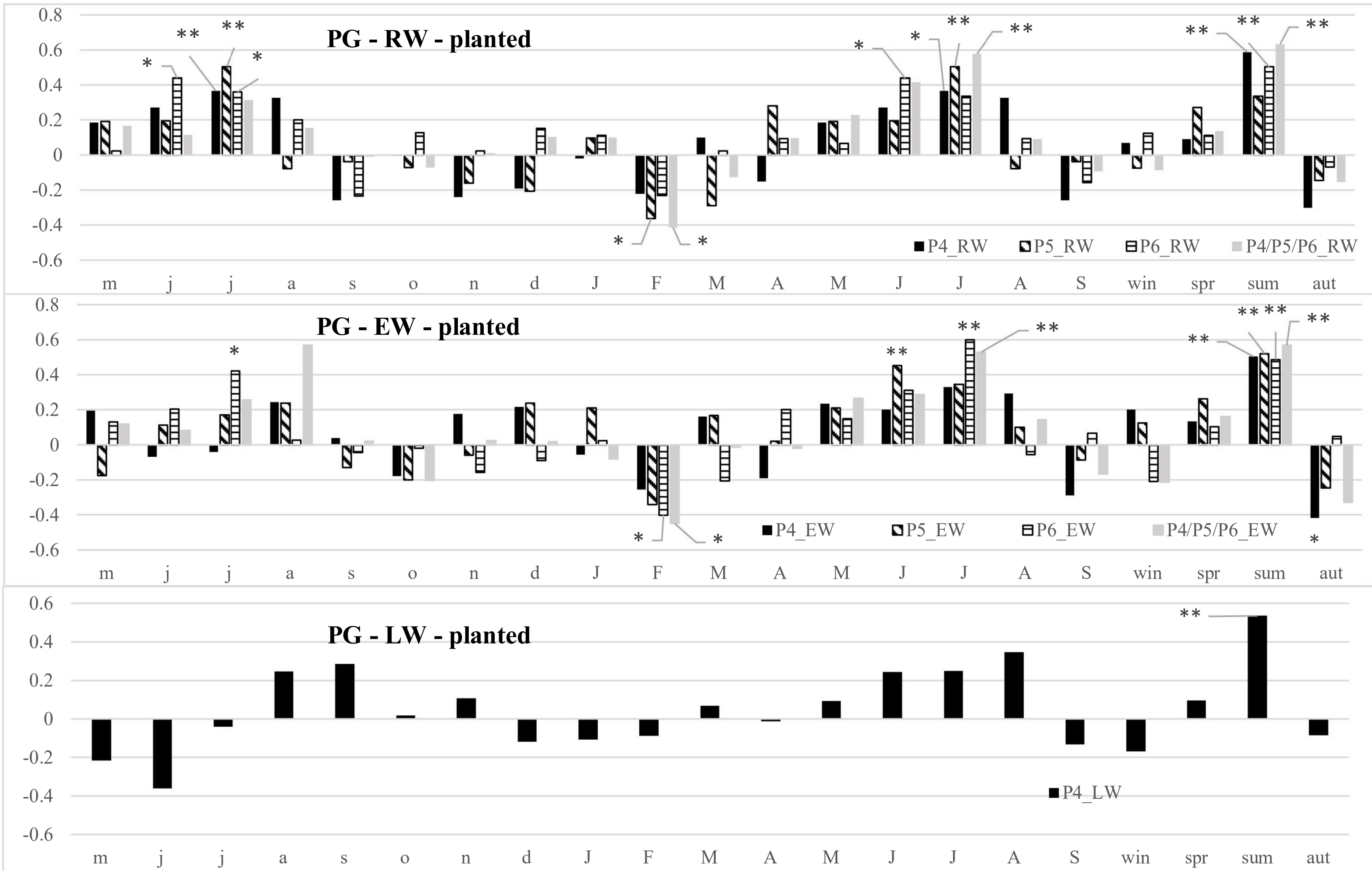

Figure 14.12 Pearson’s correlation coefficient for total monthly precipitation (mm) and ring-width *RW*, earlywood *EW* and latewood *LW* from planted (P1, P2, P3) stands surrounding Prince George. Significant correlations are represented with ** p = 0.01; * = 0.05 level. Months are represented by lower and upper case letters, respectively; win = winter, spr = spring, sum= summer, aut = autumn.

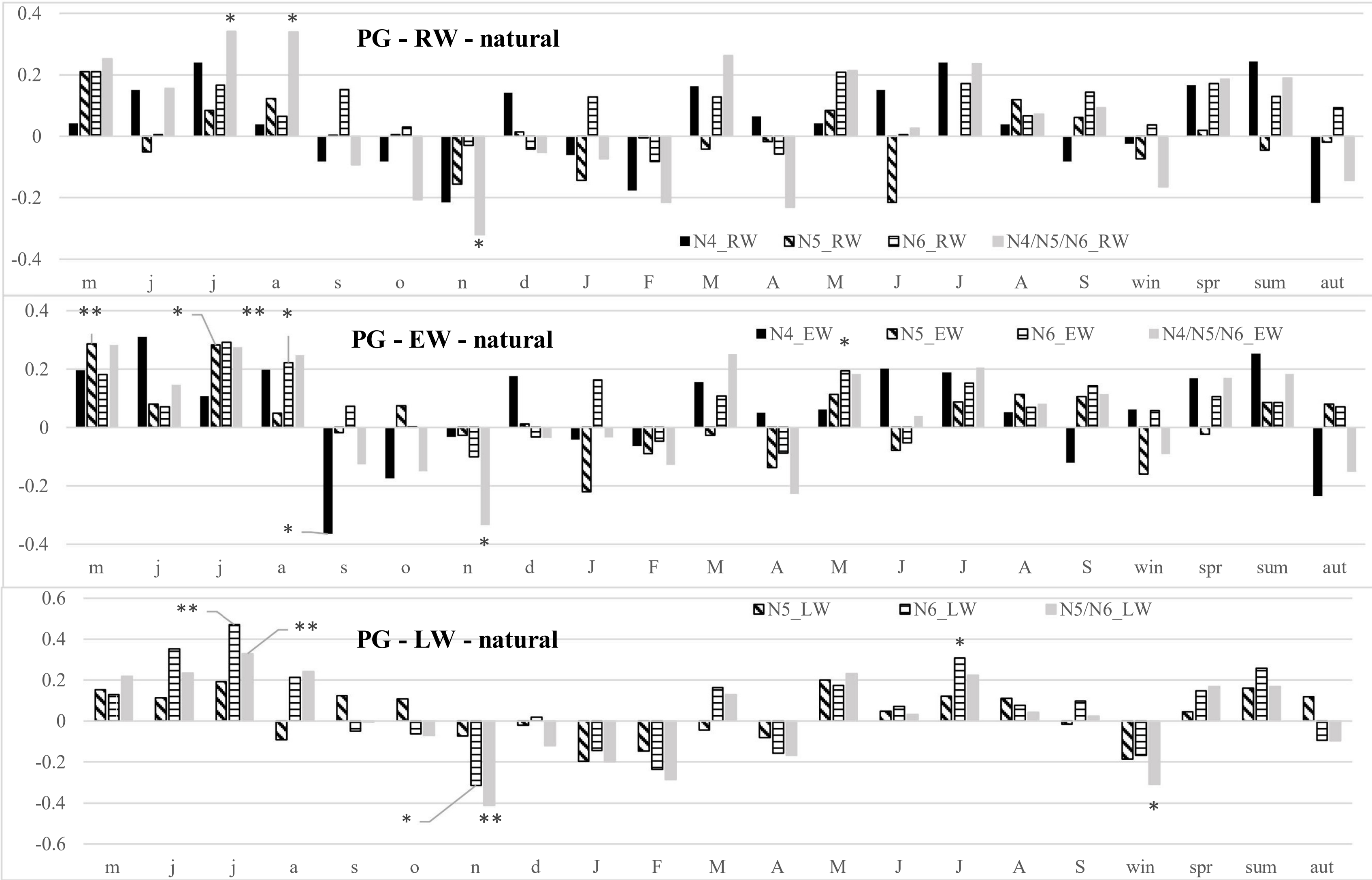

Figure 15.13. Pearson's correlation coefficient for total monthly precipitation (mm) and ring-width *RW*, earlywood *EW* and latewood *LW* from natural (N4, N5, N6) stands surrounding Prince George. Significant correlations are represented with ** p = 0.01; * = 0.05 level. Months are represented by lower and upper case letters, respectively; win = winter, spr = spring, sum= summer, aut = autumn.

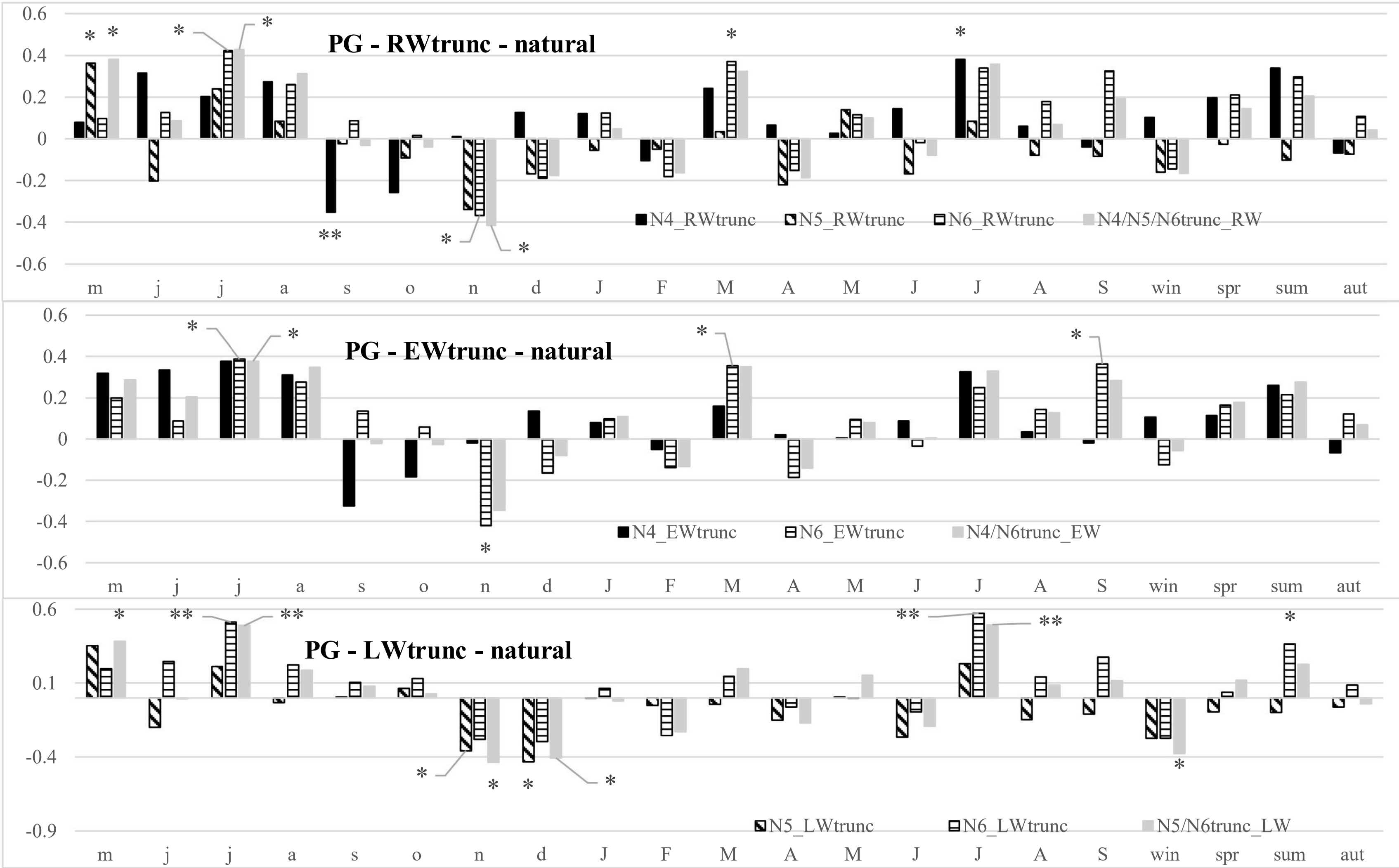

Figure 16.14. Pearson's correlation coefficient for total monthly precipitation (mm) and ring-width *RW*, earlywood *EW* and latewood *LW* from natural (N4, N5, N6) stands truncated to the last 30-years of growth, NXtrunc, surrounding Prince George. Significant correlations are represented with ** p = 0.01; * = 0.05 level. Months are represented by lower and upper case letters, respectively; win = winter, spr = spring, sum= summer, aut = autumn.

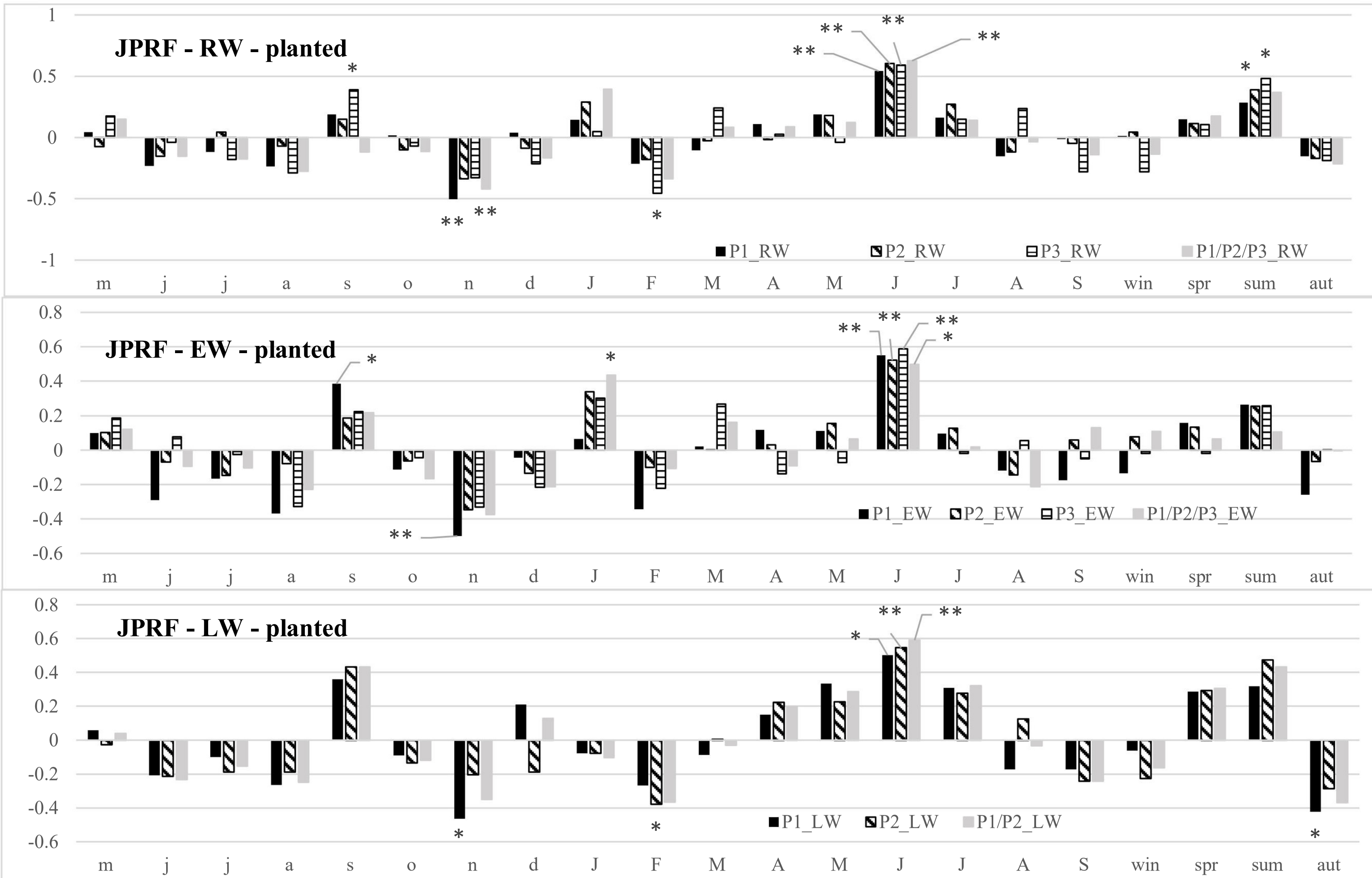

Figure 17.15. Pearson's correlation coefficient for total monthly precipitation (mm) and ring-width *RW*, earlywood *EW* and latewood *LW* from planted (P1, P2, P3) stands surrounding the John Prince Research Forest. Significant correlations are represented with ** p = 0.01; * = 0.05 level. Months are represented by lower and upper case letters, respectively; win = winter, spr = spring, sum= summer, aut = autumn.

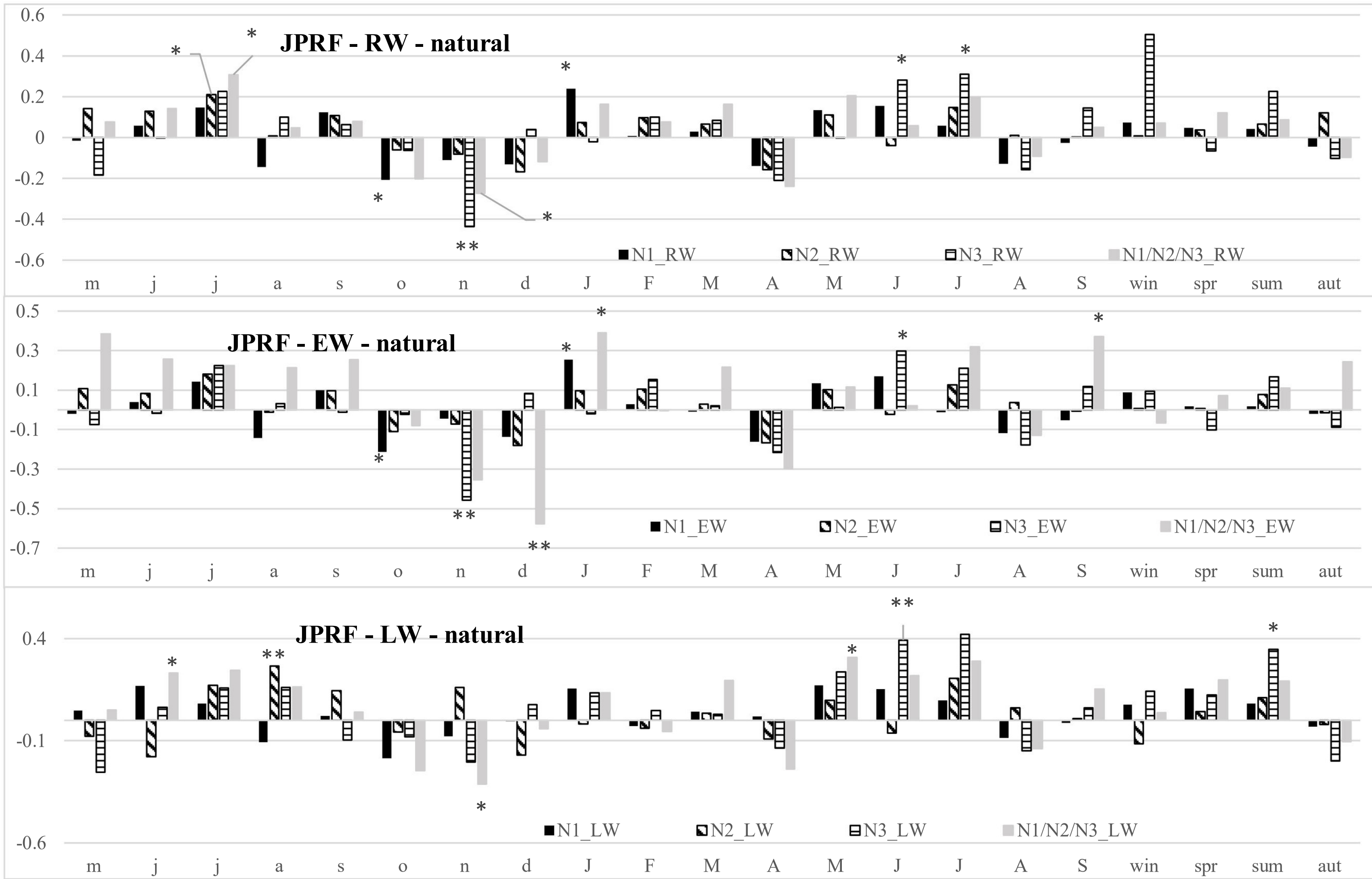

Figure 18.16. Pearson's correlation coefficient for total monthly precipitation (mm) and ring-width *RW*, earlywood *EW* and latewood *LW* from planted (N1, N2, N3) stands surrounding the John Prince Research Forest (JPRF). Significant correlations are represented with ** p = 0.01; * = 0.05 level. Months are represented by lower and upper case letters, respectively; win = winter, spr = spring, sum= summer, aut = autumn.

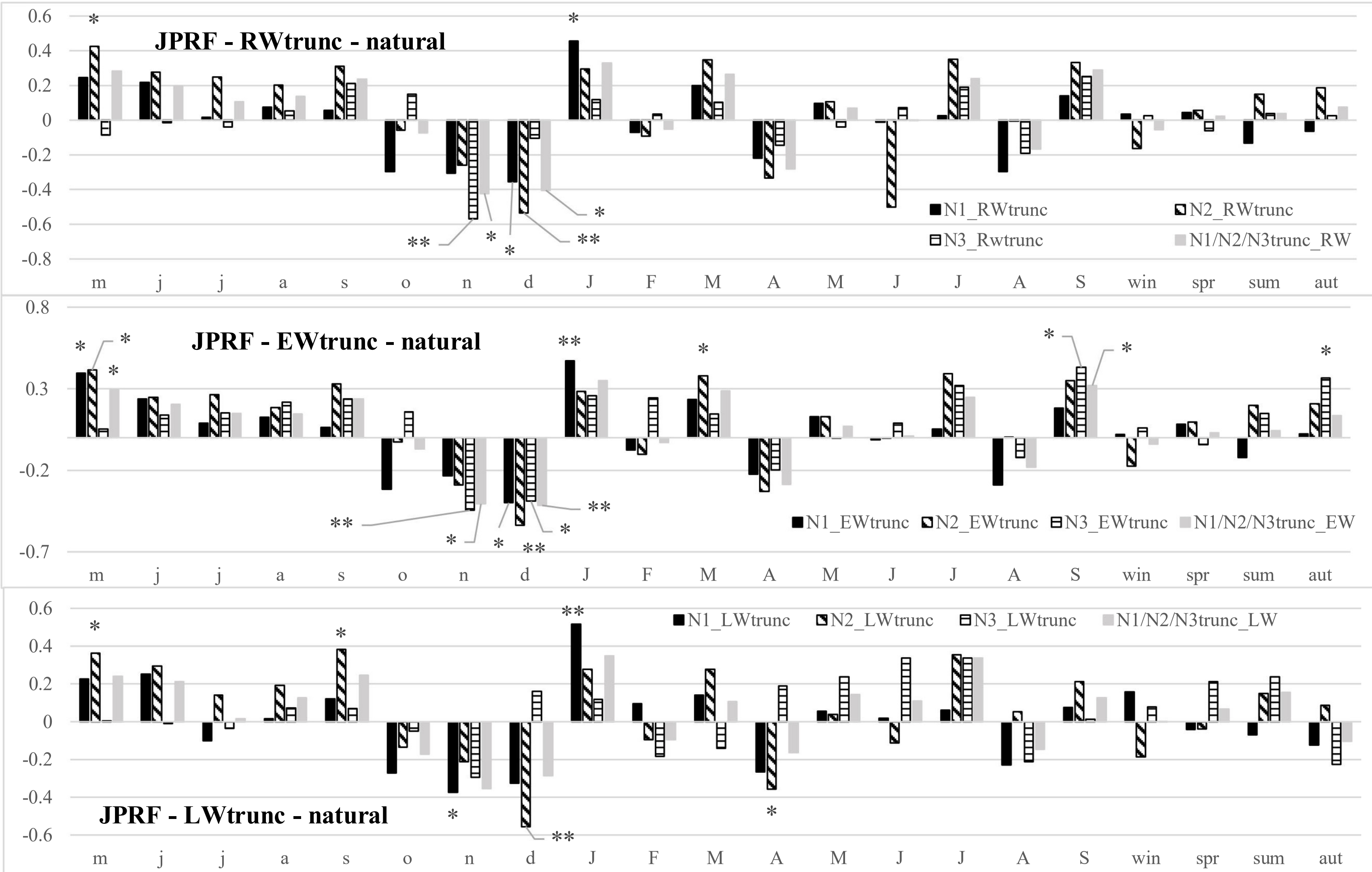

Figure 19.17 Pearson's correlation coefficient for total monthly precipitation (mm) and ring-width *RW*, earlywood *EW* and latewood *LW* from planted (N1, N2, N3) stands truncated to the last 30 years of growth (NXtrunc) surrounding the John Prince Research Forest. Significant correlations are represented with ** p = 0.01; * = 0.05 level. Months are represented by lower and upper case letters, respectively; win = winter, spr = spring, sum= summer, aut = autumn.

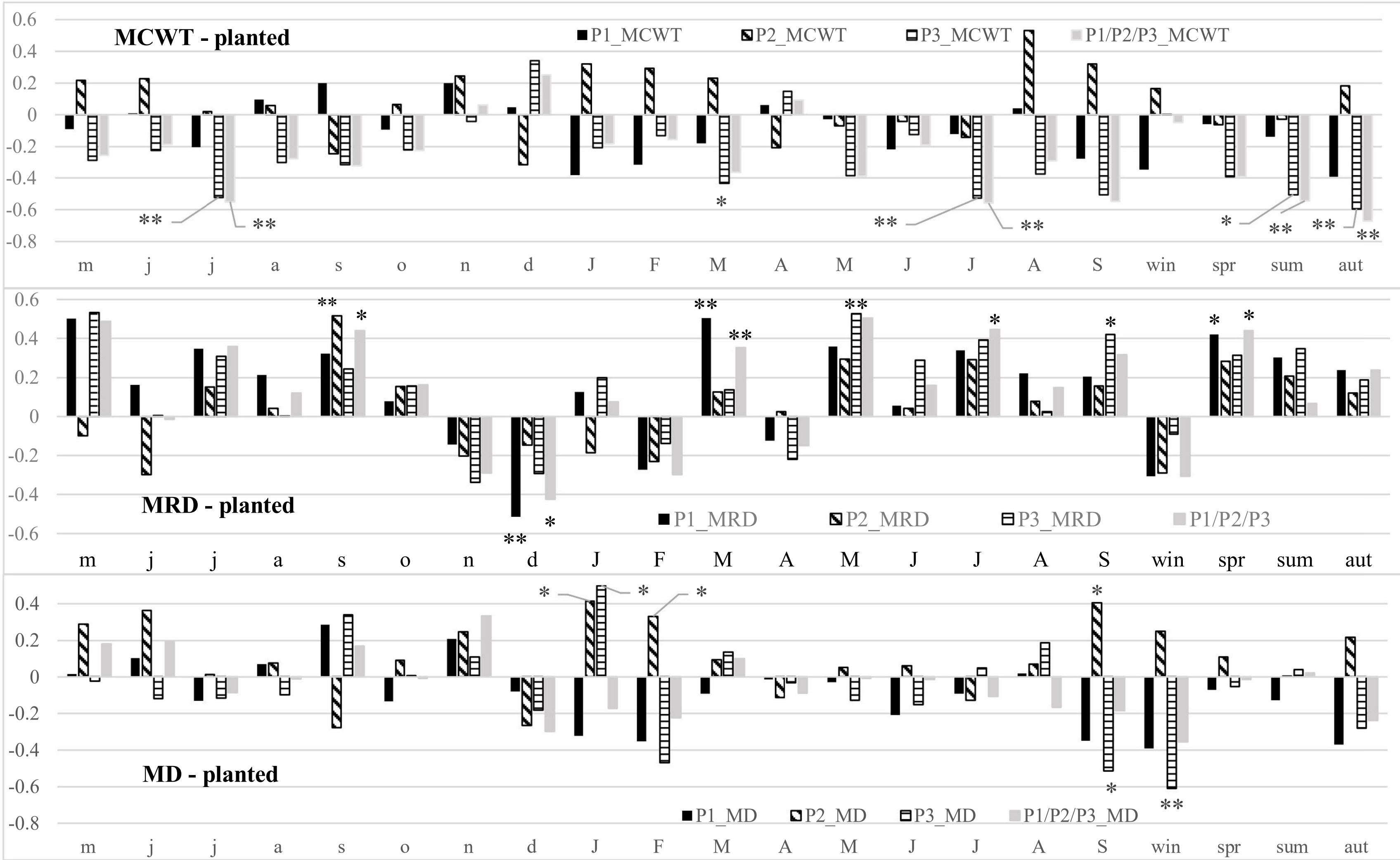

Figure 20.18. Pearson's correlation coefficient for total monthly precipitation from planted (P1, P2, P3) stands surrounding the John Prince Research Forest for mean cell wall thickness *MCWT*, mean radial diameter *MRD* and mean density *MD*. Significant correlations are depicted by ** p = 0.01 and * = 0.05. Months are represented by lower and upper case letters, respectively; win = winter, spr = spring, sum= summer, aut = autumn.

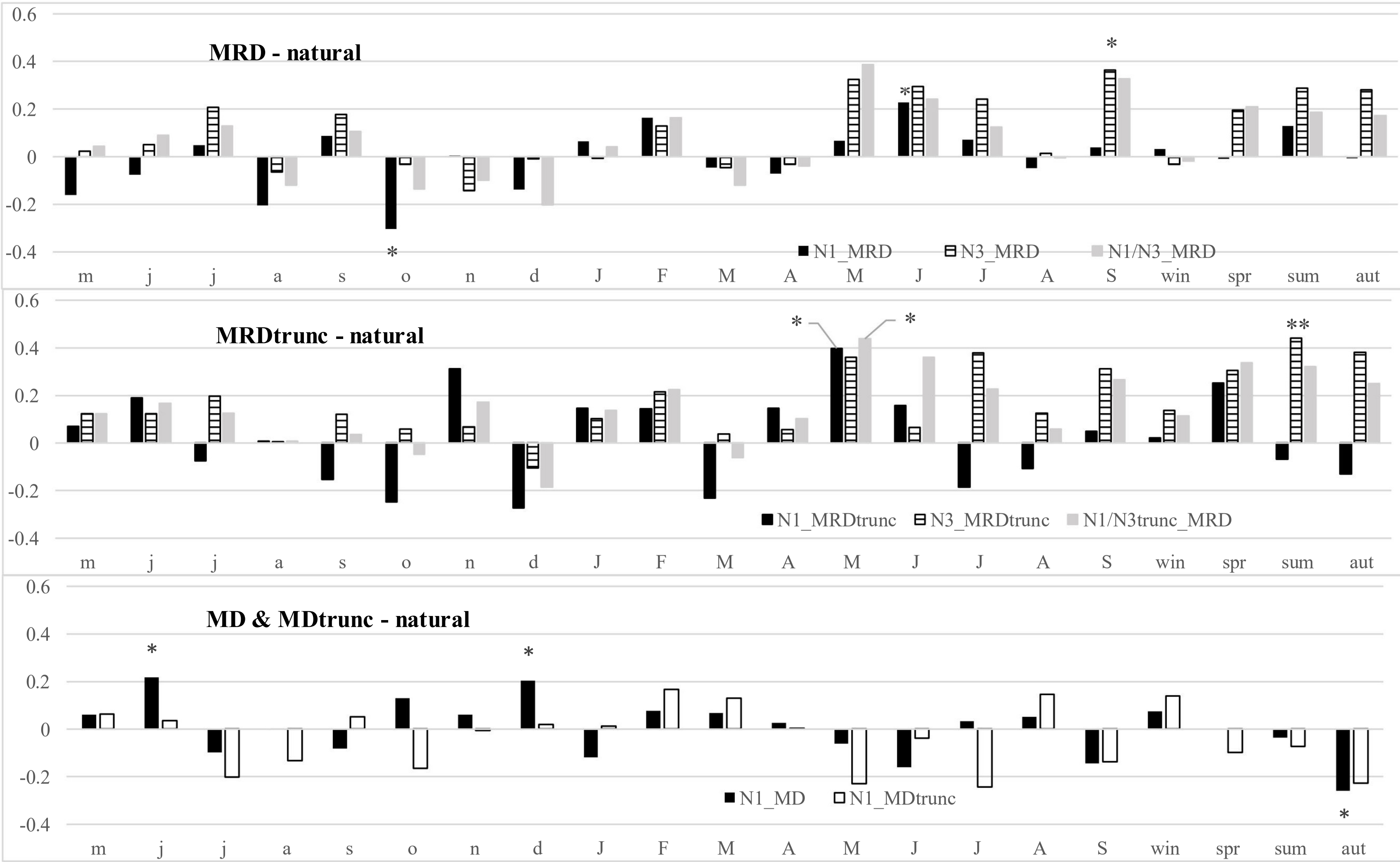

Figure 21.19. Pearson's correlation coefficient for total monthly precipitation from natural (N1, N3) stands surrounding the John Prince Research Forest for mean radial diameter *MRD* and mean density *MD*. Significant correlations are depicted by ** p = 0.01 and * = 0.05. NXtrunc indicates mature chronologies truncated at 30 years. Months are represented by lower and upper case letters, respectively; win = winter, spr = spring, sum= summer, aut = autumn.

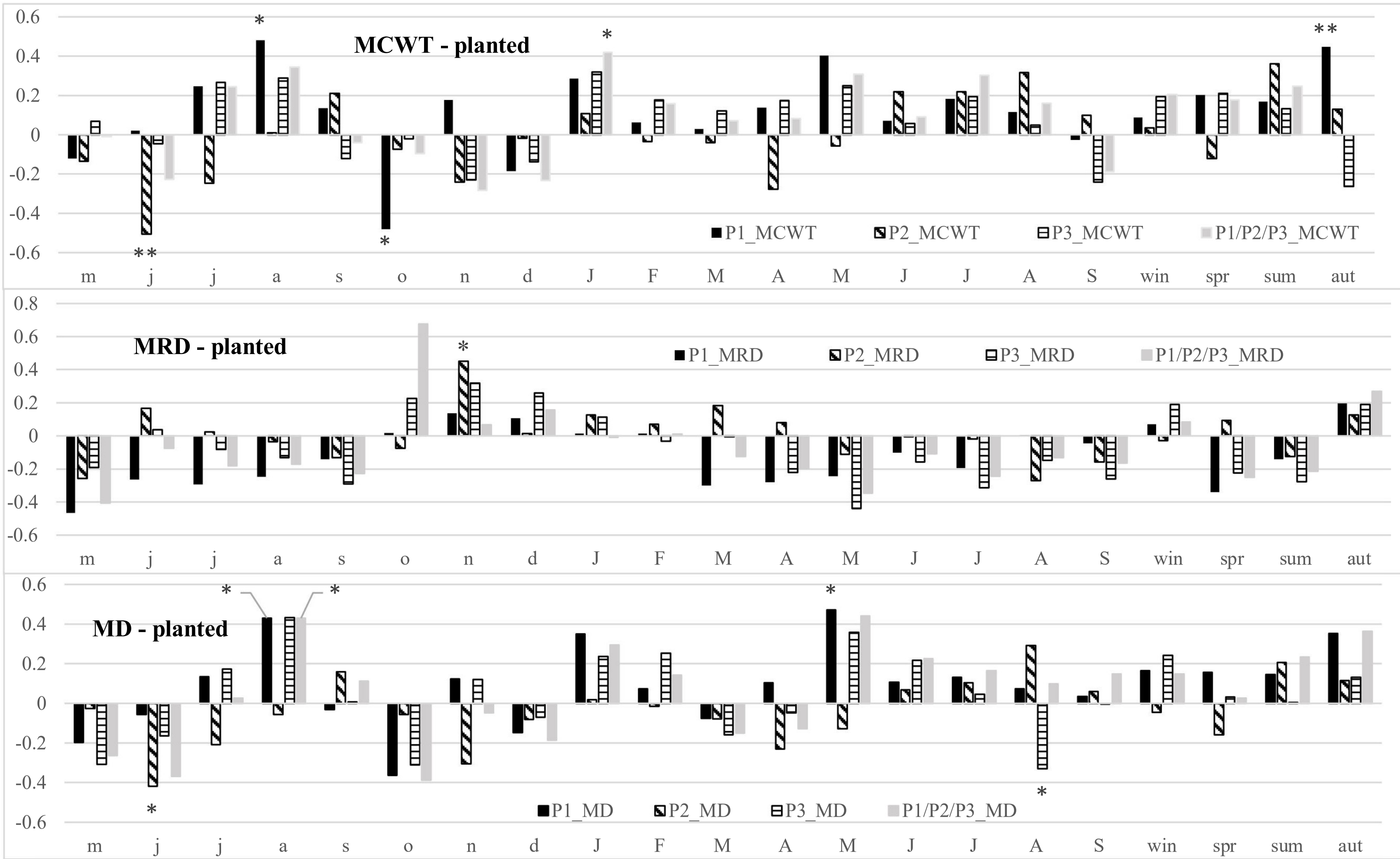

Figure 22.20. Pearson's correlation coefficient for mean monthly temperature and planted (P1, P2, P3) stands surrounding the John Prince Research Forest from mean cell wall thickness *MCWT*, mean radial diameter *MRD* and mean density *MD*. Significant correlations are depicted by ** p = 0.01 and * = 0.05. Months are represented by lower and upper case letters, respectively; win = winter, spr = spring, sum= summer, aut = autumn.

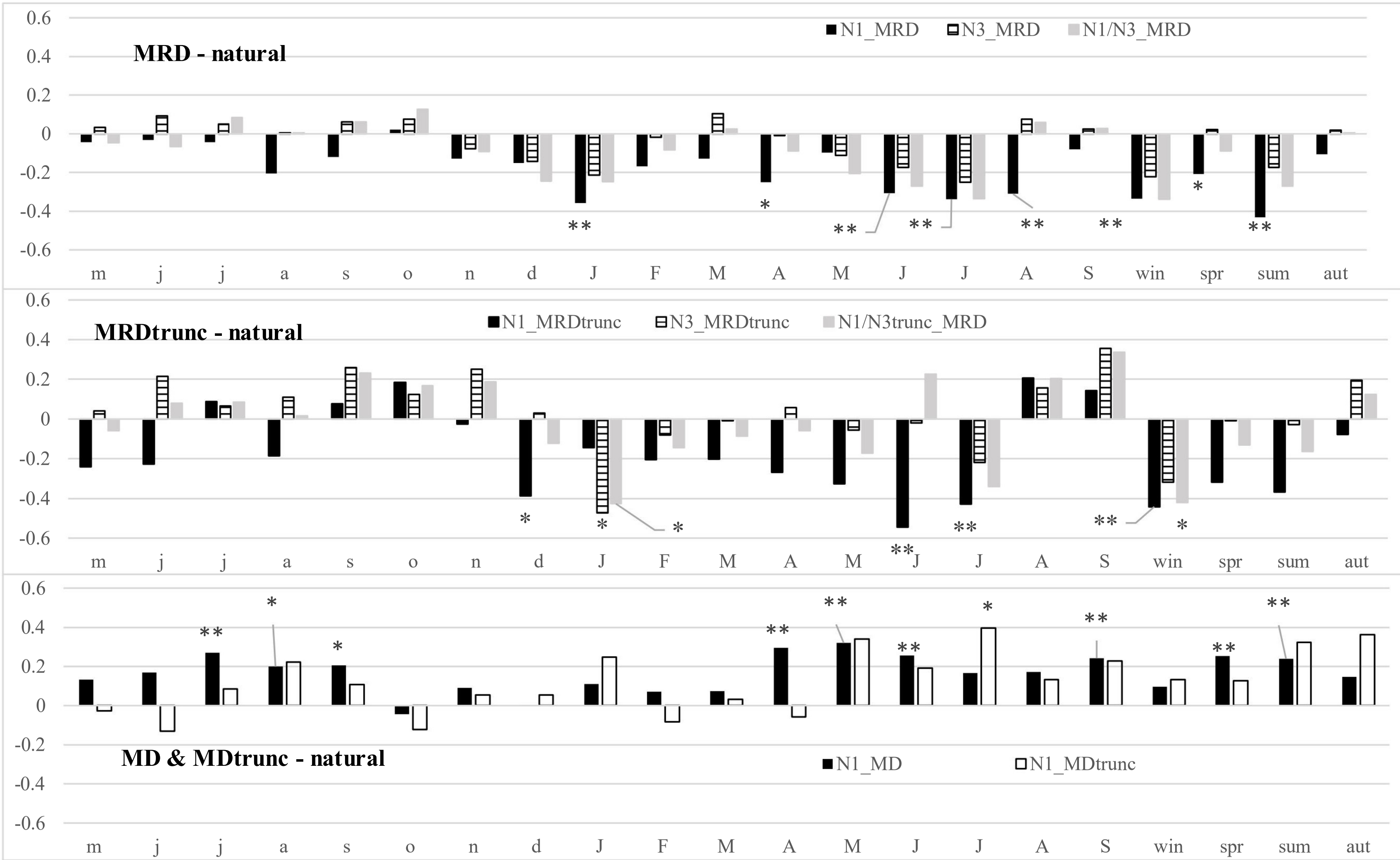

Figure 23.21. Pearson's correlation coefficient for mean monthly temperature for natural (N1, N3) stands surrounding the John Prince Research Forest from mean radial diameter *MRD* and mean density *MD*. Significant correlations are depicted by ** p = 0.01 and * = 0.05. NXtrunc indicates mature chronologies truncated at 30 years. Months are represented by lower and upper case letters, respectively; win = winter, spr = spring, sum= summer, aut = autumn.

Table 2.7. Regression analysis between average monthly temperature (°C) (T), total monthly precipitation (mm) (P) and ring-width (RW), earlywood (EW) and latewood (LW) chronologies for natural (N4, N5, N6) and planted (P4, P5, P6) stands surrounding Prince George. R_2 values only accepted if > 0.25. ** p = 0.01; * = 0.05 level. Grey shading indicates natural stand chronologies; NXtrunc indicates natural stand chronologies truncated at the last 30 years of growth. Months are represented by lower and upper case letters. Pearson correlation statistic and p-value results between measured (M) and modelled (MX) RW, EW and LW also presented for every model.

P	Site	RW (R_2)	EW (R_2)	LW (R_2)	MvsMX (Pearson's R)	p-value
jul	N6trunc			0.263**	0.513	0.003
	P5	0.267**			0.517	0.003
JUL	N6trunc			0.327**	0.572	0.001
	N5/N6trunc			0.246**	0.496	0.005
	P5	0.256**			0.506	0.002
	P6		0.338*		0.6	<0.0001
	P4/P5/P6	0.335**	0.280**		0.578; 0.529	0.001; 0.003
SUM	P4	0.346**	0.254**	0.286**	0.588; 0.504; 0.535	0.001; 0.005; 0.003
	P5		0.271**		0.521	0.002
	P6	0.253**			0.503	0.003
	P4/P5/P6	0.402**	0.323**		0.634; 0.569	<0.0001; 0.001

T	Site	RW (R_2)	EW (R_2)	LW (R_2)	MvsMX (Pearson's R)	p-value
JAN	P4	0.332**	0.276**		0.576; 0.526	0.001; 0.003
	P5	0.254**			0.504	0.002
	P4/P5/P6	0.365**	0.290**		0.604; 0.539	<0.0001; 0.003
aug	P4			0.266**	0.516	0.005
WIN	P4	0.360**	0.365**		0.6; 0.596	<0.0001; 0.001
	P4/P5/P6	0.298**	0.251**		0.546; 0.501	0.001; 0.006

Table 2.8. Regression results from regression analysis between average monthly temperature (°C) (T), total monthly precipitation (mm) (P) and ring-width (RW), earlywood (EW) and latewood (LW) chronologies for natural (N1, N2, N3) and planted (P1, P2, P3) stands surrounding the John Prince Research Forest. R_2 values only accepted if > 0.25.** p = 0.01; * = 0.05 level. Grey shading indicates natural stand; NXtrunc indicates natural stand chronologies truncated at the last 30 years of growth. Months are represented by lower and upper case letters, respectively. Pearson correlation statistic and p-value results between measured (MX) and modelled (M) RW, EW and LW also presented for every model.

P	Site	RW (R_2)	EW (R_2)	LW (R_2)	MvsMX (Pearson's R)	p-value
JAN	N1trunc			0.267**	0.516	0.003
JUN	P1	0.294**	0.302**	0.253**	0.542; 0.550; 0.503	0.002; 0.003; 0.010
	P2	0.363**	0.273**	0.298**	0.603; 0.522; 0.546	<0.0001; 0.003; 0.002
	P3	0.353**	0.345**		0.593; 0.588	0.001; 0.003
	P1/P2/P3	0.392**			0.626	<0.0001
nov	N3		0.201**		0.458	0.001
	N3trunc	0.342**			0.569	0.001
	P1	0.255*			0.504	0.004
dec	N2trunc	0.286**	0.287**	0.310**	0.535; 0.536; 0.556	0.002; 0.002; 0.001
	N1/N2/N3trunc		0.332**		0.577	0.001

T	Site	RW (R_2)	EW (R_2)	LW (R_2)	MvsMX (Pearson's R)	p-value
JAN	N3trunc			0.286**	0.535	0.002
	P3	0.337**			0.581	0.001
	P1/P2/P3	0.254**			0.504	0.007
JUL	N3			0.277**	0.527	<0.0001
	N3trunc			0.258**	0.508	0.004
	P1			0.395**	0.628	<0.0001
	P1/P2			0.459**	0.678	<0.0001
sep	P1			0.330**	0.575	0.003
	P1/P2			0.341**	0.584	0.002
SUM	P1			0.340**	0.538	0.002
	P1/P2			0.358**	0.598	0.002

Table 2.9. Regression results from regression analysis between total monthly precipitation (mm) (P) and average monthly temperature (°C) (T) for mean cell wall thickness (MCWT), mean radial diameter (MRD) and mean density (MD) natural (Nx) and planted (Px) stand chronologies near the John Prince Research Forest. R_2 values only accepted if > 0.2. ** p = 0.01; * = 0.05 level. Grey shading indicated natural stand chronologies; NXtrunc indicates natural stand chronologies truncated at 30 years. Months are represented by lower and upper case letters, respectively Correlation statistics (Pearson's R & p-value) results between measured (M) and modelled (MX) cell properties are also presented for every model.

P	Site	MCWT (R_2)	MRD (R_2)	MD (R_2)	MvsMX (Pearson's R)	p-value
MAR	P1		0.255**			0.01
jul	P3	0.272**			0.521	0.008
	P1/P2/P3	0.302**			0.549	0.007
JUL	P3	0.280*			0.529	0.007
	P1/P2/P3	0.311**			0.588	0.006
sep	P2		0.267**		0.517	0.005
SEP	P3	0.263*		0.263**	0.512; 0.513	0.009; 0.010
	P1/P2/P3	0.300**			0.548	0.007
dec	P1		0.263**		0.513	0.009
WIN	P3			0.371*	0.609	<0.0001
SUM	P3	0.272*			0.522	0.007
	P1/P2/P3	0.296**			0.544	0.007
T	Site	MCWT (R_2)	MRD (R_2)	MD (R_2)	MvsMX (Pearson's R)	p-value
jun	P2	0.256**			0.506	0.01
JUN	N1trunc		0.297**		0.545	0.003
SUM	N2		0.284**		0.533	<0.0001

2.4.4 Regression Analysis

Although there were numerous significant relationships found between climate and JPRF and PG radial growth properties in regression analysis, the models presented below reflect the strongest relationships found between wood properties and winter, summer, and autumn climates (Tables 2.8-2.10 and Figures 2.22 – 2.26).

Winter Relationships

RW, MD, and MRD chronologies from planted stands in JPRF and PG modelled from current and previous year winter climates compared to observed values (Figure 2.22).

Although the RW models of PG and JPRF planted stands based on January temperatures show reliability, some points are inaccurate in 1998 and between 2001-2003. Decoupling occurs between measured and modelled MD values in 2012 and 2013, and between measured and modelled MRD values from 1991-1997, 2002, and in 2012 modelled from previous December and current average winter precipitation.

Models of both truncated and full-length RW, EW, LW and MRD chronologies from natural stands in JPRF based on winter climates corresponded well with measured data; truncated natural stand data demonstrated better reliability than full-length chronologies (Table 2.9 and Figure 2.23). PG natural stands had no strong predictors of measured values based on winter climates (Table 2.8). Measured and modelled values of N1/N2/N3trunc EW from previous December precipitation decouple in 1987 and between 2008-2010. Modelled values of the N1trunc based on current January precipitation do not follow measured values in 2007 (Figure 2.23). Decoupling occurred between measured and modelled values of N3trunc LW in 1998, 2007, 2013 and 2016 based on current January temperature (Figure 2.23). Variability in measured and modelled RW, EW, LW and cell property values in both planted and natural stands from JPRF and PG coincide with fluctuations in climate as recorded in the meteorological records from PG and Fort St. James. Extreme weather events, such as in 1992, which was 10˚C warmer than the record average, corresponded to significant marker years in chronologies of wood properties (Figure 2.22 and Figure 2.23).

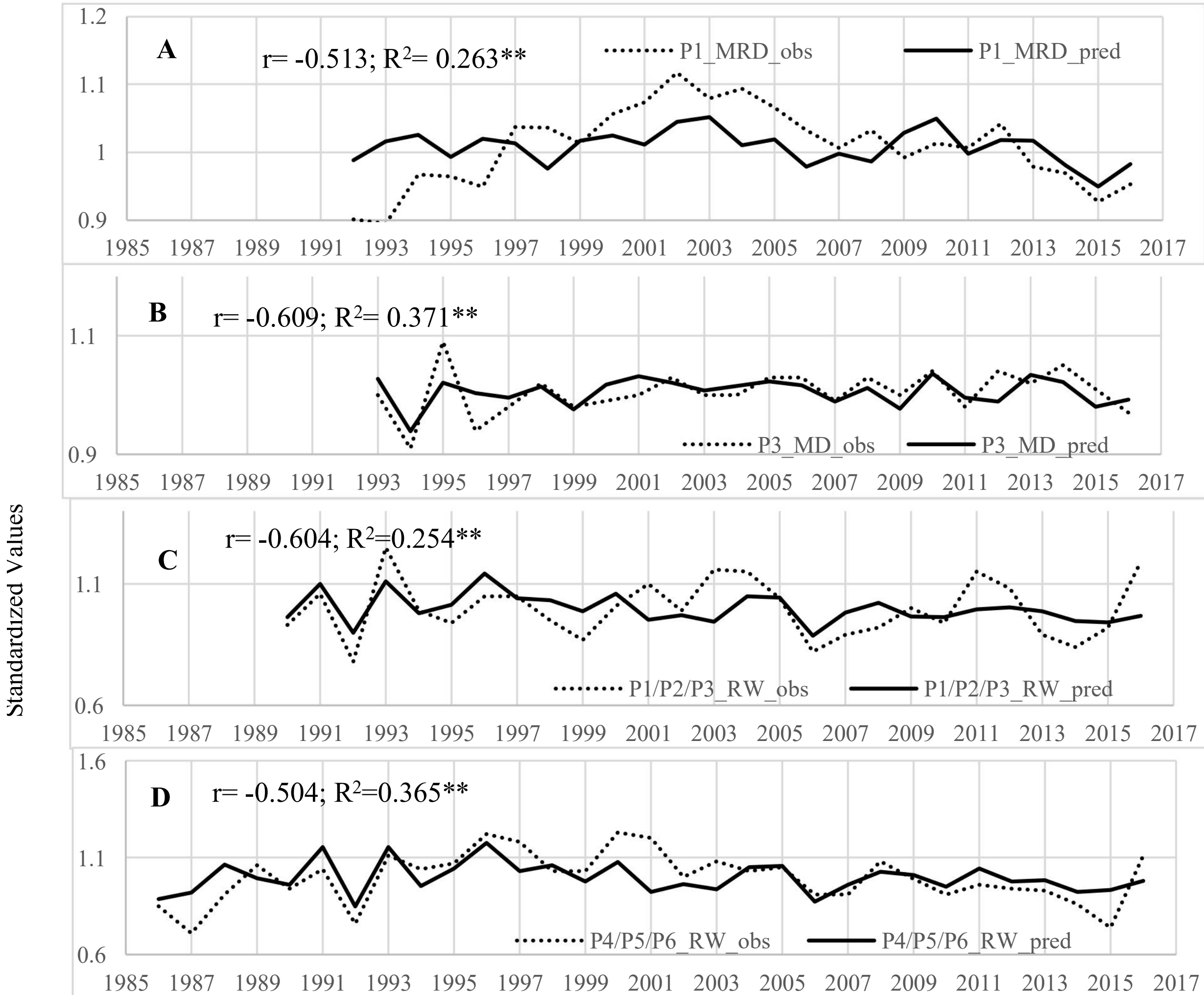

Figure 24.22. Measured (dotted line) vs modelled (solid line; crossed solid line indicates 1-year lagged data) ring width (RW), mean cell radial diameter (MRD) and mean density (MD) of regional (P1/P2/P3 & P4/P5/P6) and individual (P1, P3) planted stands of central interior British Columbia spruce. Data modeled from previous December precipitation (A), current average winter precipitation (B) and current mean January temperature (C, D) from Fort St. James and Prince George climate stations. R_2 values are presented with ** p =0.01 and * p= 0.05 Note not all axis are the same scale.

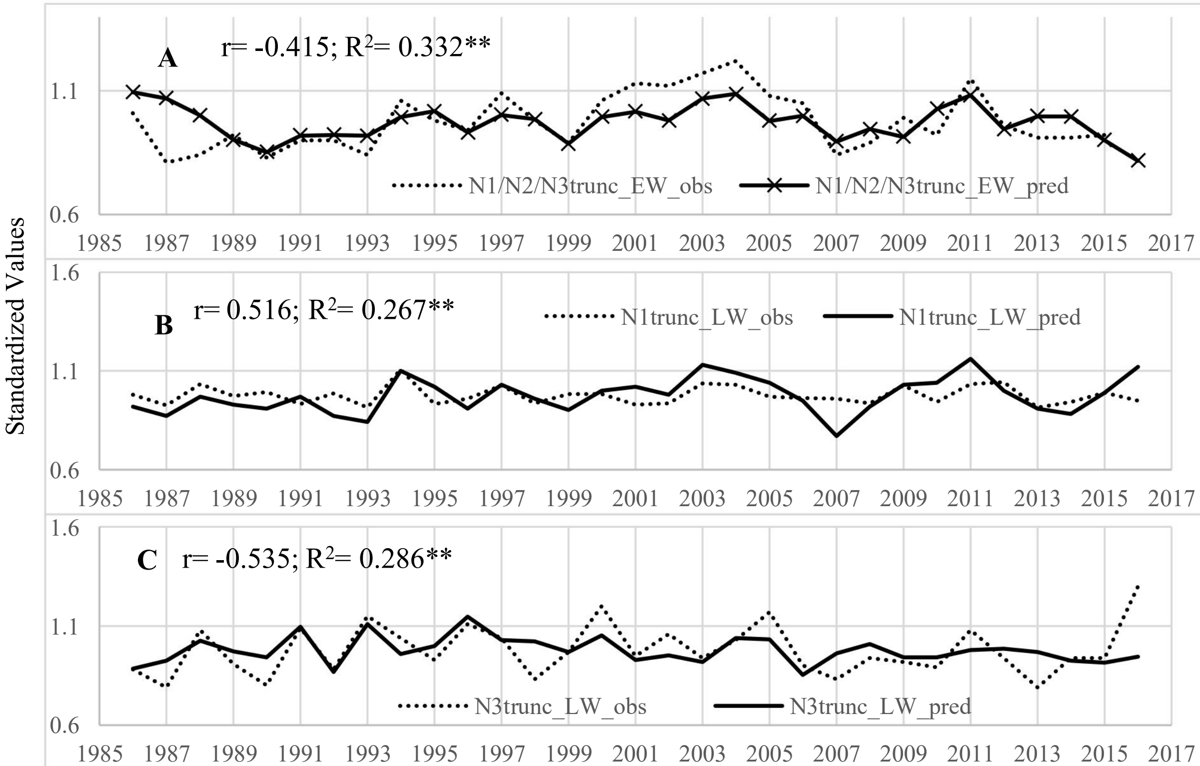

Figure 25.23. Measured (dotted line) vs modelled (solid line; crossed solid line indicates 1-year lagged data) ring width (RW), earlywood (EW), latewood (LW) and mean radial diameter (MRD) from regional (N1/N2/N3) and individual (N1, N3, N3trunc) natural stands of spruce in central British Columbia within the John Prince Research Forest. Data modelled from previous December total precipitation (A), current January total precipitation (B) and current mean January temperature (C) from Fort St. James climate stations. Thirty-year truncated natural stand chronologies indicated by NX"trunc". R2 values are presented with ** p =0.01 and * p= 0.05. Note not all axis are the same scale.

Summer Relationships

RW chronologies from regionally averaged planted stands in JPRF and PG modelled from current June and total summer precipitation levels were strongly related to measured values over most of the time series (Figure 2.24). However, modelled RW values from P4/P5/P6 in PG based on summer precipitation were poorly correlated with measured values prior to 1988 and from 2015-2016. Modelled RW values from P1/P2/P3 in JPRF, based on June precipitation levels, were poorly correlated to measured values from 1998-2003. The LW chronology from planted stands in JPRF modelled from current July mean monthly temperature was very similar to measured values despite some decoupling between 2013 and

2017 in measured and modelled values (Figure 2.24). MCWT chronology from P1/P2/P3 modelled from current July precipitation moderately followed the measured values with some areas of uncoupling occurred in this model from 1994-1996 and in 2005 (Figure 2.24).

LW chronologies from natural stands in PG (N6trunc) modelled from current July total monthly precipitation were strongly correlated with measured values (Figure 2.25). However, modelled N6trunc LW values decouple from measured values in 1988-1989, 1990-1995 1998, 2009 and 2013. N1trunc MRD chronology modelled from current June mean monthly temperature also strongly related to measured values (Figure 2.25). Decoupling from measured values only occurred from 2011-2017 in the N1trunc MRD model.

Measured wood properties were strongly related to extreme climate events. Measured wood properties were strongly related to higher-than-normal precipitation years in PG such as 1991 (190.9 mm), 1993 (254.6 mm) and 2008 (274.3 mm), and in Fort St. James such as 1993 (147 mm), 2005 (95.6 mm) and 2012 (103 mm) (Figure 2.24 and Figure 2.25). Similarly, measured values were related to lower-than-normal precipitation years in PG such as 1992 (108.9 mm) and in Fort St. James such as 1992 (22.6 mm), 1994 (49.8 mm), 2006 (11.2 mm), 2014 (8.6 mm). Relationships between growth and precipitation fluctuations are reflected in model accuracy in most cases. Wood properties were also strongly correlated to higher or lower-than-normal Fort St. James temperatures, such as 1998 (17.4˚C), 2009 (17.3˚C), 2005 (14.3˚C), and 2010 (15.9˚C) which is reflected in model accuracy (Figure 2.24 and Figure 2.25).

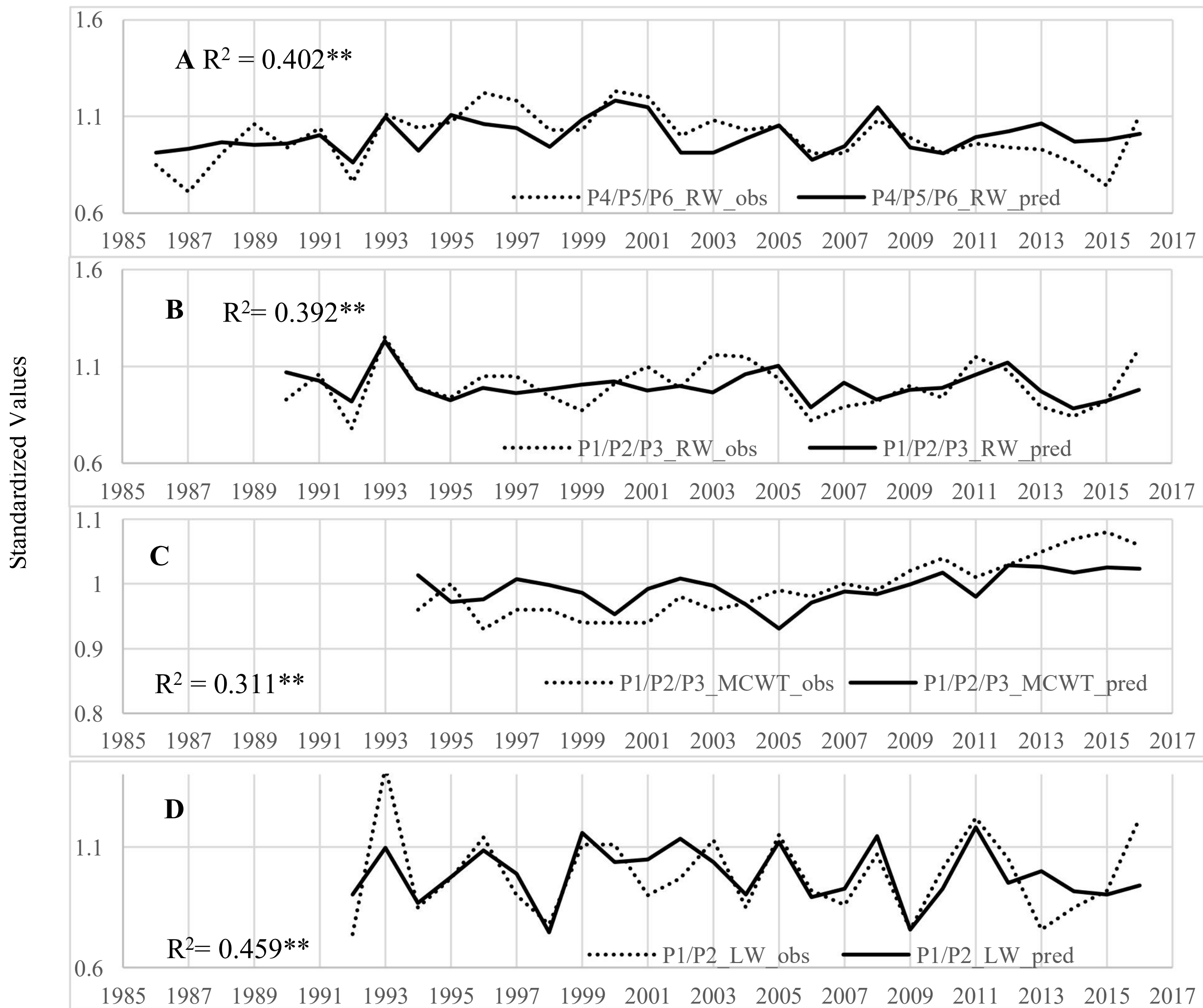

Figure 26.24. Measured (dotted line) vs modelled (solid lines) ring width (RW), latewood width (LW), mean cell radial diameter (MRD) and mean cell wall thickness (MCWT) of regionally averaged (P1/P2/P3, P1/P2 & P4/P5/P6) planted stands of spruce in central interior British Columbia modelled from current summer (A) total precipitation from Prince George climate station and current year June (B) and July (C) total precipitation and current year mean July temperature (D) from Fort St. James climate stations. R_2 values are presented with ** p =0.01 and * p= 0.05. Note not all y-axis are the same scale.

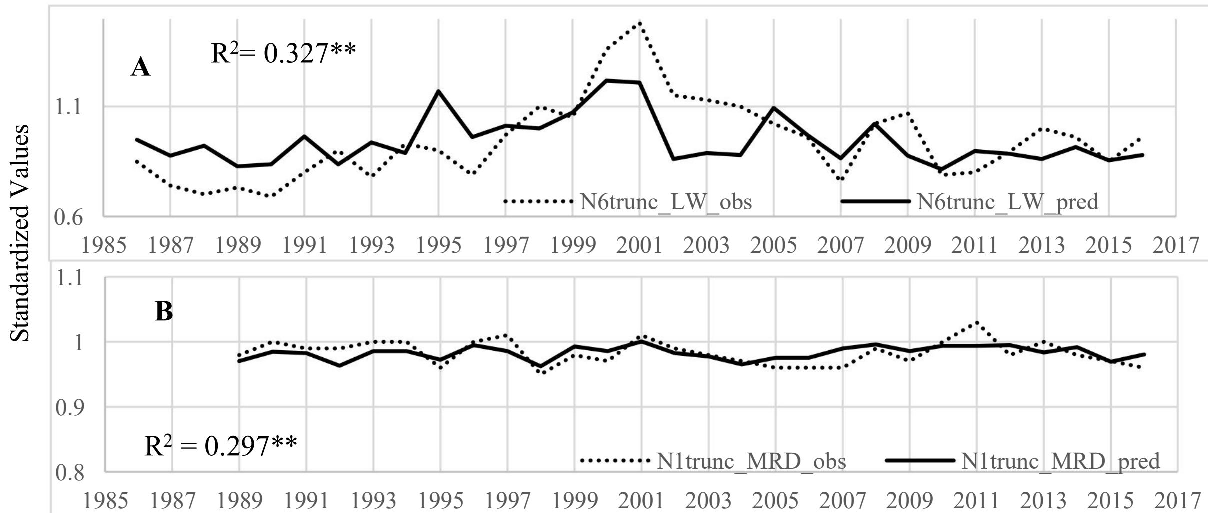

Figure 27.25. Measured (dotted line) vs modelled (solid line) latewood width (LW) and mean radial diameter (MRD) of regional (N1/N2/N3) and stand (N1trunc, N6trunc) level natural stands of central interior British Columbia modelled from current July (A) total precipitation and current June (B) mean temperature from the Fort St. James and Prince George climate stations. R_2 values are presented with ** p =0.01 and * p= 0.05. Note not all axis are the same scale.

Autumn Relationships

RW, EW, LW, MCWT, MD, and MRD chronology values from planted stands in JPRF and N3 were strongly related to models based on previous September, October and November, and current year September climate variables (Figures 2.26). No reliable models were found for planted stands from PG and the other natural stands from JPRF and PG (Tables 2.8 – 2.10). Decoupling occurred in 1997, 2006 and 2009-2010 between measured and modelled P1/P2 LW values modelled from previous September temperatures. Values of N3 RW modelled from previous November precipitation decouple from measured values in 1989, 1997, 1998 and 2006. Values of MD and MRD modelled from current September precipitation decouple from measured values between 1996-1997, 2003 and 2011-2012. Wood properties were also strongly correlated to extreme precipitation changes between 1993 and 1996 (1993 (12.9mm) to 1994 (70.6mm) to 1995 (8.6mm) to 1996 (57.9mm)) which are reflected in the models.

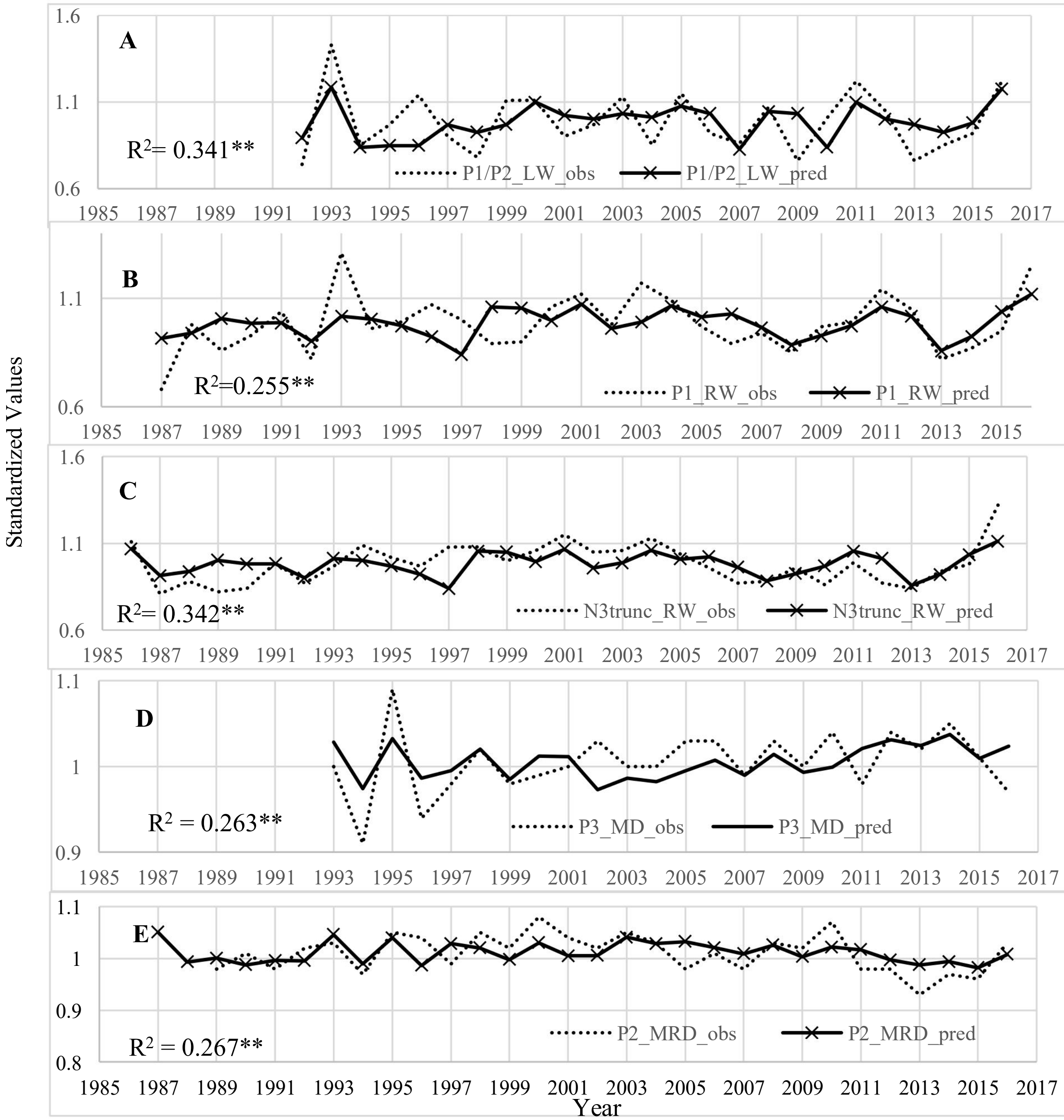

Figure 28.26. Measured (dotted line) vs modelled (solid line; crossed line indicates 1-year lagged data) values of
earlywood (EW), mean cell wall thickness (MCWT), mean density (MD) and mean radial diameter (MRD) from regional (P1/P2/P3) and/or stand (P2, P3) level planted stands of central interior British Columbia modelled from previous September mean monthly temperature (A), previous November total monthly precipitation (B, C) and current (D) and previous (E) September total monthly precipitation from Fort St. James climate station. R2 values are presented with ** p =0.01 and * p= 0.05.

2.5 DISCUSSION

Relationships between tree growth and climate over time were successfully modeled using RW, EW, LW, MCWT, MRD, and MD chronologies from planted and natural spruce stands in central interior BC and current and one-year lagged precipitation and temperature variables from Fort St. James and PG climate stations. Although there were numerous significant correlations between radial growth and climate, correlations will only be discussed where models were successfully predicted (R_2 >0.25) from climate variables. Regression analysis determined that winter and summer climate variation have the strongest influence on growth of RW, EW, LW, and cell properties in planted and natural stands of PG and JPRF. Previous autumn and current year September climate variation also had a strong effect on growth variation in JPRF planted stands. Low inter-series correlations and lack of reliable EPS values indicated that sample size was too small to create reliable stand level chronologies for MCWT in natural stands and any MMFA or MCO chronologies.

2.5.1 Climate-growth Relationships in Natural and Planted Stands of JPRF and PG

Winter

Variation in winter climate was a strong predictor of radial growth in planted stands of PG and planted and natural stands of JPRF. Correlations between January climate and chronologies suggests that recent reductions in JPRF precipitation, and rising winter temperatures in JPRF and in PG resulted in reduced annual growth (RW, LW). Higher-than-normal winter temperatures can reduce accumulated winter precipitation, or insulation, and trigger soil freezing to depths that can prevent or reduce absorption of melting snow leading to reduced water reserves for spring growth (Jarvis and Linder 2000). These events can cause drought-like conditions that will reduce cell expansion, or radial growth, by physical inhibition through loss of cell turgor pressure (Abe et al. 2003). In this study, RW (P1/P2/P3; P4/P5/P6) and LW (N1trunc) modelled from January temperature show strong correlation with measured values in years with higher-than-normal temperatures, such as 1992. Years with higher-than-normal winter temperatures can also cause midwinter dehardening and freezing injury that will substantially reduce growth, an observation seen in other studies (Strimbeck et al. 1995; Carolyn et al. 2017). Differences were found in relationships between winter precipitation and LW and EW. Relationships between winter precipitation and LW/MRD/MD chronologies of JPRF suggest that years with higher-than-normal precipitation related to increased LW production in natural stands and production of larger, less dense cells in planted stands. However, relationships between winter precipitation and EW in natural stands of JPRF suggest that years with higher-than-normal precipitation produce limited EW proportions. These differences are likely due to timing of cell formation, as substantial buildup of snow can delay spring growth, an observation found in other studies (Watson and Luckman 2001; Watson and Luckman 2016).

Summer

Radial growth over time in planted stands of PG and planted and natural stands of JPRF were strongly related to summer climates. Relationships between summer climate and JPRF planted and natural stands suggest that recent reductions in summer precipitation and higher-than-normal temperatures both coincided with reduced radial growth (RW, LW) and increased MCWT during what should be typical optimal cell enlargement periods (Fritts 1967; Flower and Smith 2011). These results are consistent with previous studies with BC interior spruce that show unfavourable summer climate conditions will reduce cell expansion with increased density and cell wall thickness and reduced RW and LW proportions (Zhang et al. 1999; Flower and Smith 2011; Oberhuber et al. 2014). However, in more favourable conditions in the PG area, relationships between summer precipitation and planted and natural stands of PG suggest that increases in summer precipitation produced increased radial growth (RW, LW), an observation found for several conifer species in BC, Canada, including white spruce (Kienholz 1931; Peterson and Peterson 1994; Ettl and Peterson 1995; Larocque and Smith 2005; Miyamoto et al. 2010). Model reliability was not consistent in all years and less reliable in models of cell properties. This outcome is particularly apparent in 2013 in models of RW, (P4/P5/P6), LW (P1/P2 and N6trunc), MCWT (P1/P2/P3) and MRD (N1trunc) where measured values poorly correlated with modelled values. Given that JPRF climate in 2013 had higher-than-average temperatures coupled with 20mm above the average precipitation, this may have allowed trees to increase cell expansion in June and increase LW and secondary wall thickening in July under favourable conditions; similar conditions were seen in growth of PG stands with higher-than-average temperatures coupled with 35mm of precipitation above the average.

Autumn

Radial growth in the stands investigated may not be as sensitive to previous autumn and current September variation as they are to other climate factors. Relationships were only found between autumn climate factors and planted stands of JPRF and N3 chronologies. Increasing autumn temperatures in JPRF were correlated with reduced LW for the P1/P2 LW chronologies. Maintaining summer-like temperatures in previous autumn months can promote active photosynthesis and carbohydrate food storage used for growth in the following year, however, results of this study show that precipitation is limiting in JPRF, and therefore is not able to adequately match climbing temperatures (Chinn et al. 2008).

Similarly, recent reductions in JPRF previous and current September precipitation appear to be related to production of cells with reduced radial diameter and higher density. These results are consistent with previous studies suggesting that water deficiency, characterized by decreasing precipitation coinciding with rising temperatures, may become the limiting growth factor in central interior boreal forests of Canada (Lo et al. 2010; Jiang et al. 2016). Although reductions in previous November precipitation were correlated with increased RW (P1; N3trunc), investigation revealed that measured and modelled values were only strongly related in years with higher-than-normal precipitation. This suggests that the negative correlation between previous November and RW is misrepresentative and that trees may be able to take advantage of years with higher-than-normal precipitation that compensates for rising temperatures.

2.5.2 Differences between Natural and Planted Stand Growth

Results from this study show that planted stands may be suffering greater growth reductions than natural stands with changing climates, an observation found in other studies comparing climate to planted and natural stand growth (Sánchez-Salguero et al. 2012; Sánchez-Salguero et al. 2013). Although the differences in response of radial growth to climate between planted and natural stands cannot be determined, several characteristics of this study's planted stands may have made them more sensitive to variation in temperature and precipitation (Szeicz and MacDonald 1993; Sánchez-Salguero et al. 2013). Younger trees, like the planted stands in this study, lack the substantial buildup of carbohydrate reserves in mature trees that helps to mitigate climate stress (Nobel and Alexander 1977; Lazarus et al. 2018). Planted trees also lack rooting depth that leads to reduced surface area for soil moisture absorption compared to older, larger trees with far reaching root systems that can continue to photosynthesize and transpire even during low precipitation periods (Wu et al. 2013). Previous studies have also shown that natural stands are able to recover from low precipitation periods or droughts substantially better than planted stands, which might account for the strong correlations between planted stands and precipitation (Sanchez-Salugero et al. 2013). Thus, results from this study suggest that variability in planted stand growth is more related to warming temperatures and/or reductions in precipitation compared to natural stands.

2.5.3 Differences between Planted, Natural, and Truncated Natural Stand Chronologies

Natural stand chronologies truncated to the last 30 years were used to compare growth in natural and planted stands with climate over the same time period and to investigate if recent natural stand growth was more influenced by climate than full-length natural stand chronologies. Although planted stand growth appears to be more sensitive to variations in temperature and precipitation than natural stands, stronger correlations were observed between climate and natural stands chronologies truncated to the last 30 years in JPRF and PG compared to the full-length chronologies. These relationships suggests that temperature and precipitation variation have become more influential in determining growth variation than earlier in the time series, an observation seen in other studies (Tardif et al. 2003; Camarero et al. 2015; Peñuelas et al. 2007; Martin-Benito et al. 2013). Prolonged warming and frequent drought can reduce deep soil moisture that supports mature tree growth during years of lower-than-normal precipitation (Chapin et al. 2002). Trees that are dependent on deeper soil moisture regimes are expected to experience longer and more intense water stress compared to younger, artificially managed, shallower rooted trees in the long-term (Carrer and Urbinati 2004; Trugman et al. 2018; Chitra-Tarak et al. 2018).

Although this study shows that reductions in planted stand growth is more strongly related to variation in precipitation and temperature, relationships between the last 30 years of natural stand growth and temperature and precipitation variation may indicate that long-term warming is beginning to affect growth in natural stands. As current projections suggest that temperatures will continue to rise in central interior BC, reductions in growth in planted and natural stands should be expected.

2.5.4 JPRF and PG Radial Growth Climate Variability

The differences in radial growth variation and growth models between JPRF and PG are probably due to the distinct differences in regional climate. Although results of this study indicate that rising temperatures of Fort St. James and PG both negatively influence radial growth (RW, LW), Fort St. James climate records report roughly 200 mm less average precipitation than PG. Previous research has shown hybrid white spruce growth in warm arid areas is more climatically sensitive to precipitation changes than areas with adequate moisture regimes, as regional differences (stronger and more numerous correlations between precipitation with JPRF than PG) in this study also suggest (Lo et al. 2010; Trindade et al. 2011; Wilmking and Myers-Smith 2008; Cortini et al. 2017). The relationships between precipitation and radial growth in JPRF may be amplified with recent reductions in precipitation. Although PG has rising temperature, adequate moisture regimes suggest that conditions for growth are more favorable than the warmer, drier conditions of JPRF. However, it is pertinent to note that the measured and modelled growth in PG is strongly correlated in years where lower-than-normal precipitation coincides with higher-than-normal temperatures in PG. This suggests that precipitation may not always be able to alleviate the negative effects of rising temperatures on radial growth in PG.

Differences in the relationships between climate and radial growth in JPRF and PG may also be due to the distance of sampled stands from climate stations and proximity of stands to one another. Although meteorological station data is relatively accurate, increasing distance or variability in distance from climate station will decrease accuracy (Coop et al. 2014). As climate stations are at fixed locals, data from the stations can be more representative of one area over another. This may explain stronger more numerous correlations in JPRF than PG. Differences in climate correlation results could have also been influenced by proximity of sites within each region to one another. Closer proximity of JPRF stands to one another could allow for better regional representation in planted and natural stand variability in tree growth and better model predictability with similar distances to climate stations than stands of PG.

2.6 CONCLUSION

This study aimed to investigate the effect of temperature and precipitation on radial growth properties (RW, EW, LW MCWT, MRD, MD, MCO and MMFA) in natural and planted stands of hybrid white spruce in areas surrounding PG and JPRF. Review of historical climate records shows annual temperature has increased in JPRF and PG areas. Precipitation showed an overall increase since 1930 with stark decreases in the last 30 years in JPRF.

Correlation analysis and regression models determined that radial growth in JPRF and PG planted stands was strongly influenced by previous autumn, winter, summer, and current September climate variables. Rising winter and summer temperatures were associated with reduced radial growth in planted stands of JPRF and PG and in natural stands of JPRF; rising autumn temperatures were also related to reduced LW in planted stands of JPRF but had poorer statistical strength. Higher-than-normal winter precipitation reduced EW but encouraged LW production in JPRF stands, likely due to timing of cell formation. Reduction in summer and autumn precipitation was associated with reduced growth in stands of JPRF, however, increases in summer precipitation related to growth in PG.

Stronger and more numerous relationships between climate with radial growth in planted than natural stands may be attributed to differences in age and size. Planted stands may have greater dependency on moisture reserves on the first decade of juvenile growth and have a lack of substantial carbohydrate reserves that help mitigate climate stressors. Although planted stands had stronger relationships between radial growth and climate than natural stands, assessment of the last 30 years of natural stand radial growth suggests increased sensitivity to climate variability than full-length natural stand chronologies. Increased sensitivity could be caused by long-term reductions in deep soil water reserves used by that deeper root systems of mature stands, especially during climate warming and reductions in precipitation.

Finally, stronger and more robust regression models occurred from stands surrounding JPRF than those in PG, likely due to distinct differences in regional climate, climate station location and proximity of sampled stands to one another. In natural and planted stands of PG, adequate precipitation in cool-moist areas appear to support increased growth in current climates. However, rising temperatures coupled with reduced precipitation have been shown in this study to reduce annual radial growth rate in natural and planted stands within warm-arid areas of JPRF. Closer proximity of stands to one another coupled with similar distances to the climate station could have allowed for better regional representation of natural and planted stand growth in JPRF than PG. Future projections of rising temperatures and reduced precipitation may lead to increase drought-induced mortality in spruce plantations and mature forests in warm-arid areas.

2.7 REFERNCES

Abe H, Nakai T, Utsumi Y, Kagawa A. 2003. Temporal water deficit and wood formation in Cryptomeria japonica. Tree Physiology. 23(12): 859–863. https://doi.org/10.1093/treephys/23.12.859

Adamopoulos S, Passialis CVE. 2006. Strength properties of juvenile and mature wood in black locust (*Robina Psudoacacia* L.). Wood and Fiber Science. 39(2): 241–249.

Alexander RR. and Nobel DL. 1971. Effects of watering treatments on germination, survival, and growth on Engelmann spruce: a greenhouse study. USDA For. Serv. Res. Note RM-182.

Alteyrac J, Cloutier A, Zhang ASY. 2006. Characterization of juvenile wood to mature wood transition age in black spruce (*Picea mariana* (Mill.) B.S.P.) at different stand densities and sampling heights. Wood Science & Technology. 40: 124–138. https://doi.org/10.1007/s00226-005-0047-4

Arenas-castro S, Fernandez-Haeger J, Jordano-Barbudo D. 2015. A Method for Tree-Ring Analysis Using Diva-Gis Freeware on Scanned Core Images. Tree-Ring Research. 71(2): 118–129. https://doi.org/10.3959/1536-1098-71.2.118

Barnett JR and Jeronimidis (eds). 2003. Tree growth and wood quality. Blackwell Publishing: Oxford (UK).

Barnett JR and Bonham VA. 2004. Cellulose microfibril angle in the cell wall of wood fibres. Biological Reviews of the Cambridge Philosophical Society. 79(2): 461–472. https://doi.org/Doi 10.1017/S1464793103006377

Blanchette D, Fournier RA, Luther JE, Cote JF. 2015. Predicting wood fiber attributes using local-scale metrics from terrestrial LiDAR data: A case study of Newfoundland conifer species. Forest Ecology and Management. 347: 116–129. https://doi.org/10.1016/j.foreco.2015.03.013

Bouriaud O, Leban JM, Bert D, Deleuze C. 2005. Intra-annual variations in climate influence growth and wood density of Norway spruce. Tree Physiology. 25(6): 651–660. https://doi.org/10.1093/treephys/25.6.651

Bower AD, Adams WT, Birkes D, Nalle D. 2005. Response of annual growth ring components to soil moisture deficit in young, plantation-grown Douglas-fir in coastal British Columbia. Canadian Journal of Forest Research. 35(10): 2491–2499. https://doi.org/10.1139/x05-146

Burenina TA, Shishikin AS, Onuchin AA. 2014. Snow cover on logged sites in fir-Siberian pine forests of the Yenisey Ridge. Contemporary Problems of Ecology. 7(7): 778–787. https://doi.org/10.1134/S1995425514070038

Camarero JJ, Gazol A, Sangüesa-Barreda G, Oliva J, Vicente-Serrano SM. 2015. To die or not to die: Early warnings of tree dieback in response to a severe drought. Journal of Ecology. 103(1): 44–57. https://doi.org/10.1111/1365-2745.12295

Cameron AD, Lee SJ, Livingston AK, Petty JA. 2005. Influence of selective breeding on the development of juvenile wood in Sitka spruce. Canadian Journal of Forest Research. 35(12): 2951–2960. https://doi.org/10.1139/x05-219

Carrer M and Urbinati C. 2004. Age-Dependent Tree-Ring Growth Responses to Climate in *Larix decidua* and *Pinus cembra*. Ecology. 85(3): 730-740

Chapin FS, Matson PA, Mooney HA. 2002. Principles of terrestrial ecosystem ecology. Springer, New York, p 106.

Chavardès RD, Daniels LD, Waeber PO, Innes JL, Nitschke CR. 2013. Unstable climate-growth relations for white spruce in southwest Yukon, Canada. Climatic Change. 116(3–4): 593–611. https://doi.org/10.1007/s10584-012-0503-8

Chen F, Yuan YJ, Wei WS, Yu SL, Li Y, Zhang RB, Zhang T, Shang H. 2010. Chronology development and climate response analysis of Schrenk Spruce (*Picea Schrenkiana*) tree-ring parameters in the Urumqi River basin, China. Geochronometria. 36: 17–22. https://doi.org/10.2478/v10003-010-0014-4

Chitra-Tarak R, Ruiz L, Dattaraja HS, Mohan Kumar MS, Riotte J, Suresh HS, McMahon SM, Skumar R. 2018. The roots of the drought: Hydrology and water uptake strategies mediate forest-wide demographic response to precipitation. Journal of Ecology 106(4): 1495–1507. https://doi.org/10.1111/1365-2745.12925

Cook ER. and Peters K. 1981. The smoothing spline: A new approach to standardizing forest interior tree-ring width series for dendroclimatic studies. Tree-Ring Bulletin, 41: 45-53.

Cook ER. and Holmes RI. 1999. Users manual for program ARSTAN. Tucson, AZ.

Coop AJ, Hubbard KG, Shulski MD, You J, Marx DB. 2014. Spatial accuracy of climate networks: A case study in Nebraska. Journal of Applied Meteorology and Climatology. 53(8): 1932–1942. https://doi.org/10.1175/JAMC-D-13-0296.1

Cortini F, Comeau PG, Strimbu VC, Hogg EH, Bokalo M, Huang S. 2017. Survival functions for boreal tree species in northwestern North America. Forest Ecology and Management, 402: 177–185. https://doi.org/10.1016/j.foreco.2017.06.036

DeSoto L, Cruz M, Fonti P. 2011. Intra-annual patterns of tracheid size in the Mediterranean tree *Juniperus thurifera* as an indicator of seasonal water stress. Canadian Journal Forest Research. 41: 1280–1294. https://doi.org/10.1139/X11-045

Dale MRT, Fortin MJ. 2014. Spatial analysis: a guide for ecologists. Cambridge University Press.

Delong C, Tanner D, Jull MJ. 1993. A field guide for site identification and interpretation for the southwest portion of the Prince George forest region. Province of British Columbia: Ministry of Forests: https://www.for.gov.bc.ca/hfd/pubs/docs/Lmh/Lmh24.pdf.

Dickerson-Lange SE, Gersonde RF, Hubbart JA, Link TE, Nolin AW, Perry GH, Roth TR, Wayand NE, Lundquist JD. 2017. Snow disappearance timing is dominated by forest effects on snow accumulation in warm winter climates of the Pacific Northwest, United States. Hydrological Processes. 31(10): 1846–1862. https://doi.org/10.1002/hyp.11144

Erickson HD, Arima T. 1974. Douglas-fir wood quality studies. Part II: Effects of age and simulated growth on fibril angle and chemical constituents. Wood Sci. Technol. 8: 255-265.

Evans R. and Ilic J. 2001. Rapid prediction of wood stiffness from microfibril angle and density. Forest Products Journal: 51(2): 53.

Fleming SW and Whitfield PH. 2010. Spatiotemporal mapping of ENSO and PDO surface meteorological signals in British Columbia , Yukon , and southeast Alaska Spatiotemporal Mapping of ENSO and PDO Surface Meteorological Signals in British Columbia, Yukon , and Southeast Alaska. Canadian Meteorological and Oceanographic Society. 48(2): 122–131. https://doi.org/10.3137/AO1107.2010

Flower A and Smith DJ. 2011. A dendroclimatic reconstruction of June-July mean temperature in the northern Canadian Rocky Mountains. Dendrochronologia. 29(1): 55–63. https://doi.org/10.1016/j.dendro.2010.10.001

Franceschini T, Lundqvist SO, Bontemps JD, Grahn T, Olsson L, Evans R, Leban JM. 2012. Empirical models for radial and tangential fibre width in tree rings of Norway spruce in north-western Europe. Holzforschung. 66(2): 219–230. https://doi.org/10.1515/HF.2011.150

Fritts HC. 1976. Tree rings and climate. New York (NY): Academic Press Inc.

George J.-P, Grabner M, Campelo F, Karanitsch-Ackerl S, Mayer K, Klumpp RT, Schüler S 2019. Intra-specific variation in growth and wood traits under water-limited conditions: long term-, short-term-, and sudden responses of four conifers grown in common garden experiments. Science of the Totatl Environment. 660: 631–643. https://doi.org/10.1016/j.scitotenv.2018.12.478

Gindl W, Grabner M, Wimmer R. 2000. The influence of temperature on latewood lignin content in treeline Norway spruce compared with maximum density and ring width. *Trees* - Structure and Function. 14(7): 409–414. https://doi.org/10.1007/s004680000057

Gou X, Chen F, Yang M, Li J, Peng J, Jin L. 2005. Climatic response of thick leaf spruce (*Picea crassifolia*) tree-ring width at different elevations over Qilian Mountains, northwestern China. 61: 513–524. https://doi.org/10.1016/j.jaridenv.2004.09.011

Grissino-Mayer HD. 2001. Evaluating crossdating accuracy: a manual and tutorial for the computer program COFECHA. Tree-Ring Research. 57(2): 205–221.

Grissino-Mayer HD 2003. A manual and tutorial for the proper use of an increment borer. Tree-Ring Research, 59(2): 63-79.

Groffman PM, Driscoll CT, Fahey TJ, Al E. 2001. Colder soils in a warmer world: A snowmanipulation study in a northern hardwood forest ecosystem. Biogeochemistry, 56(56): 135–150.

Hardy JP, Groffman PM, Fitzhugh RD, Henry KS, Welman AT, Demers JD, Fahey TJ, Discoll CT, Tierney FL, Nolan S. 2001. Snow depth manipulation and its influence on soil frost and water dynamics in a northern hardwood forest. Biogeochemistry 56(2): 151–174. https://doi.org/10.1023/A:1013036803050

Havimo M, Rikala J, Sirviö J, Sipi M. 2008. Distributions of tracheid cross-sectional dimensions in different parts of Norway spruce stems. Silva Fennica. 42: 89–99.

Heinrichs D, Tardif JC, Bergeron Y. 2007. Xylem production in six tree species growing on an island in the boreal forest region of western Quebec, Canada. Canadian Journal of Botany. 85(5): 518–525. https://doi.org/10.1139/B07-041

Jarvis P and Linder S. 2000. Constraints to growth of boreal forests. Nature. 405: 904–905. https://doi.org/10.1038/nn.3432

Jiang X, Huang J, Stadt KJ, Comeau PG, Chen HYH. 2016. Spatial climate-dependent growth response of boreal mixedwood forest in western Canada. Global and Planetary Change. 139: 141–150. https://doi.org/10.1016/j.gloplacha.2016.02.002

Kienholz R. 1931. Effect of Environmental Factors on the Wood Structure of Lodgepole Pine, *Pinus Contorta* Loudon. 12(2): 354–379.

Kostiainen K, Saranpää P, Lundqvist SO, Kubiske ME, Vapaavuori E. 2014. Wood properties of Populus and Betula in long-term exposure to elevated CO2 and O3. Plant, Cell and Environment. 37(6): 1452–1463. https://doi.org/10.1111/pce.12261

Larocque SJ and Smith DJ. 2005. A dendroclimatological reconstruction of climate since AD 1700 in the Mt. Waddington area, British Columbia Coast Mountains, Canada. Dendrochronologia. 22(2): 93–106. https://doi.org/10.1016/j.dendro.2005.02.003

Lazarus BE, Castanha C, Germino MJ, Kueppers LM, Moyes AB. 2018. Growth strategies and threshold responses to water deficit modulate effects of warming on tree seedlings from forest to alpine. Journal of Ecology. 106(2): 571–585. https://doi.org/10.1111/1365-2745.12837

Lindstrom H. 1997. Fiber length, trachied diameter, and latewood percentage in Norway spruce: Development from pith outwards. Wood and Fiber Science. 29: 21–34.

Lo YH, Blanco JA, Seely B, Welham C, Kimmins JP. 2010. Relationships between climate and tree radial growth in interior British Columbia, Canada. Forest Ecology and Management, 259(5): 932–942. https://doi.org/10.1016/j.foreco.2009.11.033

Lundgren C. 2004. Cell wall thickness and tangential and radial cell diameter of fertilized and irrigated Norway spruce. Silva Fennica. 38(1): 95–106. https://doi.org/http://dx.doi.org/10.14214/sf.438

Mäkinen H, Nöjd P, Mielikäinen K. 2000. Climatic signal in annual growth variation of Norway spruce (*Picea abies)* along a transect from central Finland to the Arctic timberline. Canadian Journal of Forest Research. 30(5): 769–777. https://doi.org/10.1139/cjfr-30-5-769

Martin-Benito D, Beeckman H, Cañellas I. 2013. Influence of drought on tree rings and tracheid features of *Pinus nigra* and *Pinus sylvestris* in a mesic Mediterranean forest. European Journal of Forest Research. 132(1). https://doi.org/10.1007/s10342-012-0652-3

Martz F, Vuosku J, Ovaskainen A, Stark S, Rautio P. 2016. The snow must go on: Ground ice encasement, snow compaction and absence of snow differently cause soil hypoxia, CO2 accumulation and tree seedling damage in boreal forest. PLoS ONE. 11(6): 1–18. https://doi.org/10.1371/journal.pone.0156620

Meko DM and Baisan CH. 2001. Pilot study of latewood-width of conifers as an indicator of variability of summer rainfall in the North American monsoon region. International Journal of Climatology. 21(6): 697–708. https://doi.org/10.1002/joc.646

Mellander P.-E, Löfvenius MO, Laudon H. 2007. Climate change impact on snow and soil temperature in boreal Scots pine stands. Climatic Change. 85(1–2): 179–193. https://doi.org/10.1007/s10584-007-9254-3

Mitchell MD and Denne MP. 1997. Variation in density of *Picea sitchensis* in relation to within-tree trends in tracheid diameter and wall thickness. Forestry. 70(1): 47–60. https://doi.org/10.1093/forestry/70.1.47

Miyamoto Y, Griesbauer HP, Green SD. 2010. Growth responses of three coexisting conifer species to climate across wide geographic and climate ranges in Yukon and British Columbia. Forest Ecology and Management. 259(3): 514–523. https://doi.org/10.1016/j.foreco.2009.11.008

Newton PF. 2016. Developmental Trends of Black Spruce Fibre Attributes in Maturing Plantations. International Journal of Forestry Research. https://doi.org/10.1155/2016/7895289

Nobel DL. and Alexander RR. 1977. Environmental factors affecting natural regeneration Engelmann spruce in the central rocky mountains. For. Sci. 23(4): 420-429.

Oberhuber W, Gruber A, Kofler W, Swidrak I. 2014. Radial stem growth in response to microclimate and soil moisture in a drought-prone mixed coniferous forest at an inner Alpine site. European Journal of Forest Research. 133(3): https://doi.org/10.1007/s10342-013-0777-z

Panshin AJ, deZeeuw C. 1980. Textbook of wood technology. Fourth edition. US: McGraw-Hill Book Company.

Peñuelas J, Ogaya R, Boada M, Jump AS. 2007. Migration, invasion and decline: Changes in recruitment and forest structure in a warming-linked shift of European beech forest in Catalonia (NE Spain). Ecography. 30(6): 829–837. https://doi.org/10.1111/j.2007.0906-7590.05247.x

Peterson DW, Peterson DL, Ettl GJ. 2002. Growth responses of subalpine fir to climatic variability in the Pacific Northwest. Canadian Journal of Forest Research. 32(9): 1503–1517. https://doi.org/10.1007/BF00374331

Pike CC, Warren JC, Montgomery RA. 2017. Effects of artificial warming during quiescence on budbreak and growth of white spruce, *Picea glauca*. Canadian Journal of Forest Research, 47(11): 1538–1545. https://doi.org/10.1139/cjfr-2017-0102

Pitman KJ and Smith DJ. 2013. A dendroclimatic analysis of mountain hemlock (*Tsuga mertensiana*) ring-width and maximum density parameters, southern British Columbia Coast Mountains, Canada. Dendrochronologia. 31(3): 165–174. https://doi.org/10.1016/j.dendro.2013.05.002

Pritzkow C, Heinrich I, Grudd H, Helle G. 2014. Relationship between wood anatomy, tree-ring widths and wood density of *Pinus sylvestris* L. and climate at high latitudes in northern Sweden. Dendrochronologia. 32(4). https://doi.org/10.1016/j.dendro.2014.07.003

Robertson EO, Jozsa L. 1990. Estimating Douglas-fir wood production from soil and climate data. Can. J. For. Res., 20: 357–364.

Rossi S, Deslauriers A, Anfodillo T, Morin H, Saracino A, Motta R, Borghetti M. 2006. Conifers in cold environments synchronize maximum growth rate of tree-ring formation with day length. New Phytologist. 170(2): 301–310. https://doi.org/10.1111/j.1469-8137.2006.01660.x

Sánchez-Salguero R, Camarero JJ, Dobbertin M, Fernández-Cancio Á, Vilà-Cabrera A, Manzanedo RD, Zavala MA, Navarro-Cerrillo RM. 2013. Contrasting vulnerability and resilience to drought-induced decline of densely planted vs. natural rear-edge *Pinus nigra* forests. Forest Ecology and Management, 310, 956–967. https://doi.org/10.1016/j.foreco.2013.09.050

Sánchez-Salguero R, Navarro-Cerrillo RM, Camarero JJ, Fernández-Cancio Á. 2012. Selective drought-induced decline of pine species in southeastern Spain. Climatic Change. 113(3–4): 767–785. https://doi.org/10.1007/s10584-011-0372-6

Saranpaa P. 2003. Wood density and growth. In: Barnett JK, Jeronimidis G, editors. Wood quality and its biological basis. Great Britain: Blackwell Publishing & CRC Press, Biological Sciences Series. p. 87-117.

Shmulsky R, Jones PD. 2011. Fundamentals of tree-ring research. Tucson: The University of Arizona Press.

Strimbeck GR, Schaberg PG, DeHayes DH, Shane JB, Hawley GJ. 1995. Midwinter dehardening of montane red spruce during a natural thaw. Canadian Journal of Forest Research, 25(12): 2040–2044. https://doi.org/10.1139/x95-221

Strong WL. 2017. Episodic and systematic tree ring-width variation (Ad 1763–2013) in the Takhini valley, southwest Yukon, Canada. Arctic, 70(4): 389–402. https://doi.org/10.14430/arctic4685

Szeicz JM and MacDonald GM. 1993. Age-dependant tree-ring growth responses of subarctic white spruce to climate. Can. J. For. Res., 24: 120–132.

Tardif J, Camarero JJ, Ribas M. and Guti errez E. (2003) Spatiotemporal variability in tree growth in the Central Pyrenees: climatic and site influences. Ecological Monographs, 73, 241–257.

Taylor FW, Wang EIC, Yanchuk AMM. 1982. Specific gravity and tracheid length variation of white spruce in alberta. Canadian Journal Forest Research. 12: 561–566.

Trindade M, Bell T, Laroque C. 2011. Changing climatic sensitivities of two spruce species across a moisture gradient in Northeastern Canada. Dendrochronologia. 29(1): 25–30. https://doi.org/10.1016/j.dendro.2010.10.002

Vahey DW, Zhu J, Scott CT. 2007. Wood density and anatomical properties in suppressed-growth trees: Comparison of two methods. Wood and Fiber Science. 39(3): 462–471. Retrieved from http://swst.metapress.com/index/f05102n1n7x3059j.pdf

Vaganov EA, Hughes MK, Kirdyanov AV, Schweingruber FH, Silkin PP. 1999. Influence of snowfall and melt timing on tree growth in subarctic Eurasia. Nature. 400(6740): 149–151. https://doi.org/10.1038/22087

van Dijk AIJM and Keenan RJ. 2007. Planted forests and water in perspective. Forest Ecology and Management. 251(1–2): 1–9. https://doi.org/10.1016/j.foreco.2007.06.010

Watson E and Luckman BH. 2001. Dendroclimatic reconstruction of precipiation for sites in the southern Canadian Rockies. The Holocene. 2(2001): 203–213.

Watson E and Luckman BH. 2016. An investigation of the snowpack signal in moisture-sensitive trees from the Southern Canadian Cordillera. Dendrochronologia. 38: 118–130. https://doi.org/10.1016/j.dendro.2016.03.008

Wigley TML, Briffa KR, Jones PD. 1984. On the average value of correlated time series, with applications in dendroclimatology and hydrometeorology. Journal of Climate and Applied Meteorology.

Wilmking M and Myers-Smith I. 2008. Changing climate sensitivity of black spruce (*Picea mariana* Mill.) in a peatland-forest landscape in Interior Alaska. Dendrochronologia. 25(3): 167–175. https://doi.org/10.1016/j.dendro.2007.04.003

Wimmer R. 2002. Wood anatomical features in tree-rings as indicators of environmental change. Dendrochronologia. 20(1): 21–36. https://doi.org/10.1078/1125-7865-00005

Wood LJ and Smith DJ. 2012. Climate and glacier mass balance trends from AD 1780 to present in the Columbia Mountains, British Columbia, Canada. The Holocene. 23(5): 739–748. https://doi.org/10.1177/0959683612465450

Wood LJ, Smith DJ, Hartley ID. 2016. Predicting softwood quality attributes from climate data in interior British Columbia, Canada. Forest Ecology and Management. 361: 81–89. https://doi.org/10.1016/j.foreco.2015.11.004

Wood LJ and Smith DJ. 2015. Intra-annual dendroclimatic reconstruction for northern British Columbia, Canada, using wood properties. Trees. 29: 461–474. https://doi.org/10.1007/s00468-014-1124-9

Wu G, Xu G, Chen T, Liu X, Zhang Y, An W, Wang, W, Fang Z, Yu S. 2013. Age-dependent tree-ring growth responses of Schrenk spruce (*Picea schrenkiana*) to climate-A case study in the Tianshan Mountain, China. Dendrochronologia. 31(4): 318–326. https://doi.org/10.1016/j.dendro.2013.01.001

Yarie J. 2008. Effects of moisture limitation on tree growth in upland and floodplain forest ecosystems in interior Alaska. Forest Ecology and Management. 256(5): 1055–1063. https://doi.org/10.1016/j.foreco.2008.06.022

Zhang Q, Alfaro RI, Hebda RJ. 1999. Dendroecological studies of tree growth, climate and spruce beetle outbreaks in central British Columbia, Canada. Forest Ecology and Management. 121(3): 215–225. https://doi.org/10.1016/S0378-1127(98)00552-0

Zobel BJ, and van Buijtenen, J.P. 1989. Wood variation: its causes and controls. Berlin: Springer-Verlag.

Zubizarreta-Gerendiain A, Gort-Oromi J, Mehtätalo L, Peltola H, Venäläinen A, Pulkkinen P. 2012. Effects of cambial age, clone and climatic factors on ring width and ring density in Norway spruce (*Picea abies*) in southeastern Finland. Forest Ecology and Management. 263: 9–16. https://doi.org/10.1016/j.foreco.2011.09.011

Chapter 3: Relationships between percent carbon and wood growth and climate variation in natural and planted stands of hybrid white spruce (*Picea glauca* (Moench) *x engelmannii* (Parry)) in central interior British Columbia

3.1 ABSTRACT

Measurements of tree growth and carbon sequestration are important for accurate determination of carbon balance in terrestrial ecosystems. Using hybrid white spruce (*Picea glauca* (Moench) x *engelmannii* (Parry), this study sought to investigate relationships between percent carbon and wood properties of ring-width, earlywood, latewood, cell wall thickness, and density, determine if percent carbon between individual stands and between regional-level stand aggregates differed, and to evaluate relationships between percent carbon and climate variation over time. Significant differences between percent carbon of wood found in individual natural and planted stands were found, likely due to site-specific characteristics. Significant relationships were found between percent carbon and cell wall thickness, density, and ring-width values, which suggests these wood properties are good indicators of variation in sequestered carbon. Percent carbon accumulation in some planted stands and some natural stands appeared to be suffering reductions with increasing temperatures; however, warmer late-season conditions appear to enhance growth. The last 30 years of growth in some natural stands may be more sensitive to climate variation compared to the entire time series. The results of this study provide improved understanding of relationships between percent carbon, wood properties and climate and potential differences inherent to natural and planted stands.

3.2 INTRODUCTION

Forest growth in natural and managed stands is a key process that requires assessment to determine the impacts of environmental change to carbon balance in terrestrial ecosystems (Pompa-Garcia 2016). Simple measurements of carbon content in tree stems are a function of tree height and diameter at breast height (DBH), but can be enhanced with knowledge of wood density, carbon concentration, and wood volume (Weber et al. 2018). It has been suggested that wood density and cell wall thickness correlate with carbon concentration; cellulose and lignin are components of xylem cell walls therefore thicker, denser cell walls should have greater proportions of carbon (Elias and Potvin 2003; Thomas and Malczewski 2007; Lachenbruch and Mcculloh 2014; Weber et al. 2018). However, relationships between wood properties and carbon are not well understood as past research has focused mainly on biomass (or allometric biomass equations as determined from DBH and height measurements) instead of direct measurements of volatile and structural carbon (Zabek and Prescott 2006; Castaño-Santamaría and Bravo 2012). Expanding knowledge of the variation and relationships in natural and planted stands between wood properties, such as density and cell wall thickness, and carbon could improve projections of carbon sequestration (Weber et al. 2018).

Forest growth, and subsequent carbon accumulation, is strongly affected by changes in climate. Changes in climate are predicted to cause deviations in tree photosynthetic and respiration rates, increase disturbance, and increase tree mortality related to chronic drought (Allen et al. 2010; Schwalm et al. 2010; Haughian et al. 2012; Babst et al. 2014; McDowell and Allen 2015). Changes in British Columbia (BC) climate are predicted to include warmer and wetter conditions, with increased maximum and minimum temperatures and decreased depth and water content of snowpack that will vary across the topographic landscape

(MWLAP 2002; Lo et al. 2010; Fleming and Whitfield 2010). Over the next century, substantial changes in temperature and precipitation in central interior BC, particularly in the spruce-willow-birch (SWB) and sub-boreal spruce (SBS) biogeoclimatic zones, are expected (Spittlehouse 2007; Lo et al. 2010; Wang et al. 2012; Jiang et al. 2016). Increasing temperatures may push forests beyond sustainability thresholds, reducing the amount of carbon dioxide uptake and carbon accumulation (Millar and Stephenson 2015).

Tree ring analysis has been used to determine forest growth dynamics and has provided climate variability information through radial growth and climate reconstructions (Fritts 1967; Babst et al. 2014). Dendrochronological techniques may also be used to enhance understanding of relationships between above ground carbon accumulation and climate (Bouriaud et al. 2005). However, most carbon research relates to productivity based on climate (Grünwald and Bernhofer 2007), biomass equations (Liepiņš et al. 2018), and changes to forests after anthropogenic management (Davis et al. 2009; Ter-Mikaelian et al. 2014). These studies exclude the established large-scale spatiotemporal tree-ring records that are deemed unsuitable for carbon equations.

3.2.1 Objectives

This chapter aims to determine variations in percent carbon of hybrid white spruce (*Picea glauca* x *engelmannii*) in natural and planted stands over time, and how these variations relate to density and cell wall thickness measurements, and how these variations correspond with changes in temperature and precipitation in central interior BC. The specific objectives of this research were to:

i) Determine radial growth profiles of percent carbon, density, and cell wall thickness at annual scales;

ii) Examine the relationship between percent carbon, ring width, earlywood and latewood widths, and values of wood density and cell wall thickness;

iii) Compare percent carbon relationships among individual stands and regional-level stand aggregates;

iv) Examine the statistical correlation between monthly and seasonal climate variables and percent carbon; and,

v) Investigate relationships between climate variables and percent carbon over time.

3.3 METHODS

3.3.1 Site Selection

Hybrid white spruce trees were selected from six natural (N1-N6) and six planted stands (P1-P6) from areas of central interior BC (Figure 3.1 and Table 3.1). One group of six stands (N1-N3; P1-P3) was selected from the John Prince Research Forest (JPRF), where each stand was within 5km of one another. The second group of six stands (N4-N6; P4-P6) were within a 200km range of Prince George (PG). Biogeoclimatic variant of each site was determined with review of site characteristics and Biogeoclimatic Ecosystem Classification land management handbooks (Figure 3.1 and Table 3.1) (Delong et al. 1993). PG stands were in the willow-wet-cool (wk1) and very-wet-cool (vk1) variants, of the Sub Boreal (SBS) and biogeoclimatic zone, classified with high precipitation and cooler temperatures. JPRF stands were in the Stuart-dry-warm (dw3) variant, of the SBS zone, that is characterized by lower snow packs and warmer temperatures.

3.3.2 Sample Collection

Twenty dominant trees in each stand were selected for sampling. Sampling occurred at 5m minimum intervals to avoid concerns of spatial autocorrelation (Dale and Fortin 2014).

Trees with scars, fire or insect damage, split tops and abnormal growth patterns were avoided. Areas near roads or with open canopies were also avoided to alleviate influences on growth that would reduce the ability to obtain a stand-level climatic growth signal (Fritts 1976). One 5mm core at 90 degree spacing from each tree was collected at breast height (and at 30cm aboveground for smaller trees) that was parallel with contours (Grissino-Mayer 2003). An additional 12mm core from each tree was collected at JPRF sites for SilviScan fibre analysis. Surrounding vegetation, slope, elevation, flowing or standing water, diameter-at-breast-height and GPS site and tree location were recorded.

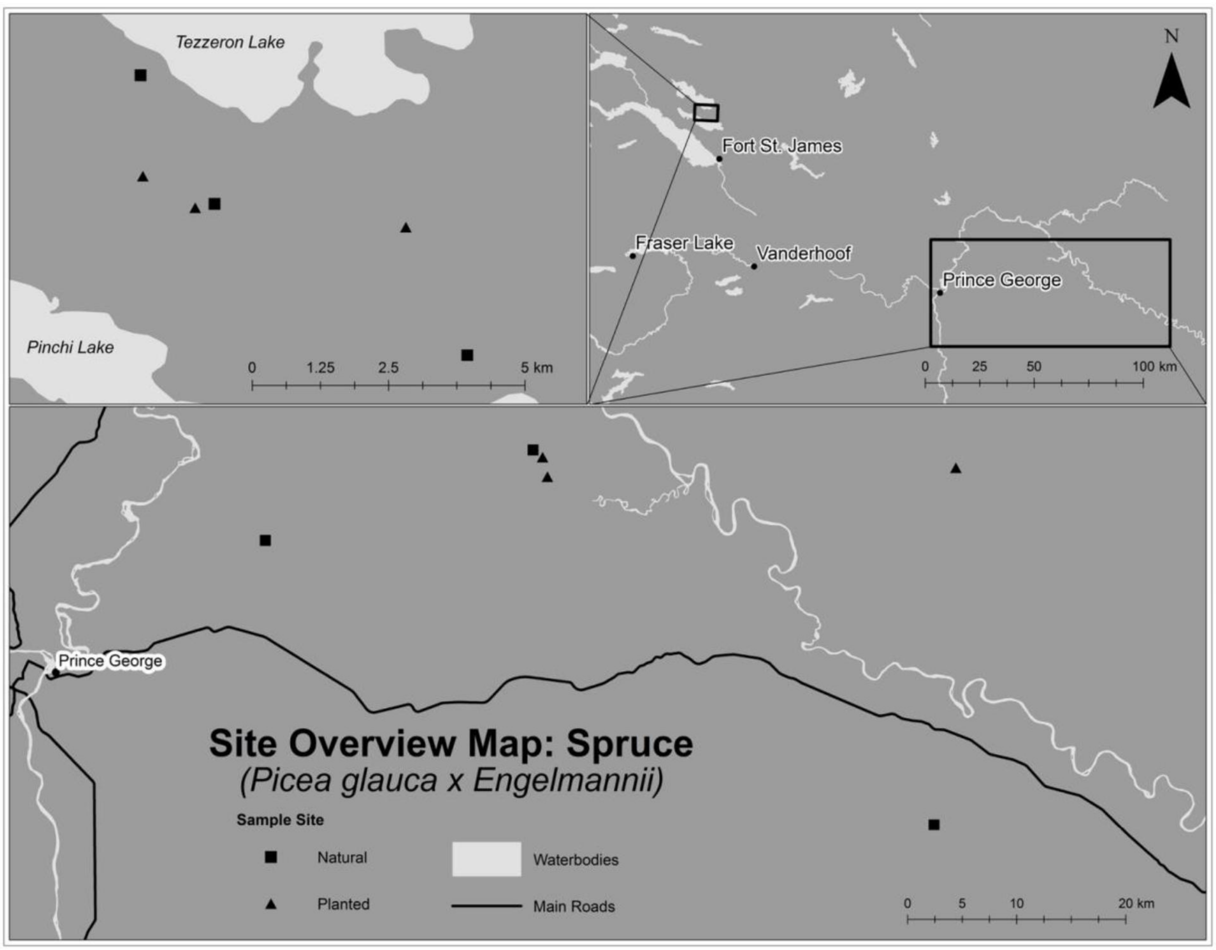

Figure 29.1. Sample site overview map of natural (squares) and planted (triangles) stands near Prince George and Fort St. James.

Table 3.10. Site and stand characteristics of natural (N1-N6) and planted (P1-P6) spruce research samples surrounding the John Prince Research Forest (JPRF) Prince George collected from 2016-2017.

	Geographic Information								Tree characteristics		
	Site	**Latitude**	**Longitude**	**Elevation (m)**	**Slope (%)**	**BEC zone**	**BEC subzone**	**BEC variant**	**Mean Age (years)**	**# of Tree Cores**	**Mean DBH (cm)**
JPRF	N1	54 38’50.80	124 23’35.1	768	<2	SBS	dw	3	101	40	26.5
	N2	54 39’46.60	124 24’36.6	833	<5	SBS	dw	3	119	35	38.3
	N3	54 36’58.21	124 19’05.5	727	0	SBS	dw	3	52	34	30.5
	P1	54 38’47.50	124 23’68.2	801	0	SBS	dw	3	28	40	17.8
	P2	54 38’48.00	124 24’34.5	866	20	SBS	dw	3	31	40	22.3
	P3	54 38’14.17	124 20’05.5	802	0	SBS	dw	3	25	36	18.9
Prince George	N4	54 04’58.90	122 01’32.3	730	0	SBS	wk	1	93	40	40.9
	N5	54 46’33.90	121 29’14.6	1113	0	SBS	vk	1	145	40	48.2
	N6	54 01’01.00	122 24’54.5	707	0	SBS	wk	1	154	40	32.4
	P4	54 04’05.90	121 26’48.8	843	<5	SBS	vk	1	30	40	26.1
	P5	54 05’19.90	122 01’31.8	713	<10	SBS	wk	1	30	40	28.2
	P6	54 04’01.10	122 01’09.7	689	0	SBS	wk	1	33	40	22.9

Note: N1 had a unidentified stream running through site.

3.3.3 Sample Preparation of 12mm Cores

Of the 120-12mm cores sampled JPRF, 89 undamaged cores were selected for SilviScan analysis. Resins were removed from selected cores via 12-hour Soxhlet acetone extraction. After extraction, cores were conditioned at 40% relative humidity and 20°C to obtain an 8% moisture content equilibrium. Once at 8% moisture content, cores were cut into 2mm X 7mm radial pith-to-bark strips (tangentially x longitudinally) with a twin-blade saw and sanded. SilviScan analysis was then performed, which included: 1) image analysis of radial and tangential cell dimensions using optical microscopy, 2) X-ray densitometry to provide measurements of wood density every 25 microns along the wood samples, and, 3) X-ray diffractometry yielding measurements of microfibril angle at 5-mm increments (Evans and Ilic 2001).

3.3.4 Percent Carbon Analysis

Increment cores from JPRF and PG were dried, sanded, and cross-dated using a dotting system. Cores were labelled with a single dot every ten years, two dots every half-century and three dots every century (Stokes and Smiley 1968); 1200 grit sandpaper was used to identify especially narrow rings. The Yamaguchi (1991) list method was implemented to determine significant marker years. Once cross-dated, twenty 5mm cores from each site were cut bark-pith into 5-year increments from the last 40 years for planted stands and 80 years for natural stands. Although one-year increments were initially sought, annual increments did not provide enough wood mass for percent carbon measurements. Each group of 20 cores (stand-level chronology) were cut into 5-year sections. These 5-year sections were grouped together by year and corresponding years were analysed together as an aggregate sample (Figure 3.2). Aggregate samples were measured for wet weight and extracted at 110 ˚C for 1.5 hours of boiling, rinsing and recovery using a Soxhlet unit to remove resins. Once dry, samples were measured for dry weight and ground into a powder with a Wiley grinder. Four replicates from each aggregate sample representing 20 cores were created (Figure 3.2). Replicates combined 4-5mg of sample and 10mg of catalyst, valdium peroxide and were placed into a small tin. Each replicate was analyzed with the PerkinElmer 2400 Series II CHNS/O Elemental Analyzer (2400 Series II) to measure carbon content as a percentage (Figure 3.2). Percent carbon content of replicates was then averaged to obtain a mean value for each 5-year segment. This process was then completed for 5-year aggregate sample and for all other sites.

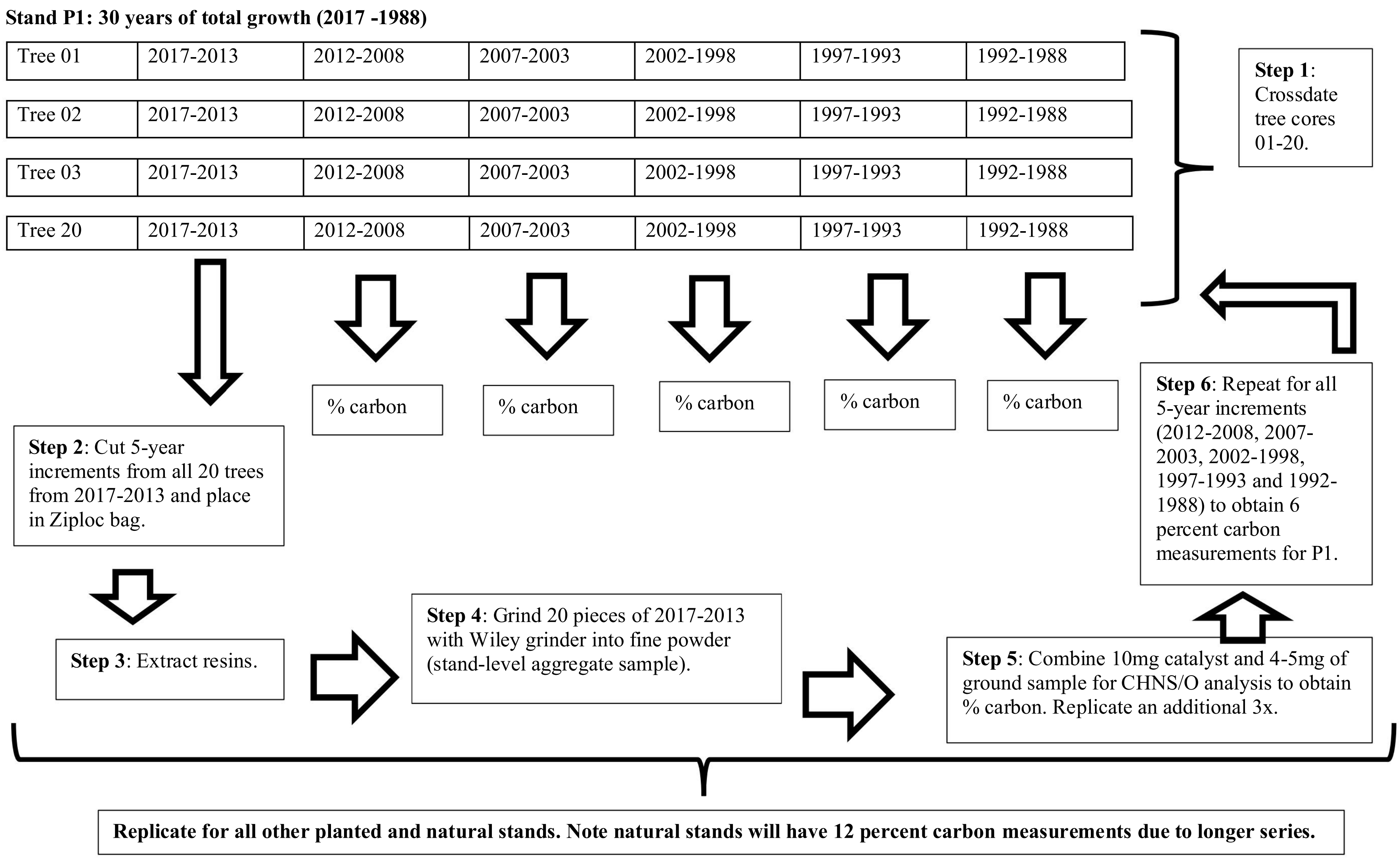

Figure 30.2 Overview of core preparation and percent (%) carbon analysis from one planted stand.

3.3.5 Percent Carbon vs JPRF Cell Wall Thickness and Density Values

Individual mean, minimum, and maximum density and cell wall thickness measurements were obtained from SilviScan data of all cores from each natural and planted stand in JPRF only (P1-P3, N1-N3) due to cost of analysis. Annual RW, EW, LW and density and cell wall thickness values from each core were averaged into 5-year increment values to correspond to 5-year carbon value increments. The 20 cores representing a stand were then averaged for each interval to obtain average stand-level values of RW, EW, LW, density, and cell wall thickness over time. Stand-level and regional-level percent carbon and average RW, EW, LW and mean, minimum, and maximum cell wall thickness and density values were tested for normality using skewness, kurtosis and Shapiro-Wilk values prior to statistical tests (Table 3.2). Shapiro-Wilk values for percent carbon were used to determine normality rather than skewness and kurtosis due to small sample sizes. Data failing one test was assessed using histograms to determine severity of skew. Data failing all tests was transformed where possible or assumed non-normal. Data that were unable to be normalized were removed from further analysis.

Several one-way ANOVAs with Bonferroni post-hoc test (alpha=0.05) tests were conducted to determine significant differences of mean percent carbon content between natural (N1 vs N2 vs N3) and planted stands (P1 vs P2 vs P3) (Table 3.3). Residuals of ANOVA tests were checked for normality. Regional data sets were created for natural and planted stands of percent carbon and mean, minimum and maximum density, and cell wall thickness were combined where no significant differences existed. An independent t-test analysis was conducted to determine if there was a significant difference between regional data sets of mean percent carbon content in natural and planted (Table 3.3).

Correlations statistics were calculated for regional data sets and natural and planted stand values between mean percent carbon values and average RW, EW, LW and mean, maximum and minimum density and cell wall thickness values over time using a Pearson's or Spearman Rank correlation coefficient (R) (Table 3.4). Correlation statistics in individual stands were graphed for visual aid (Figure 3.3 and Figure 3.4). Juvenile wood and mature wood were determined for each site using changes in cell wall thickness and density values. Although statistical tests were not possible between juvenile wood and mature wood, relationships between values of percent carbon and cell wall thickness and density in juvenile and mature wood are graphically represented (Figure 3.5).

3.3.6 Percent Carbon vs Climate

Climate Data

Historical climate information was obtained from the Adjusted Historical Canadian Climate Data website (https://www.canada.ca/en/environment-climate-change/services/climate-change/modelling-projections-analysis/adjusted-homogenized-canadian-data.html) for JPRF (Station #1092970, Latitude 54°45, Longitude -124°25, 686m elevation) and PG (Station #1096439, Latitude 53°88, Longitude -122°67, 680m elevation) stations. Climate variables included monthly mean temperature, total monthly precipitation, and winter (previous December, current January and February), spring (current March, April, May) and summer (current June, July, August), and previous autumn (previous September, November, December) seasonal averages. Random missing values within climate data were calculated by averaging four surrounding points or filled with modeled climate data from Climate BC (http://cfcg.forestry.ubc.ca/projects/climate-data/climatebcwna/) for large gaps in data. Temperature and precipitation data was averaged into 5-year intervals for comparison with 5-year average percent carbon data.

Correlation & Regression Analysis

Percent carbon was correlated to climate (mean previous monthly May-December and mean current monthly January-September, and previous autumn, winter, spring, and summer temperature and precipitation) values using Pearson's correlation coefficient (R) or Spearman's Rank coefficient for non-parametric data that could not be normalized. In addition, correlation statistics were determined for data from natural stands that were truncated to the last 30 years of growth ($N(X)_{trunc}$). Truncated natural stand data was compared with planted and entire natural stand data. Partial correlation was used to determine spurious correlations when relationships between percent carbon were found to both temperature and precipitation within the same months/seasons.

3.3.7 Regression Analysis and Comparison of Measured and Modelled Values

Regression analysis was completed where significant Pearson's correlation coefficients were detected. Significant regression values (R_2) were only accepted where R_2 >0.40 to provide the best models (Wood and Smith 2011; Blanchette et al. 2015). Modelled values were correlated back to measured values to verify model accuracy. Models with significant correlation coefficients and R_2 values were visually assessed against measured values to determine model accuracy over time.

3.4 RESULTS

3.4.1 Percent Carbon vs Cell Wall Thickness and Density

Normality testing determined normality of values for percent carbon and average RW, EW, and LW as well as mean, maximum, and minimum cell wall thickness and density values within natural (N1, N2, N3) and planted (P1, P2, P3) stands and within natural and planted regional averages (Table 3.2). Data that were not normal were transformed using inverse or log transformations (Table 3.2). ANOVA results determined average percent carbon was statistically different among natural stands at a 5% confidence level; post hoc comparisons indicated that mean percent carbon of N1(M=45.34; SD= 0.865) was significantly different from mean percent carbon of N2 and N3 ($p<0.0001$) with no significant difference seen between N2 (M= 42.38; SD = 0.218) and N3 (M= 42.06; SD= 0.070; $p=0.589$) (Table 3.3). Planted stands showed statistically different percent carbon at a 5% confidence level; post-hoc comparisons indicated that mean percent carbon of P2 (M= 44.11; SD= 0.616) was significantly different from mean percent carbon of P1 and P3 ($p<0.0001$) with no significant difference between P1 (M= 42.21; SD = 0.448) and P3 (M= 41.57; SD= 0.961; $p=0.401$) (Table 3.3). Independent sample t-test results indicated no significant difference between regional-level mean percent carbon of natural stands (N2 and N3) (M=42.23, SD = 0.24) and planted stands (P1 and P3) (M=41.89, SD = 0.73; $t = 1.950$, p-value = 0.070, two-tailed) in JPRF (Table 3.3).

Correlation statistics determined significant correlations between percent carbon and wood properties over time in stands N2, N3, and P1 (Table 3.4). Relationships between wood properties and percent carbon values are presented graphically by site in Figure 3.3 and Figure 3.4. Relationships between cell wall thickness and density properties of mature and juvenile wood are graphically presented in Figure 3.5; the majority of juvenile wood is from planted stands whereas the mature wood is generally from natural stands.

Table 3.2. Normality testing including skewness (S), kurtosis (K), and Shapiro-Wilk (SW) values for percent carbon (% C) and mean (m), maximum (max) and minimum (min) cell wall thickness (CWT) and density (D) values and average (avg) ring width (RW), earlywood (EW), and latewood (LW) from natural (N3, N1, N2) and planted (P1, P2, P3) stands surrounding the John Prince Research Forest. Although S and K values > +11 or < -1 are considered not normal data, SW values were used in cases with small sample sizes. SW <0.050 were not accepted as normal data. Some samples were transformed with inverse (y) or log (l) transformations.

Site		% C	mCWT	mD	maxCWT	maxD	minCWT	minD	avgRW	avgEW	avgLW
N1	S	0.60	-0.93	-0.67	1.48	1.47	-0.69	-0.70	1.17	1.20	1.28
	K	1.95	-0.14	-0.46	2.21	2.01	-0.66	-0.29	0.88	0.33	1.93
	SW	0.05	0.05	0.150	0.22(l)	0.24(l)	0.09	0.33	0.05(l)	0.01	0.092
N2	S	-0.73	-0.47	-0.27	1.18	1.13	-0.45	-0.35	0.49	0.68	0.78
	K	1.01	-1.06	-0.29	0.45	0.32	-0.73	-0.49	-0.36	-0.72	-0.12
	SW	0.72	0.21	0.98	0.26(l)	0.36(l)	0.50	0.88	0.43	0.10	0.23
N3	S	-0.56	-0.34	0.63	-0.95	-0.78	0.53	0.53	-0.78	-0.47	-0.35
	K	-0.24	-1.15	0.48	0.09	-0.20	0.40	-1.48	-0.47	-0.55	-0.47
	SW	0.35	0.54	0.90	0.37	0.50	0.71	0.16	0.34	0.62	0.71
P1	S	1.27	1.08	1.42	-0.92	-0.76	2.03	1.36	0.08	-0.48	-0.40
	K	1.00	1.18	1.91	0.49	0.22	4.25	1.53	-1.63	-1.50	-1.89
	SW	0.21	0.46	0.24	0.63	0.48	0.05	0.30	0.53	0.93	0.94
P2	S	0.51	0.83	1.73	-1.63	-0.76	0.80	1.55	-0.09	-0.41	-0.72
	K	0.49	0.48	3.14	2.83	0.22	0.09	2.36	-2.45	-0.51	-0.27
	SW	0.97	0.56	0.05	0.08	0.16	0.58	0.09	0.11	0.98	0.96
P3	S	1.51	1.79	1.43	-1.25	-1.90	2.02	1.74	-	-0.56	-0.44
	K	2.05	3.43	0.98	2.28	3.70	4.26	2.62	-	-1.63	1.44
	SW	0.14	0.07	0.06(y)	0.45	0.04	0.06(l)	0.06(y)	-	0.85	0.95
N	S	-0.36	-0.83	0.25	0.51	0.60	0.20	0.60			
	K	-0.31	0.21	-0.61	-1.21	-0.99	-1.40	-1.27			
	SW	0.97	0.93	0.98	0.90	0.90	0.94	0.87			
P	S	0.30	0.33	1.35	-0.19	-1.44	2.63	1.45			
	K	1.23	-1.27	1.02	2.68	1.79	7.49	1.08			
	SW	0.96	0.92	0.85	0.91	0.86	0.65	0.80			

Table 3.3. Anova and t-test results between percent carbon (% carbon) of natural (N1, N2, N3) and planted (P12, P2, P3) stands and regionally averaged natural (N) and planted (P) % carbon surrounding the John Prince Research Forest with Bonferroni (*) post hoc. Within a column numbers indicate mean and standard deviation within brackets. Anova test results are presented with letters in columns; similar letters indicate groups that have no significant difference, different letters indicate groups that have a significant difference.

Stand-level				**Regional-level**	
	% carbon (SD)*		**% carbon (SD)***		**% carbon (SD)**
N1	45.34 **a** (0.865)	P1	42.21 **a** (0.448)	N	42.23 **a** (0.24)
N2	42.38 **b** (0.218)	P2	44.11 **b** (0.616)	P	41.89 **a** (0.73)
N3	42.06 **b** (0.589)	P3	41.57 **a** (0.961)		

Table 3.4. Pearson(P) and Spearman Rank(S) correlation coefficient results between average percent carbon (C) and mean, maximum (max), minimum (min), cell wall thickness (CWT) and density (D) values and average (avg) ring width (RW), earlywood (EW) and latewood (LW) across natural (N3, N1, N2) and planted (P1, P2, P3) stands over 5-year intervals surrounding the John Prince Research Forest. ** p = 0.013; * p = 0.05 level.

	N1	N2	N3	P1	P2	P3
meanCWT vs C	0.208(S)	-0.668(S)**	0.633(S)	0.143(S)	-0.200(P)	0.886(S)
meanD vs C	0.012(S)	-0.592(P)*	0.100(P)	0.486(S)	-0.029(S)	0.771(S)
maxCWT vs C	-0.093(S)	0.712(S)**	0.558(P)	0.814(S)	0.200(S)	-0.543(S)
maxD vs C	-0.056(S)	0.712(S)**	0.605(P)	0.826(S)	0.200(P)	-0.543(S)
minCWT vs C	-0.080(S)	-0.623(P)**	-0.673(P)*	0.400(S)	-0.218(P)	0.886(S)
minD vs C	0.142(S)	-0.674(P)**	0.167(S)	0.100(S)	-0.086(S)	0.600(S)
avgRW vs C	-0.049(P)	0.691(S)**	0.559(P)	-0.855(P)**	-0.235(P)	-
avgEW vs C	-0.115(S)	0.624(P)**	0.491(P)	0.469(S)	0.272(P)	-0.696(S)
avgLW vs C	-0.134(S)	0.602(P)**	0.180(P)	0.600(S)	0.368(P)	-0.086(S)

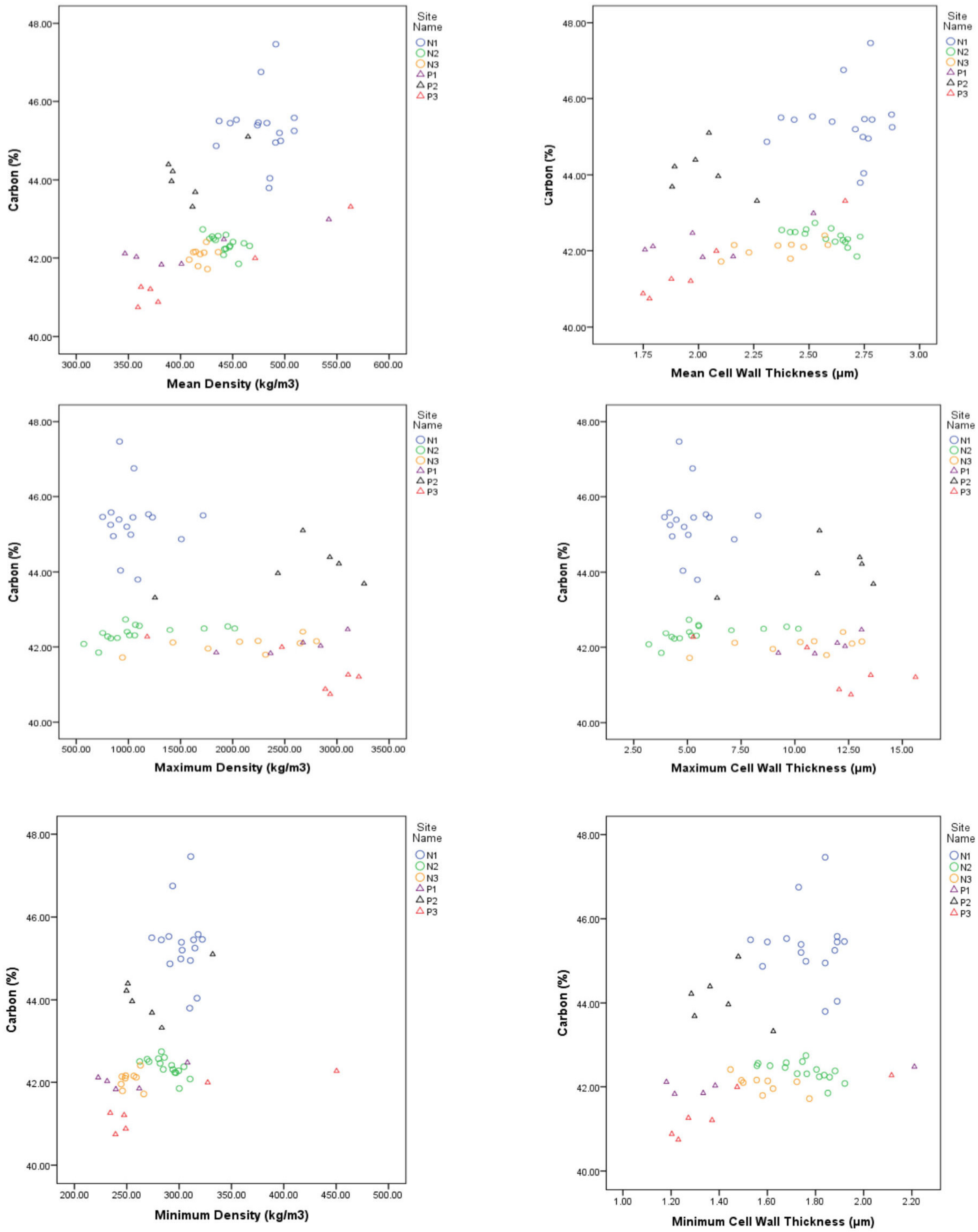

Figure 31.3. Comparison between average percent carbon (%) and mean-maximum-minimum cell wall thickness (µm) and density (kg/m3) values of natural (N1, N2, N3) and planted (P1, P2, P3) spruce stands depicted by colour and shape. Each point represents a 5-year average within each series for percent carbon and wood properties. Note that not all axis are the same.

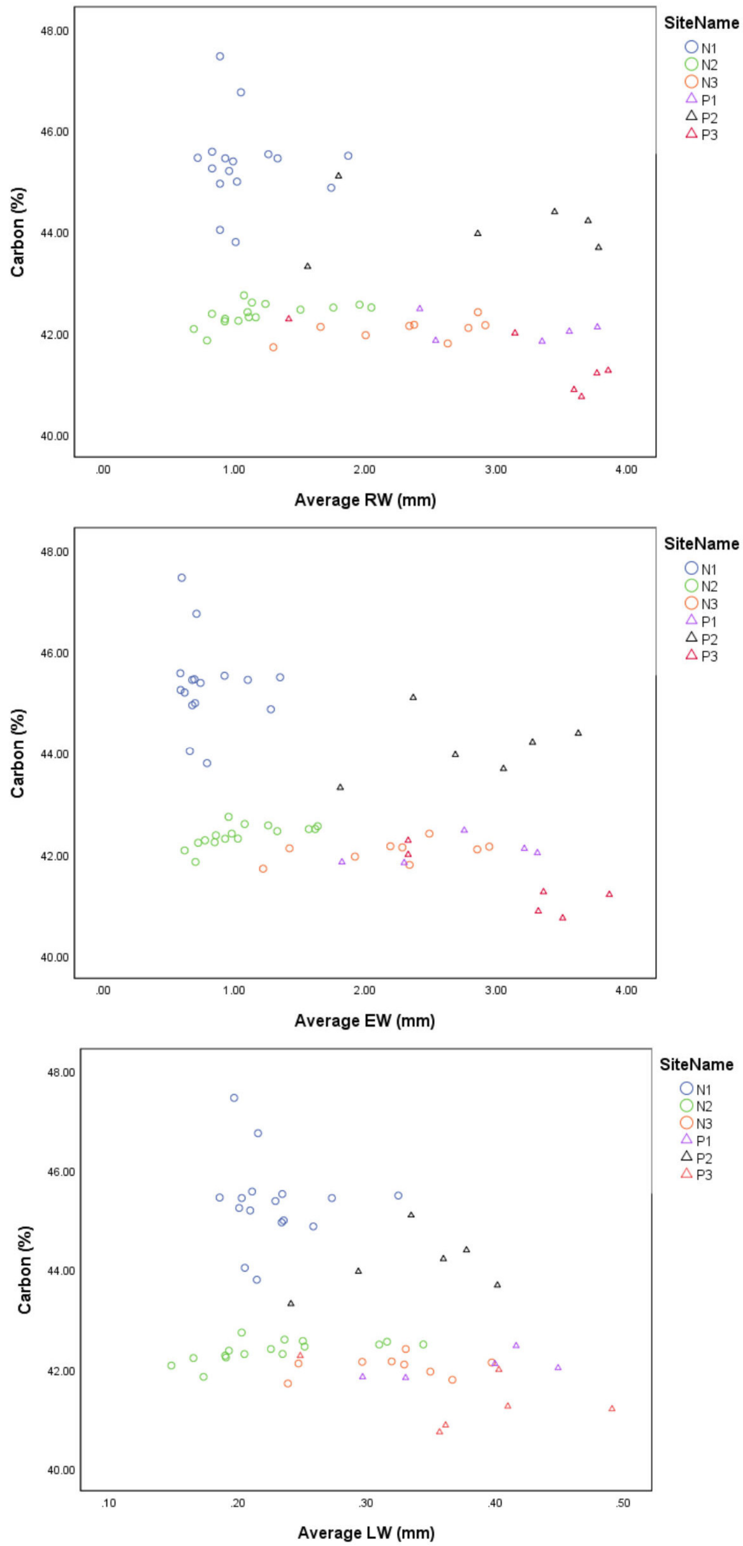

Figure 32.4. Comparison between average percent carbon (%) and average ring width (RW), earlywood (EW) and latewood (LW) values of natural (N1, N2, N3) and planted (P1, P2, P3) spruce stands depicted by colour and shape. Each point represents a 5-year average within each series for percent carbon and RW, EW and LW. Note that not all axis are the same.

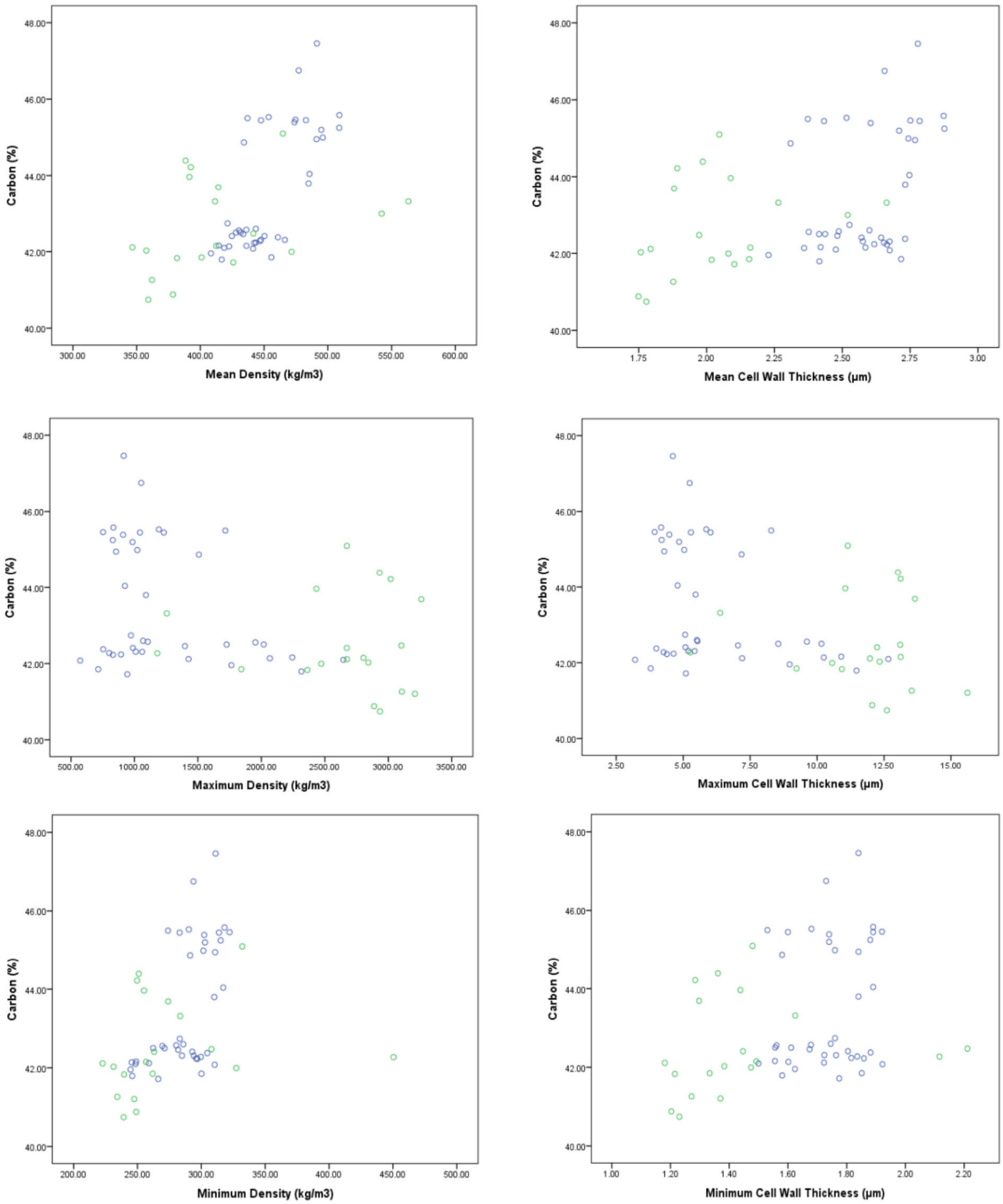

Figure 3.5. Comparison between percent carbon (%) and mean-maximum-minimum cell wall thickness (μm) and density (kg/m3) values of all spruce stands combined. Blue indicates mature wood and green indicates juvenile wood combined for all sites. Note that not all x-axis are the same.

3.4.2 Changes in Climate

Climate conditions at Fort St. James and PG weather stations have changed over the last 100 years (Figure 3.6 and Figure 3.7). Historical climate records indicate mean annual precipitation has ranged from 282-770 mm in Fort St. James, 368-934 mm in PG. Average annual precipitation and annual average temperatures have been recorded as 465 mm and 2.8 ˚C for Fort St. James and 633 mm and 3.7˚C for PG. Figure 3.6 and 3.7 depicts trend line comparison for periods 1920-1987 and 1987-2016 that illustrate changes in mean average temperatures and total annual precipitation for all regional areas. Mean average temperature increased 1.2 ˚C and 0.4 ˚C for Fort St James and PG respectively. Total annual precipitation increased 31.2 mm in PG and decreased 24.6 mm in Fort St. James.

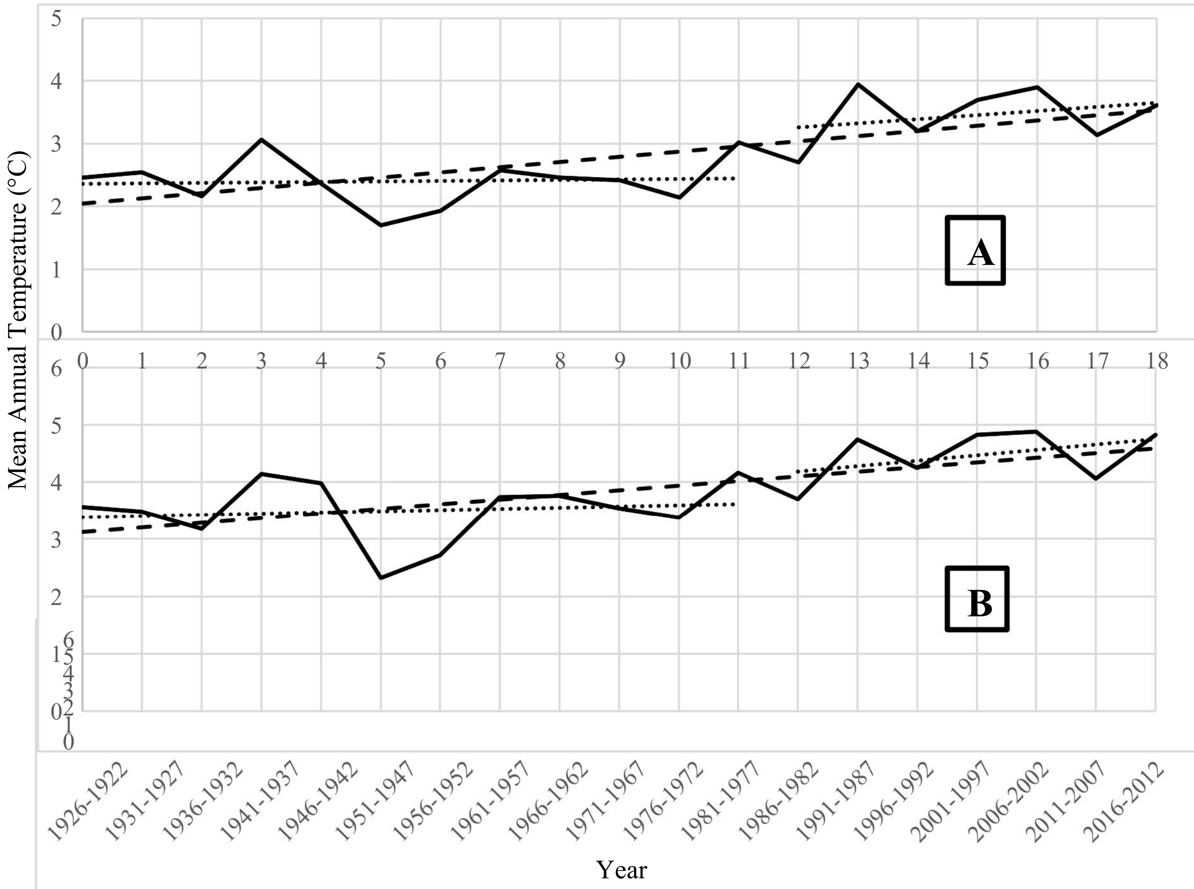

Figure 33.6. Mean annual temperature from Fort St. James (A) and Prince George (B) climate stations from 1920-2016. The solid line represents temperature variation, dotted trend lines represent differences in climate before and after 1987, or the last 30 years, dashed trend line represents entire climate history trend.

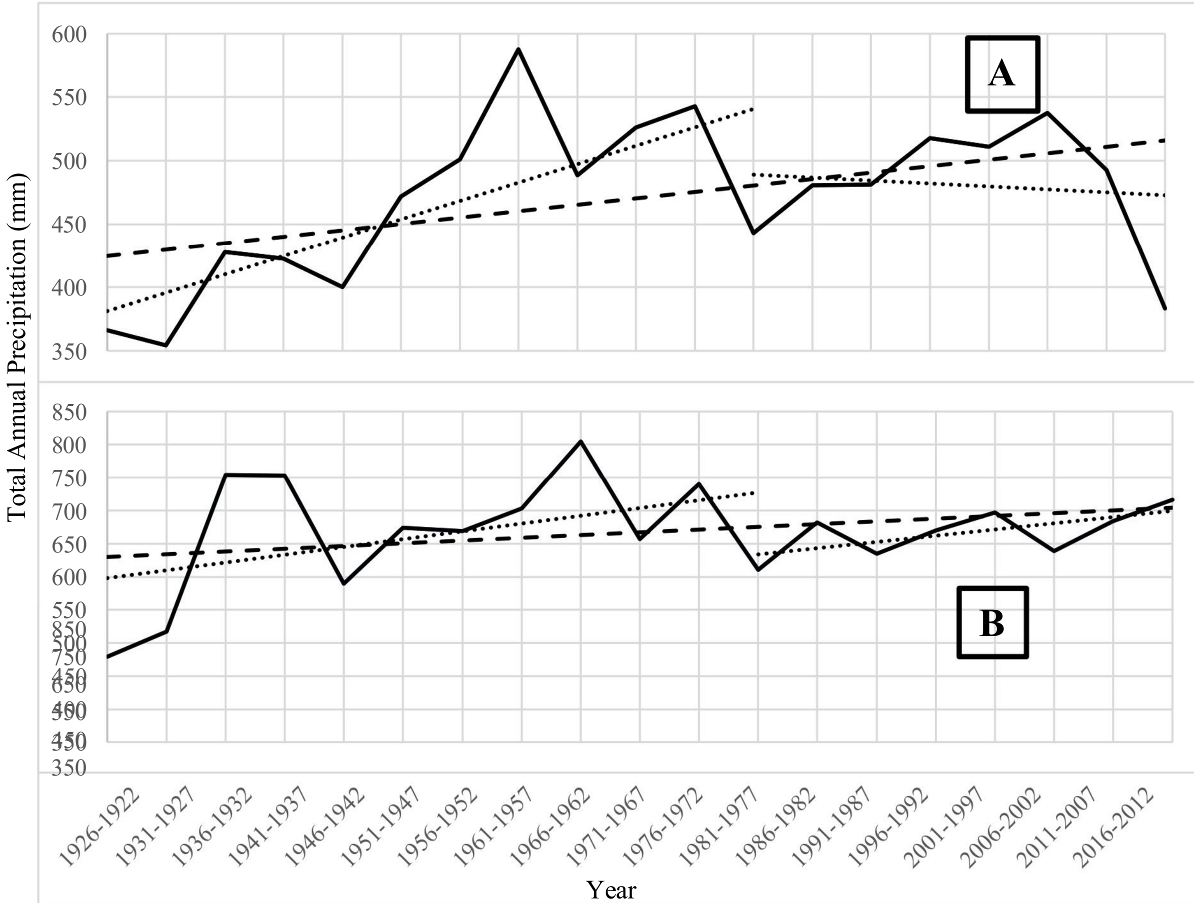

Figure 34.7. Total annual precipitation from Fort St. James (A) and Prince George (B) climate stations from 1920-2016. The solid line represents precipitation variation, dotted trend lines represent differences in climate before and after 1987, or the last 30 years.

3.4.3 Carbon-Climate Correlations

Normality testing determined most percent carbon chronologies were normally distributed excluding N4 chronology that was not used for further analysis (Table 3.5). Several significant correlations were found between percent carbon and the current and previous monthly and seasonal weather record for JPRF and PG (Figures 3.8 – 3.11).

Temperature

Percent carbon chronologies in planted stands of PG were significantly negatively correlated to previous year June, September and December and current year July temperature; significant positive correlations between temperature and percent carbon in planted stands of JPRF were only found for current year September temperatures (Figure 3.8). Percent carbon in natural stand chronologies was significantly negatively correlated in JPRF and positively correlated in PG to several previous and current monthly temperatures (Figure 3.9). Truncated natural percent carbon chronologies in PG were not significantly correlated to any temperature variables. A truncated natural percent carbon chronology in JPRF was positively correlated with previous November and current July and August temperatures.

Precipitation

Percent carbon chronologies in planted stands of JPRF were significantly positively correlated to current February, May, and winter precipitation; significant negative correlations between percent carbon in planted stands of PG were only found for previous November and average spring precipitation (Figure 3.10). Truncated chronologies indicated better sensitivity to precipitation in both JPRF and PG. JPRF full-length natural stand percent carbon chronologies were positively correlated to previous and current July and September

(Figure 3.11). Truncated JPRF natural stand percent carbon chronologies were significantly negatively correlated with current March and positively correlated with previous September and current March, September, and winter precipitation (Figure 3.11). Percent carbon chronologies in natural stands of PG were significantly negatively correlated to previous July and positively correlated to summer precipitation; truncated percent carbon chronologies in PG natural stands were significantly positively correlated to current June and summer precipitation (Figure 3.11).

Table 3.5. Normality testing for percent carbon values for natural and planted stands surrounding the John Prince Research Forest (N1-N3; P1-P3) and Prince George (N4-N6; P4-P6) including skewness, kurtosis and Shapiro-Wilk (SW) values. Although skewness and kurtosis values > +14 or < -1 are considered not normal data, SW values were used due to small sample sizes. Shapiro-Wilk values <0.050 were not accepted as normal data.

Site	Skewness	Kurtosis	SW
N1	0.592	1.951	0.054
N2	-0.730	1.011	0.719
N3	-0.557	-0.236	0.347
P1	1.269	1.000	0.207
P2	0.505	0.490	0.967
P3	1.513	2.049	0.135
N4	-2.126	4.043	0.001
N5	0.421	-1.622	0.056
N6	0.234	2.367	0.648
P4	0.504	-1.015	0.691
P5	0.943	-0.677	0.204
P6	1.154	0.548	0.202

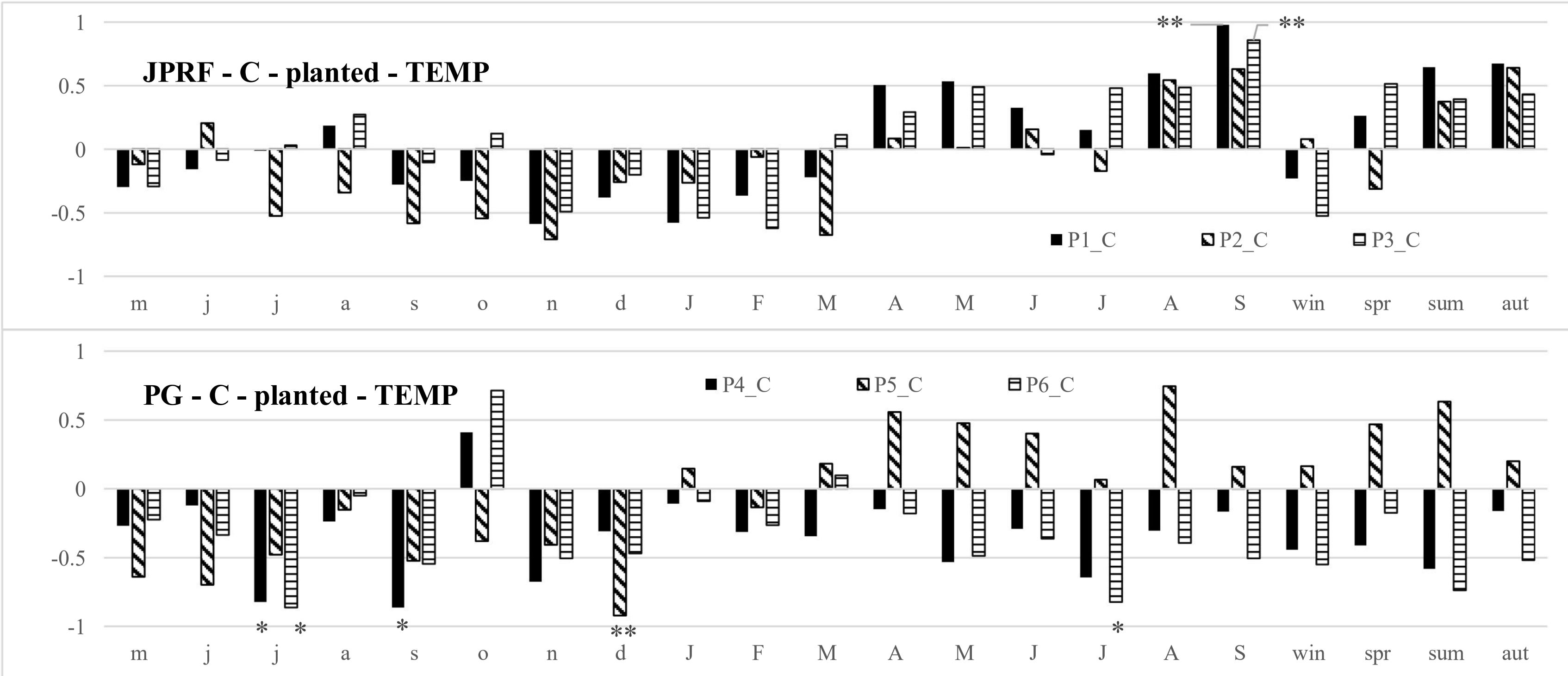

Figure 35.8. Pearson's correlation coefficient between average monthly temperature (ºC) and percent carbon for natural (N) and planted (P) stands surrounding the John Prince Research Forest (N1-N3, P1-P3) and Prince George (N4-N6, P4-P6) ** p = 0.01; * = 0.05 level. Months are represented by lower and upper case letters, respectively; win = winter, spr = spring, sum= summer, aut = autumn.

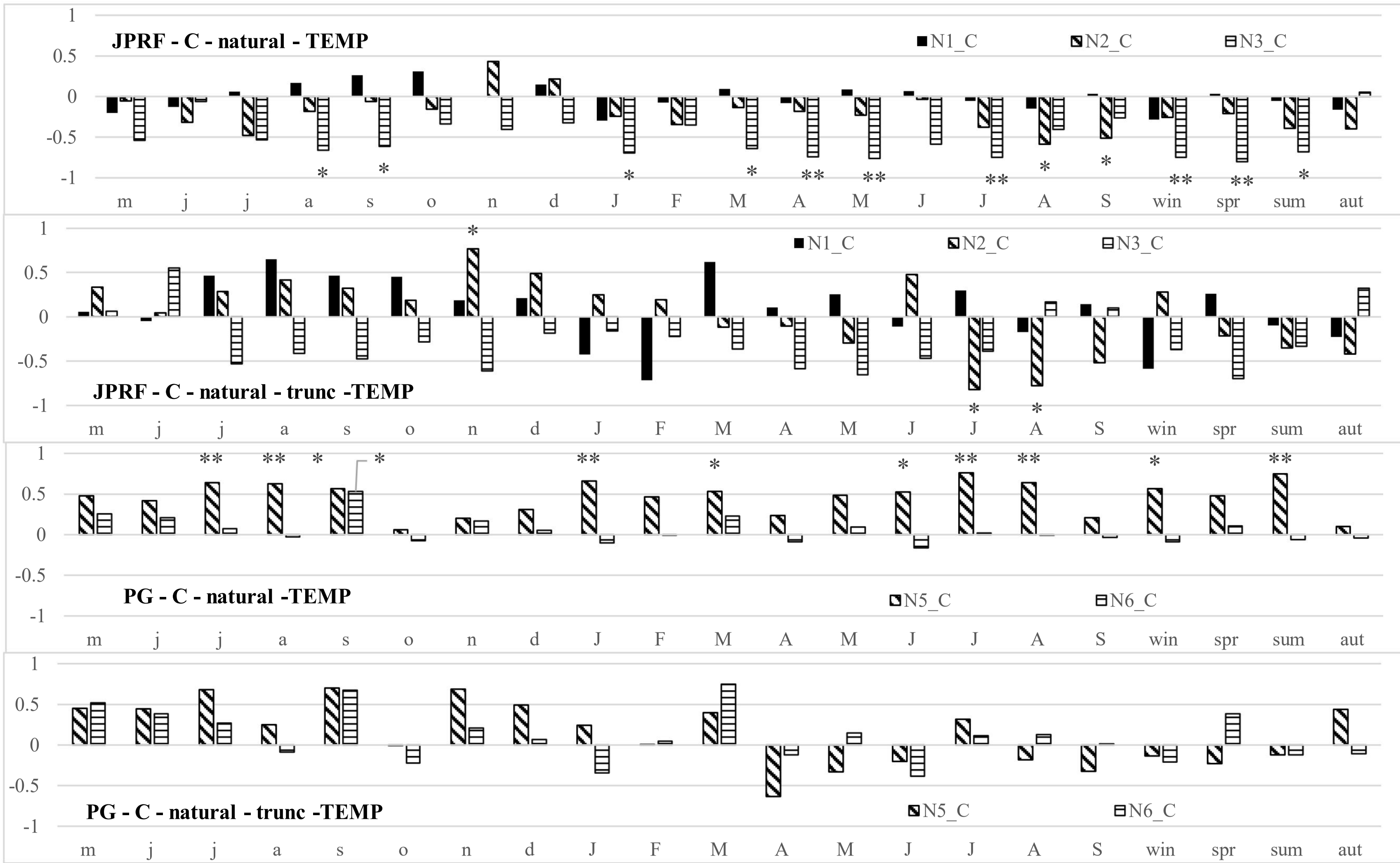

Figure 36.9. Pearson's correlation coefficient between average monthly temperature (ºC) and percent carbon for natural (N) and planted (P) stands surrounding the John Prince Research Forest (N1-N3, P1-P3) and Prince George (N4-N6, P4-P6) ** p = 0.01; * = 0.05 level. Months are represented by lower and upper case letters, respectively; win = winter, spr = spring, sum= summer, aut = autumn.

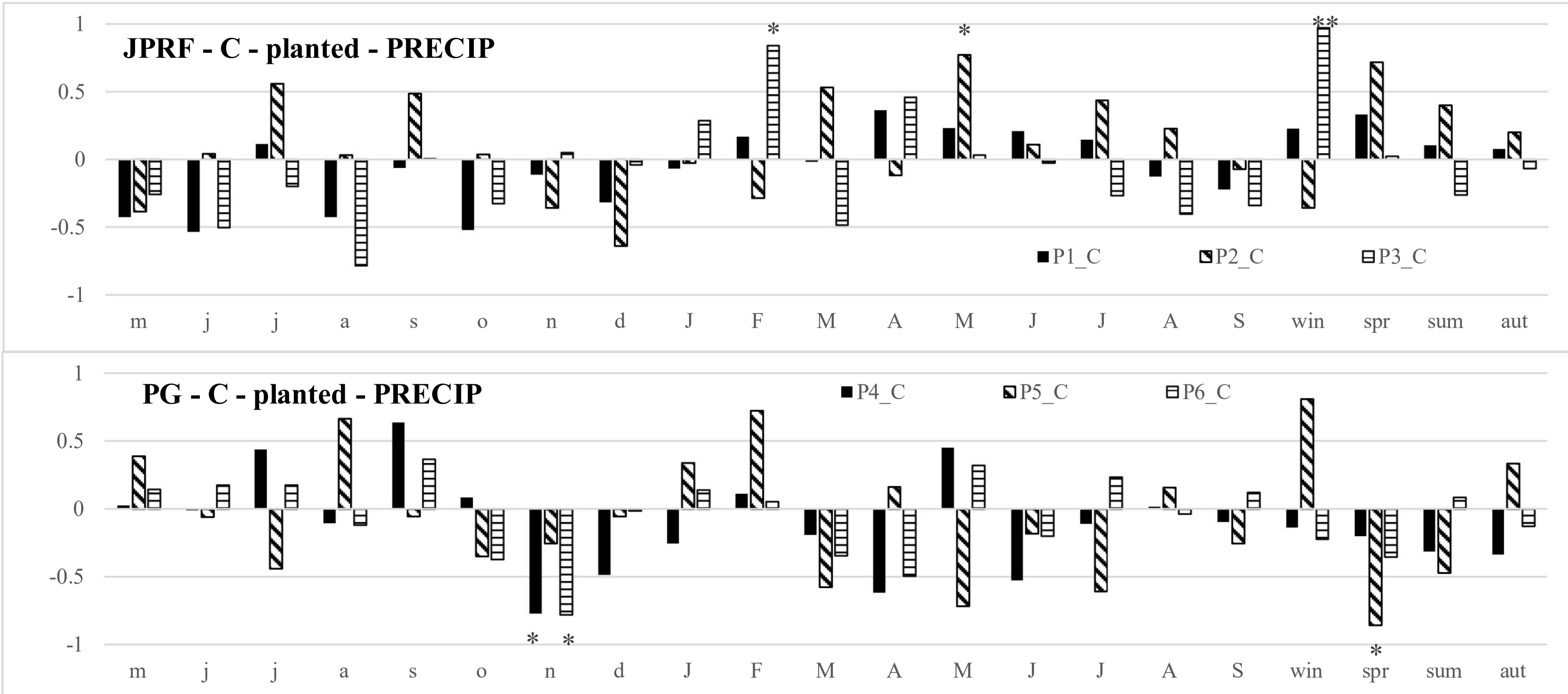

Figure 37.10. Pearson's correlation coefficient between average monthly precipitation (mm) and percent carbon for natural (N) and planted (P) stands surrounding the John Prince Research Forest (N1-N3, P1-P3) and Prince George (N4-N6, P4-P6) ** p = 0.01; * = 0.05 level. Months are represented by lower and upper case letters, respectively; win = winter, spr = spring, sum= summer, aut = autumn.

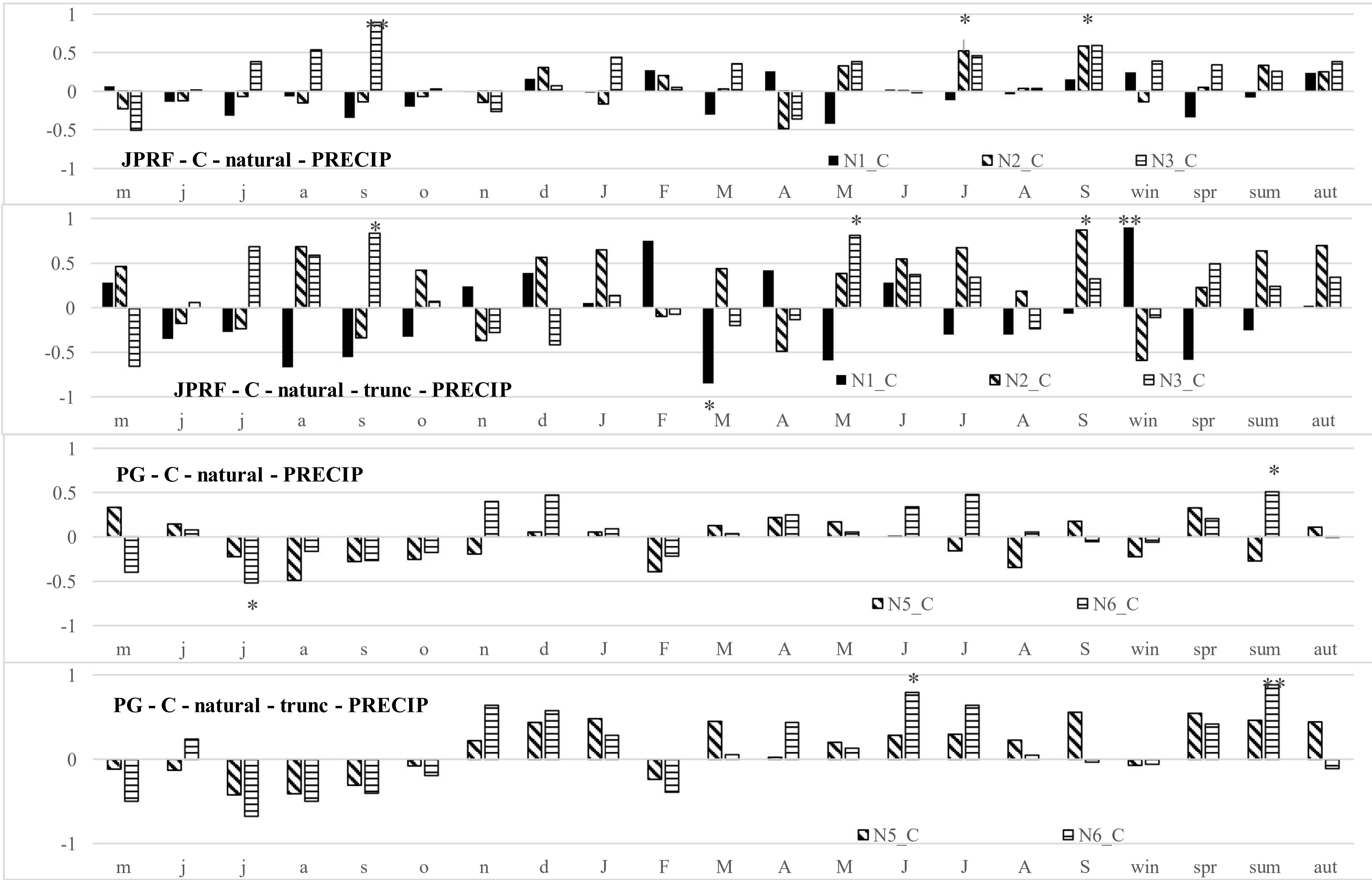

Figure 38.11. Pearson's correlation coefficient between average monthly precipitation (mm) and percent carbon for natural (N) and planted (P) stands surrounding the John Prince Research Forest (N1-N3, P1-P3) and Prince George (N4-N6, P4-P6) ** p = 0.01; * = 0.05 level. Months are represented by lower and upper case letters, respectively; win = winter, spr = spring, sum= summer, aut = autumn.

3.4.4 Regression Analysis and Comparison of Measured and Modelled Values

Percent carbon values were modelled from climate variables and correlations between measured percent carbon and modelled percent carbon are found in Table 3.6 and Table 3.7. Although numerous significant relationships were found between climate and JPRF and PG percent carbon in regression analysis, the models presented below reflect the strongest relationships found between percent carbon and winter, spring, and summer climates (Figures 3.11-3.14). Unusually high R_2 values were found in planted stands (e.g. P3) that may be a result of small sample size.

Table 3.6. Regression analysis between total monthly precipitation (mm) (Precip), average monthly temperature (ºC) (Temp) and percent carbon chronologies for natural (N) and planted (P) stands surrounding John Prince Research Forest (JPRF) (N15-N3, P1-P3). R_2 values only accepted if > 0.4. ** p = 0.01; * = 0.05 level. Months are represented by lower and upper case letters, respectively. Correlation statistics (Pearson's R & p-value) results between measured (M) and modelled (MX) percent carbon values also presented for every model. Grey shading indicates natural stand chronologies.

Precip	Site	C (R_2)	MvsMX (Pearson's R)	p-value	**Temp**	Site	C (R_2)	MvsMX (Pearson's R)	p-value
FEB	P3	0.709*	0.842	0.035	JAN	N3	0.485**	0.696	0.017
MAR	N1trunc	0.718**	0.848	0.016	MAR	N3	0.411*	0.641	0.033
MAY	P2	0.599*	0.774	0.041	APR	N3	0.547**	0.74	0.009
SEP	N2	0.757**	0.87	0.011	JUL	N2trunc	0.669*	0.818	0.025
WIN	P3	0.941**	0.97	0.001		N3	0.555**	0.745	0.009
	N1trunc	0.809**	0.899	0.006	aug	N3	0.439*	0.663	0.026
					AUG	N2trunc	0.608*	0.779	0.039
					SEP	P1	0.959**	0.908	0.001
						P3	0.736*	0.663	0.026
					nov	N2trunc	0.591*	0.769	0.044
					SPR	N3	0.639**	0.8	0.003
					SUM	N3	0.466*	0.683	0.021
					WIN	N3	0.559**	0.8	0.003

Table 3.7. Regression analysis between total monthly precipitation (mm) (Precip), average monthly temperature (ºC) (Temp) and percent carbon chronologies for natural (N) and planted (P) stands surrounding Prince George (N4-N6, P4-P6). R_2 values only accepted if > 0.4. ** p = 0.016; * = 0.05 level. Months are represented by lower and upper case letters, respectively. Correlation statistics (Pearson's R & p-value) results between measured (M) and modelled (MX) percent carbon values also presented for every model. Grey shading indicates natural stand chronologies.

Precip	Site	C (R_2)	MvsMX (Pearson's R)	p-value	**Temp**	Site	C (R_2)	MvsMX (Pearson's R)	p-value
JUN	N6	0.627**	0.792	0.034	JAN	N5	0.432**	0.657	0.006
nov	P4	0.593*	0.770	0.043	jul	N5	0.414**	0.643	0.007
	P6	0.609*	0.781	0.038		P4	0.675*	0.822	0.023
SPR	P5	0.734*	0.857	0.029		P6	0.748**	0.865	0.012
					JUL	N5	0.574**	0.758	0.001
						P6	0.678*	0.823	0.023
					AUG	N5	0.408**	0.639	0.008
					sep	P4	0.748**	0.865	0.012
					dec	P5	0.851**	0.922	0.009

Winter Relationships

Measured values had a close relationship with modelled percent carbon values based on winter temperatures in N3, N5, and P5 (Figure 3.12). The models had some areas of poor association with measured values in 1951-1947 and 1981-1977 in N1, 1982-1996 and 2002-2011 in N5, and 1998-2002 in P5 (Figure 3.12).

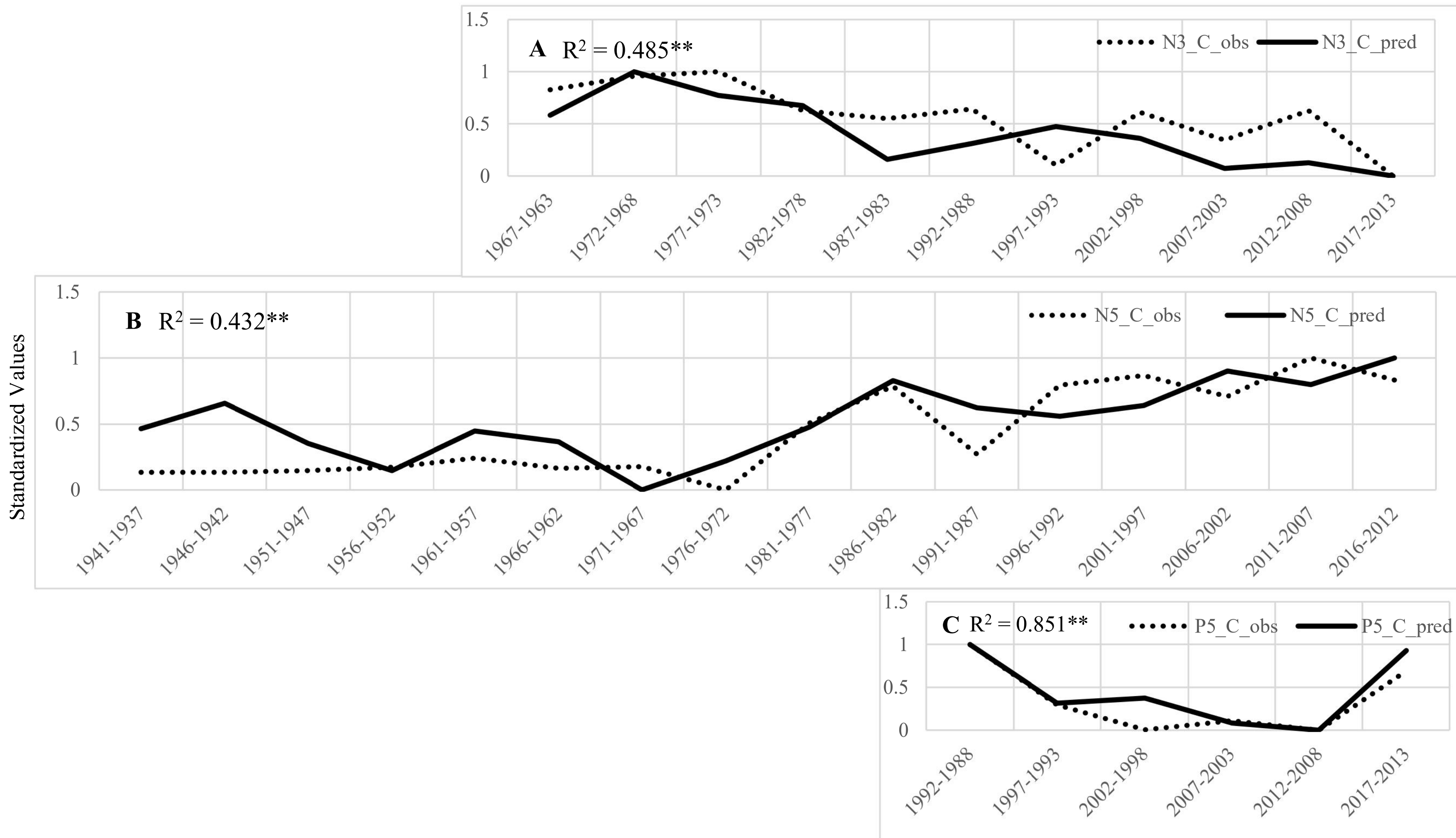

Figure 39.12. Measured (dotted line) vs modelled (solid line) normalized percent carbon values from natural (N3, N5) and planted (P5) stand of spruce in central interior British Columbia within the John Prince Research Forest and surrounding Prince George. Data modelled from current year January temperature (A, B) and previous year December temperature (C) from Fort St. James and Prince George climate stations. R_2 values are presented with ** p =0.01 and * p= 0.05. Note not all axis are the same scale.

Spring Relationships

Measured values had a close relationship with modelled percent carbon values based on spring precipitation and temperature in P5, N1trunc, and N3; however, measured and modelled values decouple in 1963-1972 in N1trunc and 1983-1987 in N3 (Figure 3.13). Modelled percent carbon values from P2 are poorly correlated to measured values from 1982-1996 (Figure 3.13).

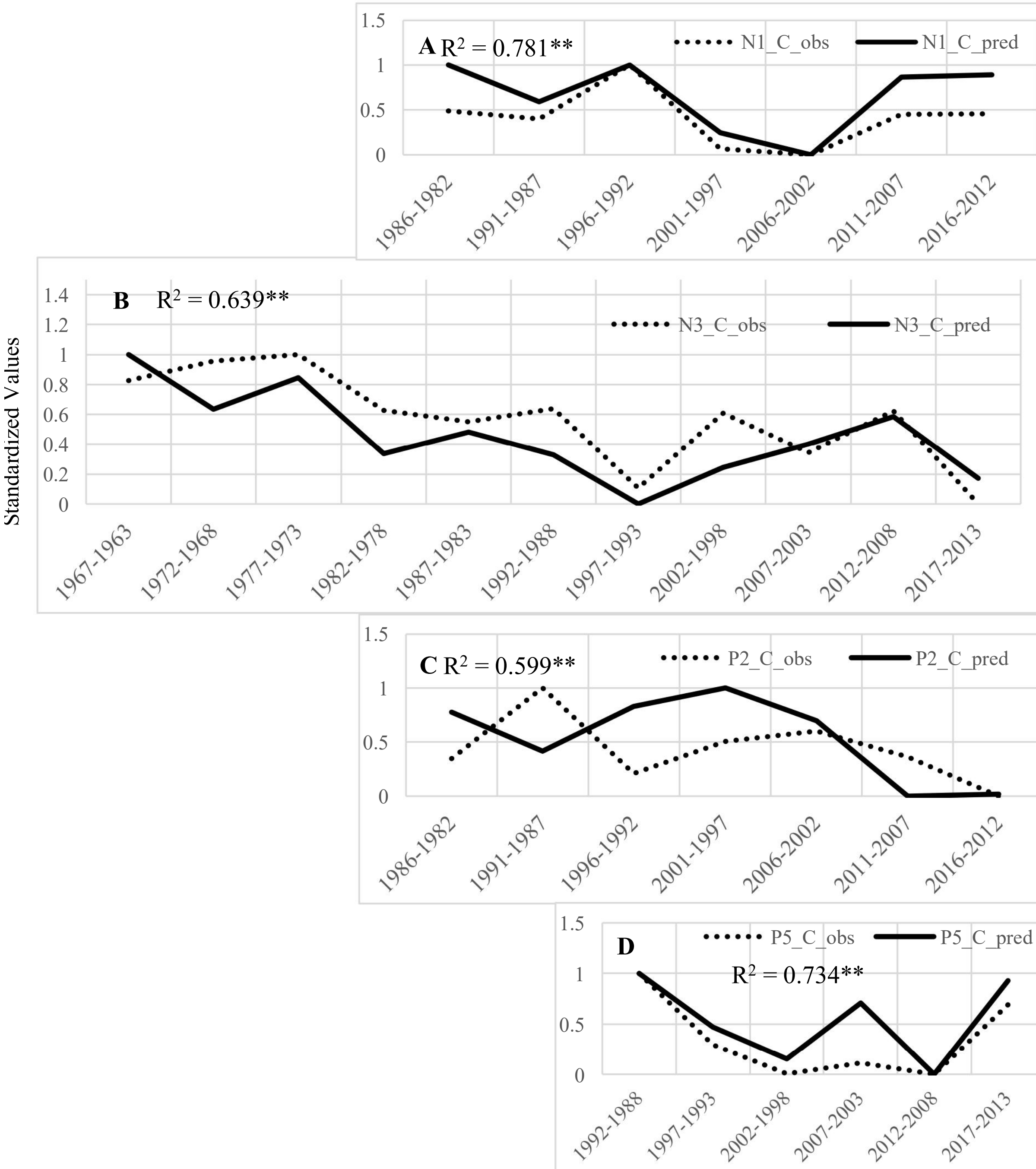

Figure 40.13. Measured (dotted line) vs modelled (solid line) normalized percent carbon values of planted (P2, P5) and natural (N1trunc, N3) stands of central interior British Columbia spruce. Data modelled from current mean March (A), May (C), and average spring precipitation (D) and average spring temperature values (B). Note not all x-axis the same. R_2 values are presented with ** p =0.01 and * p= 0.05. Note not all axis are the same scale.

Summer relationships

Measured values and values of percent carbon modelled from previous July temperatures are strongly correlated in planted stands from PG with some decoupling occurring between 1997-2006 in P4 and 1982-1986 in P6 (Figure 3.14). Values of percent carbon in natural stands modelled from current July temperatures accurately predict measured values (Figure 3.15). Some areas of decoupling between measured and modelled values of percent carbon occur between 2012-2016 in N2trunc, between 1983-1992 and 2003-2007 in N3 and between 1937-1941, 1982-1991 and 2007-2016 in N5 (Figure 3.15).

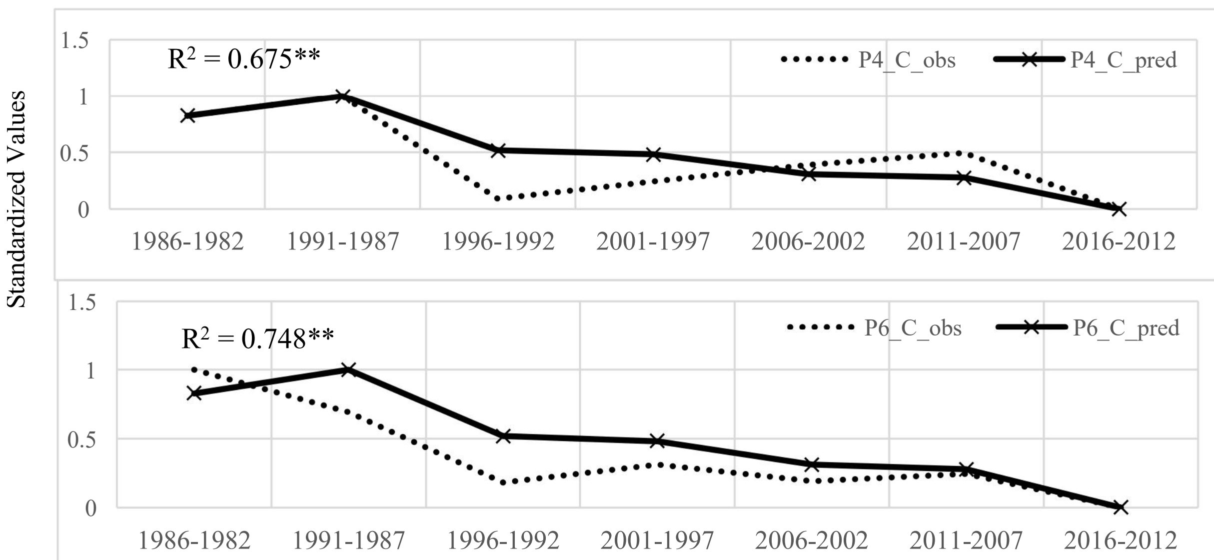

Figure 41.14. Measured (dotted line) vs modelled (solid line; crossed solid line indicates 1-year lagged data) normalized percent carbon values from planted (P4, P6) stands of spruce in central interior British Columbia surrounding Prince George. Data modelled from previous July temperature from Prince George climate stations. R2 values are presented with ** p =0.01 and * p= 0.05.

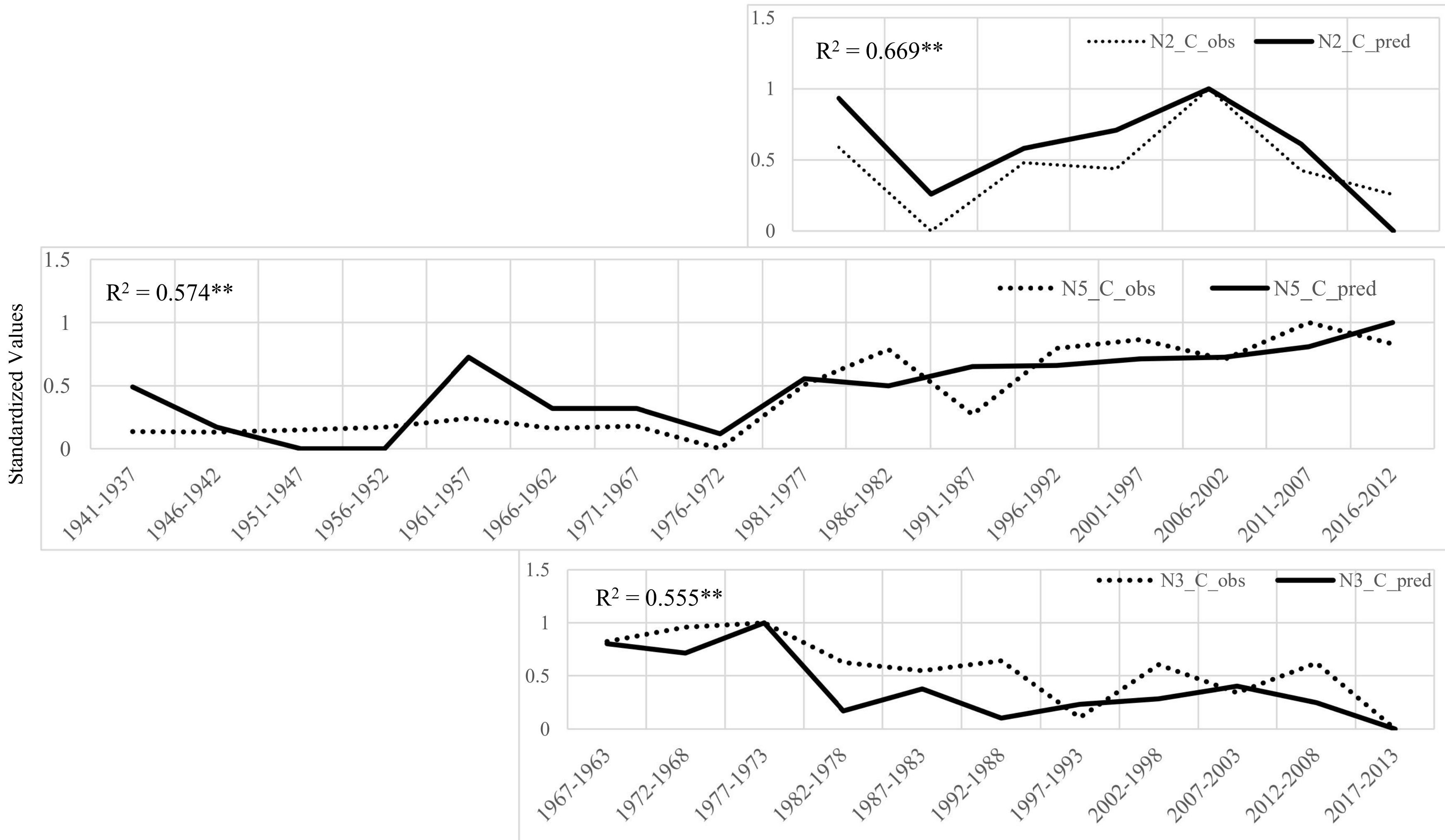

Figure 42.15. Measured (dotted line) vs modelled (solid line) normalized percent carbon values from natural stands (N2trunc, N3, N5) of spruce in central interior British Columbia within the John Prince Research Forest and surrounding Prince George. Data modelled from current July temperature from Fort St. James and Prince George climate stations. R_2 values are presented with ** p =0.01 and * p= 0.05. Note not all axis are the same scale.

3.5 DISCUSSION

3.5.1 Individual Stands and Average Regional Percent Carbon Content

Results of this study show significant differences between individual stand percent carbon values in JPRF. Literature suggests that carbon content can vary depending on geographical and environmental factors (Pettersen 1984; Hughes et al. 1999; Elias and Potvin 2003; Martin and Thomas 2011). Higher percent carbon content of P2 and N1 may be attributed to site-specific differences, similar to relationships between radial growth and soil water volume, crown cover, nutrient availability, and topography (Wang et al. 2003; Weber et al. 2018). For example, the warmer south-facing slope of P2 receives more sunlight and may allow for increased snow-melt and soil thaw in comparison with the flat topography of P1 and P3. These conditions in P2 may result in increased growing season length that could directly affect percent carbon accumulation (Rossi et al. 2007). Higher percent carbon content of N1 may be attributed to the stream at this site that could stabilize or increase the soil moisture content. This increased moisture in N1 could counteract the unfavourable conditions of rising temperatures coupled with reduced precipitation seen in Fort St. James climate, an observation found in other studies with similar climatic conditions (Guehl 1985; McMahon et al. 2010; Hember et al. 2012). There is also evidence of increased carbon sequestration in trees grown in wet versus dry conditions (Li et al. 2015).

Results suggest that there are no significant differences between average percent carbon in natural versus planted stands at the regional level. This observation was somewhat unexpected because the younger planted stands have larger proportions of juvenile wood than natural stands. Although it has been reported that juvenile wood contains higher percent carbon than mature wood due to the larger proportions of lignin and extractive concentrations, samples within this study had chemical extractives, or non-structural carbon, removed (Zobel and Van Buijtenen 1989; Bert et al 2006). Therefore, based on structural cell properties alone, fast-growing, thin-walled, and low-density cells typical of juvenile wood should have a lower structural percent carbon content than denser, thicker cells, found in mature wood (Bao et al. 2001). Although not statistically tested, Figure 3.4 shows general trends in percent carbon of juvenile wood being less than that of mature wood. However, the high variability in juvenile wood percent carbon and the small sample size limit our confidence in this finding.

3.5.2 Percent Carbon and Cell Wall Thickness and Density

Relationships between percent carbon and average RW, EW, LW and mean, maximum, and minimum cell wall thickness and density values of JPRF natural and planted stands only existed in N2, N3 and P1; lack of more significant relationships between percent carbon and RW, EW, LW, cell wall thickness, and density in planted stands was likely due to small sample size. Relationships between percent carbon and average RW, EW, LW and maximum cell wall thickness and density values in N2 suggest that higher amounts of cellulose and lignin (as represented by a thicker cell wall and denser wood) correspond to greater proportions of percent carbon; maximum values appeared to have stronger relationships than RW, EW, or LW values. Relationships found between percent carbon and mean and minimum cell wall thickness and density values of N2 and N3 and average RW in P1 suggest that increases in cell materials contributing to larger, thicker cells and larger rings, such as cellulose and lignin, corresponded to reduced proportions of percent carbon. These results are similar to previous work in western Canada and Alaska showing correlations between forest productivity and LW(max) and other studies relating carbon to biomass and density, with maximum values of cell wall thickness and density as the best predictors of percent carbon (Elias and Potvin 2003; Zhang et al. 2009; Martin and Thomas 2011; Castaño-Santamaría and Bravo 2012; Beck et al. 2013; Navarro et al. 2013; Weber et al. 2018). Average RW, EW, and LW are also good indicators of percent carbon and may be preferred as proxies over maximum cell wall thickness and density due to their ease of measurement and the reduced cost of analysis. However, the lack of standardized sampling protocols to prepare samples for carbon measurements, such as kiln-drying (Lamlom and Savidge 2003), freeze-drying and oven-drying at varying temperatures, such as 105 ºC (Thomas and Malczewski 2007) and 70 ºC (Gower et al. 2001; Wang et al. 2003), makes cross-study comparisons difficult to interpret (Zhang et al. 2009; Jones and Hara 2017). Nevertheless, the relationships identified here suggest that maximum cell wall thickness and density and average RW, EW, and LW values may be good indicators of percent carbon variation in natural and planted stands (Beck et al. 2013). Although other studies have found similar trends in relationships with mean density (Xiang et al. 2014), the use of maximum values may improve statistical strength in relationships between percent carbon and cell wall thickness and density because they provide additional detail regarding radial growth that is lost in investigation of average (mean) values. Finally, the relationships between carbon and density and cell wall thickness could provide greater accuracy in carbon approximations that are often crudely determine biomass/carbon content as a function of tree height and DBH (Somogyi et al. 2007; Kearsley et al. 2013; Ali et al. 2016; Weber et al. 2018). Although there is evidence that in some species tree DBH is a good variable for carbon estimations, as increasing tree diameter allows for increased biomass and thus increased carbon (Elias and Potvin 2003; Usuga et al. 2010; Navarro et al. 2013), this trend is not consistent across studies (Clark et al 2003; Navarro et al. 2013).

3.5.3 Percent Carbon vs Climate

Relationships between percent carbon and climate over time were successfully modeled using percent carbon chronologies from planted and natural spruce stands in central interior BC and current and one-year lagged precipitation and temperature variables from Fort St. James and PG climate stations. These results could provide a novel approach for estimates of climate effects on carbon accumulation. However, planted stand models lacked reliability due to small sample sizes, which can increase the likelihood of type II statistical error of failing to reject a false null hypothesis (Knudson and Lindsey 2014). Increased sampling error and outlier influences that question validity may also occur with small sample sizes (Knudson and Lindsey 2014). Consequently, few regression models of planted stands were compared to measured values. Nonetheless, some generalizations can be made of the relationship between percent carbon and precipitation and temperature in most of the planted stands in addition to natural stand relationships. Although there were numerous significant correlations between percent carbon and climate, winter and spring temperature and precipitation and current July temperatures had the strongest influence on percent carbon in planted and natural stands of PG and JPRF. Correlations also suggest that September temperatures also influenced radial growth, however, models lacked reliability.

Winter, Spring, and Summer Temperature

Results from this study show that reductions in percent carbon in planted stands of PG and natural stands in JPRF are related to increases in Fort St. James and PG previous December, current January, average spring, and previous and current July temperatures. Increased temperatures during winter months can reduce length of snow cover and reduce accumulated winter precipitation, or insulation, leading to deeper soil freezing (Jarvis and

Linder 2000). These conditions can prevent or reduce absorption of melting snow thus delaying bud burst and percent carbon accumulation in spring months (Peterson et al. 2002; Chavardès et al. 2013). Additionally, increasing spring or summer temperatures beyond optimal growth thresholds have been shown to reduce or halt growth, and subsequent carbon accumulation, in previous studies of BC interior spruce (Zhang et al. 1999; Flower and Smith 2011; Oberhuber et al. 2014). Alternatively, rising winter and summer temperatures in PG were related to increased percent carbon of N5, which is likely due to favourable site-specific characteristics. Rising temperature coupled with N5's higher elevation, typically higher precipitation, and cooler temperatures (SBS very-wet-cool), may have allowed for increased percent carbon accumulation; similar relationships have been found between warming temperatures and forest productivity under favourable conditions (Guehl 1985; McMahon et al. 2010; Hember et al. 2012).

Spring Precipitation

Percent carbon accumulation in JPRF and PG was related to spring precipitation variation. Various site-specific differences occurred in relationships between spring precipitation and percent carbon in natural (N1trunc) and planted (P2, P5) stands of JPRF and PG. Results suggest that decreases in Fort St. James spring precipitation were related to reduced percent carbon accumulation in P2 and enhanced carbon accumulation in N1trunc. Although the model of percent carbon in P2 was poorly related to measured values, reductions in May precipitation may have negatively affected percent carbon accumulation in P2 due to the south-facing slope. The warmer south-facing slope of P2 could cause increased rates of evaporation and transpiration and reduced soil moisture that may lead to reduced carbon accumulation in P2 compared to the other planted stands. Reductions in March precipitation, which typically falls as snow in this region, were related to increases in carbon accumulations in N1trunc. Reductions in March precipitation, or snow depth, could lead to earlier bud burst and an extension of the growing season length and subsequent increased radial growth and carbon accumulation (Peterson et al. 2002; Chavardès et al. 2013). In PG, results suggest that reductions in percent carbon in P5 related to increasing average spring precipitation. Increased and prolonged precipitation could have been related to reduced cell production and subsequent carbon accumulation in P5 with decreases in light availability and allowable energy for photosynthesis with increases in cloud cover (Polge 1970; Kozlowski 1979; Martin and Thomas 2011).

3.5.4 Relationships in Natural and Planted Stands with Climate

Percent carbon accumulation in planted and natural stands in JPRF and PG appear to be negatively influenced by rising temperatures with some site-specific differences in relationships with spring climate variation. However, only general statements can be made comparing relationships between natural and planted stands with climate due to the inability to evaluate percent carbon of planted and natural stands within the same time period of growth. Percent carbon was only determined for the last 40 years of growth for planted stands and the last 80 years of growth for natural, which resulted in greater proportions of juvenile wood in planted stands (Cameron et al. 2005; Alteyric et al. 2006). Attempts to separate juvenile wood and mature wood were not possible and standardized detrending techniques have not been developed for percent carbon. However, several studies have suggested that mature trees may be more resilient to acute changes in climate than planted trees whereas others have suggested that mature trees have higher climate sensitivity than younger trees (Merian and Lebourgeois 2011; Schuster and Oberhuber 2013; Oberhuber 2017).

3.5.5 Differences between Truncated and Full-length Natural Chronologies in JPRF and PG

Percent carbon measurements from JPRF natural stands from the last 30 years were more strongly related to climate variation compared to full-length JPRF natural stand chronologies; these relationships were not seen in natural stand data from PG. These relationships could indicate that temperature and precipitation variation in JPRF have become more influential in determining percent carbon accumulation than earlier in the time series, an observation seen in radial growth and climate in other studies (Tardif et al. 2003; Camarero et al. 2015; Peñuelas et al. 2007; Martin-Benito et al. 2013). Historical climate of Fort St. James shows rising temperatures coupled with stark reductions in precipitation, which may explain stronger relationships between climate variation and percent carbon in recent decades. Similar relationships may not have been seen in truncated percent carbon chronologies of PG natural stands because of differences in climate regimes. Historical records of PG climate report roughly 200 mm higher average precipitation and 1˚C higher average temperature than Fort St. James climate. In recent decades, records in PG also show stable increases in precipitation that contrasts stark decreases in Fort St. James. Higher and stable average precipitation coupled with increasing temperatures, as seen in the PG climate records, suggests conditions are more favorable for growth than in warmer, drier conditions of JPRF. This may explain fewer relationships between full-length natural stand chronologies of PG and the lack of relationships in truncated natural stand chronologies of PG. Results from this study may indicate trees in JPRF are reaching growth-thresholds with long-term climate warming coupled with recent reduction in precipitation, not yet seen in PG stands (Lo et al. 2010; Camarero et al. 2015; Lazarus et al. 2018).

3.6 CONCLUSION

This study sought to determine relationships between percent carbon and cell wall thickness, density, and climate in natural and planted stands of hybrid white spruce of central interior BC surrounding JPRF and PG. Comparisons were made between percent carbon in individual stands and between regional-level stand aggregates. Although regional-level stand aggregates were not found to differ, differences in percent carbon between individual stands may be due to site-specific differences. Comparing structural percent carbon measurements to cell wall thickness and density and comparing percent carbon to climate over time provide novel approaches that may improve estimates of carbon sequestration as past research has mainly focused on biomass equations instead of direct measurements of volatile and structural carbon (Zabek and Prescott 2006; Castaño-Santamaría and Bravo 2012).

Relationships between percent carbon and RW, EW, LW and mean, minimum and maximum density and cell wall thickness suggest that RW, EW, LW and maximum values may be good indicators of percent carbon in some natural or planted stands. Use of maximum cell wall thickness and density values may improve statistical strength over mean values because they provide greater detail in radial growth that is lost in investigation of average (mean) values. These relationships presented here could improve carbon approximations in above ground tree biomass calculations that are normally derived from tree height and DBH.

Review of historical climate indicated annual temperature has increased in JPRF and PG areas with some indication of marginal reductions in temperatures within the last 30 years in JPRF. Historical records of total annual precipitation in JPRF and PG have shown an overall increase since 1930 with stark decreases in JPRF within the last 30 years. Relationships between climate and percent carbon indicate that rising winter, spring and summer temperatures coupled with reduced precipitation were strongly related to reduced percent carbon accumulation in most natural and planted stands. Relationships between spring climates and percent carbon were variable, likely due to site-specific variation. Some percent carbon chronologies from JPRF natural stands more strongly related to climate variation in the last 30 years of growth compared to the entire time series. Truncated data from natural stands in the PG region did not have similar relationships. These results may indicate that increased temperatures coupled with reduced precipitation has an amplified effect on recent natural stand percent carbon accumulation in JPRF. Regional climate of JPRF and PG appear to effect statistical relationships with carbon. In areas with adequate precipitation and increasing temperatures, like PG, carbon sequestration processes were shown to be less associated with climate compared to drier sites, like JPRF.

Development of a standardized percent carbon measurement sampling protocol for comparison with wood properties would be valuable to improve on understanding relationships found in this study. Validation of modelled percent carbon accumulation within natural and planted stands of JPRF and PG is critical as this methodology is under-utilized in determining relationships between climate and carbon. Changes in tree productivity with projected changes in climate may be better understood with analysis in future studies of percent carbon measurements within natural and planted stands (Montwé et al. 2014).

3.7 REFERENCES

Allen CD, Macalady AK, Chenchouni H, Bachelet D, McDowell N, Vennetier M, Kitzberger T, Bigling A, Breshears DD, Hogg EH, Gonzalez P, Fensham R, Zhang Z, Castro J, Demidova N, Lim J-H, Allard G, Running SW, Semerci A, Cobb N. 2010. A global overview of drought and heat-induced tree mortality reveals emerging climate change risks for forests. Forest Ecology and Management. 259(4): 660–684. https://doi.org/10.1016/j.foreco.2009.09.001

Ali A, Yan ER, Chen HYH, Chang SX, Zhao YT, Yang XD, Xu MS. 2016. Stand structural diversity rather than species diversity enhances aboveground carbon storage in secondary subtropical forests in Eastern China. Biogeosciences, 13(16): 4627–4635. https://doi.org/10.5194/bg-13-4627-2016

Alteyrac J, Cloutier, Zhang ASY. 2006. Characterization of juvenile wood to mature wood transition age in black spruce (*Picea mariana* (Mill.) B.S.P.) at different stand densities and sampling heights. Wood Science & Technology, 40; 124–138. https://doi.org/10.1007/s00226-005-0047-4

Babst F, Alexander MR, Szejner P, Bouriaud O, Klesse S. Roden J, Ciais P, Poulter B, Frank D, Moore DJP, Trouet V. 2014. A tree-ring perspective on the terrestrial carbon cycle. Oecologia. 176(2): 307–322. https://doi.org/10.1007/s00442-014-3031-6

Bao FC, Jiang ZH, Jiang XM, Lu X,. Luo XQ, Zhang SY. 2001. Differences in wood properties between juvenile wood and mature wood in 10 species grown in China. Wood Science and Technology. 35: 363-375.

Beck PSA, Andreu-Hayles L, D'Arrigo R, Anchukaitis KJ, Tucker CJ, Pinzón JE, Goetz SJ. 2013. A large-scale coherent signal of canopy status in maximum latewood density of tree rings at arctic treeline in North America. Global and Planetary Change. 100: 109–118. https://doi.org/10.1016/j.gloplacha.2012.10.005

Bert D, Danjon F. 2006. Carbon concentration variations in the roots , stem and crown of mature *Pinus pinaster* (Ait.). Forest Ecology and Management. 222: 279–295. https://doi.org/10.1016/j.foreco.2005.10.030

Blanchette D, Fournier RA, Luther JE, Cote JF. 2015. Predicting wood fiber attributes using local-scale metrics from terrestrial LiDAR data: A case study of Newfoundland conifer species. Forest Ecology and Management. 347: 116–129. https://doi.org/10.1016/j.foreco.2015.03.013

Bouriaud O, Bréda N, Dupouey J.-L, Granier A. 2005. Is ring width a reliable proxy for stem-biomass increment? A case study in European beech. Canadian Journal of Forest Research. 35(12): 2920–2933. https://doi.org/10.1139/x05-202

Camarero JJ, Gazol A, Sangüesa-Barreda G, Oliva J, Vicente-Serrano SM. 2015. To die or not to die: Early warnings of tree dieback in response to a severe drought. Journal of

Ecology, 103(1): 44–57. https://doi.org/10.1111/1365-2745.12295

Cameron AD, Lee SJ, Livingston AK, Petty JA. 2005. Influence of selective breeding on the development of juvenile wood in Sitka spruce. Canadian Journal of Forest Research, 35(12): 2951–2960. https://doi.org/10.1139/x05-219

Carrer M and Urbinati C. 2004. Age-Dependent Tree-Ring Growth Responses to Climate in *Larix decidua* and *Pinus cembra*. Ecology. 85(3): 730-740

Castaño-Santamaría J, Bravo F. 2012. Variation in carbon concentration and basic density along stems of sessile oak (*Quercus petraea* (Matt.) Liebl.) and Pyrenean oak (*Quercus pyrenaica* Willd.) in the Cantabrian Range (NW Spain). Annals of Forest Science. 69(6): 663–672. https://doi.org/10.1007/s13595-012-0183-6

Chitra-Tarak R, Ruiz L, Dattaraja HS, Mohan Kumar MS, Riotte J, Suresh HS, McMahon SM, Skumar R. 2018. The roots of the drought: Hydrology and water uptake strategies mediate forest-wide demographic response to precipitation. Journal of Ecology 106(4): 1495–1507. https://doi.org/10.1111/1365-2745.12925

Clark DA, Piper SC, Keeling CD, Clark DB. 2003. Tropical rain forest tree growth and atmospheric carbon dynamics linked to interannual temperature variation during 1984-2000. Proceedings of the National Academy of Sciences. 100(10): 5852–5857. https://doi.org/10.1073/pnas.0935903100

Davis SC, Hessl AE, Scott CJ, Adams MB, Thomas RB. 2009. Forest carbon sequestration changes in response to timber harvest. Forest Ecology and Management. 258(9): 2101–2109. https://doi.org/10.1016/j.foreco.2009.08.009

Elias M and Potvin C. 2003. Assessing inter- and intra-specific variation in trunk carbon concentration for 32 neotropical tree species. Canadian Journal of Forest Research. 33(6): 1039–1045. https://doi.org/10.1139/x03-018

Fleming SW and Whitfield PH. 2010. Spatiotemporal mapping of ENSO and PDO surface meteorological signals in British Columbia , Yukon , and southeast Alaska Spatiotemporal Mapping of ENSO and PDO Surface Meteorological Signals in British Columbia, Yukon , and Southeast Alaska. Canadian Meteorological and Oceanographic Society. 48(2): 122–131. https://doi.org/10.3137/AO1107.2010

Fritts HC. 1976. Tree rings and climate. New York (NY): Academic Press Inc.

Gower ST, Krankina IO, Olson RJ, Apps M, Linder S, Wangi C. 2001. Net primary production and carbon allocation patterns of boreal forest ecosystems. Ecological Applications. 11(5): 1395–1411.

Grünwald T and Bernhofer C. 2007. A decade of carbon, water and energy flux measurements of an old spruce forest at the Anchor Station Tharandt. Tellus, Series B: Chemical and Physical Meteorology. 59(3): 387–396. https://doi.org/10.1111/j.1600-

0889.2007.00259.x

Guehl JM. 1985. Étude comparée des potentialités hivernales d'assimilation carbonée de trois conifères de la zone tempérée (*Pseudotsuga menziesii* Mirb., *Abies alba* Mill. et *Picea excelsa* Link.). Ann. Sci. For. 42: 23-38.

Haughian SR, Burton PJ, Taylor SW, Curry C. 2012. Expected effects of climate change on forest disturbance regimes in British Columbia. BC Journal of Ecosystems and Management. 13(1): 1–24.

Hember RA, Kurz WA, Metsaranta JM, Black T, Guy RD, Coops NC. 2012. Accelerating regrowth of temperate-maritime forests due to environmental change. Global Change Biology. 18(6): 2026–2040. https://doi.org/10.1111/j.1365-2486.2012.02669.x

Jones DA and Hara KLO. 2017. The influence of preparation method on measured carbon fractions in tree tissues. Tree Physiology. 36: 1177–1189.

Kauppi PE, Posch M, Pirinen P. 2014. Large impacts of climatic warming on growth of boreal forests since 1960. PLoS ONE, 9(11): 1–6.

Kearsley E, De Haulleville T, Hufkens,K. Kidimbu A, Toirambe B, Baert, G, Huygens D, Kebede Y, Defourny P, Bogaert J, Beckman H, Steppe K, Boeckx P, Verbeeck H. 2013. Conventional tree height-diameter relationships significantly overestimate aboveground carbon stocks in the Central Congo Basin. Nature Communications. 4. https://doi.org/10.1038/ncomms3269

Knudson DV and Lindsey C. 2014. Type I and Type II errors in correlations of various sample sizes. Comprehensive Psychology, 3(1): 2165-2228. https://doi.org/10.2466/03.CP.3.1

Lachenbruch B and Mcculloh KA. 2014. Tansley review Traits , properties, and performance : how mechanical functions in a cell, tissue, or whole. New Phytologist. 204(4): 747–764.

Lamlom SH and Savidge RA. 2003. A reassessment of carbon content in wood: variation within and between 41 North American species. Biomass and Bioenergy, 25: 381–388. https://doi.org/10.1016/S0961-9534(03)00033-3

Lazarus BE, Castanha C, Germino MJ, Kueppers LM, Moyes AB. 2018. Growth strategies and threshold responses to water deficit modulate effects of warming on tree seedlings from forest to alpine. Journal of Ecology. 106(2): 571–585. https://doi.org/10.1111/1365-2745.12837

Li T, Ren B, Wang D, Liu G. 2015. Spatial variation in the storages and age-related dynamics of forest carbon sequestration in different climate zones-evidence from black locust plantations on the loess plateau of China. PLoS ONE, 10(3). https://doi.org/10.1371/journal.pone.0121862

Liepiņš J, Lazdiņš A, Liepiņš K. 2018. Equations for estimating above- and belowground biomass of Norway spruce, Scots pine, birch spp. and European aspen in Latvia. Scandinavian Journal of Forest Research, 33(1): 58–70. https://doi.org/10.1080/02827581.2017.1337923

Lo YH, Blanco JA, Seely B, Welham C, Kimmins JP. 2010. Relationships between climate and tree radial growth in interior British Columbia, Canada. Forest Ecology and Management. 259(5): 932–942. https://doi.org/10.1016/j.foreco.2009.11.033

Martin AR and Thomas SC. 2011. A reassessment of carbon content in tropical trees. PLoS ONE, 6(8). https://doi.org/10.1371/journal.pone.0023533

Martin-Benito D, Beeckman H, Cañellas I. 2013. Influence of drought on tree rings and tracheid features of *Pinus nigra* and *Pinus sylvestris* in a mesic Mediterranean forest. European Journal of Forest Research. 132(1). https://doi.org/10.1007/s10342-012-0652-3

McDowell NG and Allen CD. 2015. Darcy's law predicts widespread forest mortality under climate warming. Nature Climate Change, 5(7): 669–672. https://doi.org/10.1038/nclimate2641

McMahon MS, Parker GG, Miller DR. 2010. Evidence for a recent increase in forest growth is questionable. Proceedings of the National Academy of Sciences. 107(8): 3611–3615. https://doi.org/10.1073/pnas.1002725107

Millar CI and Stephenson NL. 2015. Temperate forest health in an era of emerging megadisturbance. Science. 349(6250): 823–826. https://doi.org/10.1126/science.aaa9933

Montwé D, Spiecker H, Hamann A. 2014. An experimentally controlled extreme drought in a Norway spruce forest reveals fast hydraulic response and subsequent recovery of growth rates. Trees - Structure and Function, 28(3): 891–900. https://doi.org/10.1007/s00468-014-1002-5

Navarro M, Moya R, Chazdon R, Ortiz E, Vilchez B. 2013. Successional variation in carbon content and wood specific gravity of four tropical tree species. Bosque, 34(1): 9–10. https://doi.org/10.4067/S0717-92002013000100005

Oberhuber W. 2017. Soil water availability and evaporative demand affect seasonal growth dynamics and use of stored water in co-occurring saplings and mature conifers under drought. Trees - Structure and Function, 31(2): 467–478. https://doi.org/10.1007/s00468-016-1468-4

Oberhuber W, Gruber A, Kofler W, Swidrak I. 2014. Radial stem growth in response to microclimate and soil moisture in a drought-prone mixed coniferous forest at an inner Alpine site. European Journal of Forest Research, 133(3).

https://doi.org/10.1007/s10342-013-0777-z

Peñuelas J, Ogaya R, Boada M, Jump AS. 2007. Migration, invasion and decline: Changes in recruitment and forest structure in a warming-linked shift of European beech forest in Catalonia (NE Spain). Ecography, 30(6): 829–837. https://doi.org/10.1111/j.2007.0906-7590.05247.x

Schuster R and Oberhuber W. 2013. Age-dependent climate-growth relationships and regeneration of Picea abies in a drought-prone mixed-coniferous forest in the Alps. Canadian Journal of Forest Research, 43(7): 609–618. https://doi.org/10.1139/cjfr-2012-0426

Schwalm CR, Williams CA, Schaefer K, Arneth A, Bonal D, Buchmann N, Chen J, Law BL, Lindroth A, Luyssaert S, Reichstein, Richardson AD. 2010. Assimilation exceeds respiration sensitivity to drought: A FLUXNET synthesis. Global Change Biology, 16(2): 657–670. https://doi.org/10.1111/j.1365-2486.2009.01991.x

Somogyi Z, Cienciala E, Mäkipää R, Muukkonen P, Lehtonen A, Weiss P. 2007. Indirect methods of large-scale forest biomass estimation. European Journal of Forest Research, 126(2): 197–207. https://doi.org/10.1007/s10342-006-0125-7

Ter-Mikaelian MT, Colombo SJ, Chen J. 2014. Effect of age and disturbance on decadal changes in carbon stocks in managed forest landscapes in central Canada. Mitigation and Adaptation Strategies for Global Change. 19(7): 1063–1075. https://doi.org/10.1007/s11027-013-9460-4

Thomas SC and Malczewski G. 2007. Wood carbon content of tree species in eastern China: Interspecific variability and the importance of the volatile fraction. Journal of Environmental Management. 85(3): 659–662. https://doi.org/10.1016/j.jenvman.2006.04.022

Usuga JCL, Toro JAR, Alzate MVR, de Jesús Lema Tapias, Á. 2010. Estimation of biomass and carbon stocks in plants, soil and forest floor in different tropical forests. Forest Ecology and Management, 260(10): 1906–1913.

Wang C, Bond-Lamberty B, Gower ST. 2003. Carbon distribution of a well- and poorly-drained black spruce fire chronosequence. Global Change Biology. 9(7): 1066–1079. https://doi.org/10.1046/j.1365-2486.2003.00645.x

Weber JC, Sotelo Montes C, Abasse T, Sanquetta CR, Silva, DA, Mayer S, Muniz GIB, Garcia, RA. 2018. Variation in growth, wood density and carbon concentration in five tree and shrub species in Niger. New Forests. 49(1): 35–51. https://doi.org/10.1007/s11056-017-9603-7

Zabek LM and Prescott CE. 2006. Biomass equations and carbon content of aboveground leafless biomass of hybrid poplar in coastal British Columbia. Forest Ecology and Management. 223(1–3): 291–302. https://doi.org/10.1016/j.foreco.2005.11.009

Zhang Q, Alfaro RI, Hebda RJ. 1999. Dendroecological studies of tree growth, climate and spruce beetle outbreaks in central British Columbia, Canada. Forest Ecology and Management. 121(3): 215–225. https://doi.org/10.1016/S0378-1127(98)00552-0

Zhang Q, Wang C, Wang X, Quan X. 2009. Carbon concentration variability of 10 Chinese temperate tree species. Forest Ecology and Management. 258(5): 722–727. https://doi.org/10.1016/j.foreco.2009.05.009

Zobel, B.J., and van Buijtenen, J.P. 1989. Wood variation: its causes and controls. Berlin: Springer-Verlag.

Zubizarreta-Gerendiain A, Gort-Oromi J, Mehtätalo L, Peltola H, Venäläinen A, Pulkkinen P. 2012. Effects of cambial age, clone and climatic factors on ring width and ring density in Norway spruce (*Picea abies*) in southeastern Finland. Forest Ecology and Management. 263: 9–16. https://doi.org/10.1016/j.foreco.2011.09.011

Chapter 4: Concluding Synthesis

This thesis aimed to determine how wood properties of RW, EW, LW, cell wall thickness, density, radial diameter, microfibril angle, coarseness, and percent carbon in natural and planted stands of hybrid white spruce (*Picea glauca* (Moench) *x engelmannii* (Parry)) in central interior British Columbia, Canada vary over time and with climate. This thesis also aimed to determine if relationships existed between percent carbon and mean, maximum, and minimum cell wall thickness and density values in the natural and planted stands. Finally, this thesis aimed to determine if significant differences occurred between percent carbon in individual stands and regional-level stand aggregates of the natural and planted stands of spruce.

4.1 KEY POINTS

Results presented in Chapter 2 and Chapter 3 suggest that hybrid white spruce radial growth and percent carbon accumulation in areas surrounding Prince George (PG) and within the John Prince Research Forest (JPRF) are dependent on variation in temperature and precipitation, as suggested by other research (Wood al. 2016; Charney et al. 2016). Further, although planted stand variability was more sensitive to climate variation than natural stand growth, results suggest that natural stand growth within the last 30 years appears to be more sensitive to climate variation than full-length chronologies.

Results suggest that variation in winter, summer, and autumn temperature and precipitation was a strong predictor of radial growth and percent carbon in planted and natural stands of PG and/or JPRF. Increases in winter, summer, and autumn temperatures were strongly related to reduced radial growth in planted stands (RW, LW) and natural stands (LW, MRD). Planted stands of PG and natural stands in JPRF also appear to be fixing less carbon as a result of increases in Fort St. James and PG previous December, current January, average spring, and previous and current July temperatures. However in some cases, beneficial site-specific differences contributed to positive relationships between rising temperatures and percent carbon accumulation.

Relationships between radial growth and percent carbon and precipitation appear to be influenced by differences in climate regimes of Fort St. James (warm-dry) and PG (cold-wet). Stronger relationships with precipitation are expected in areas with lower average precipitation coupled with rising temperatures (Wood and Smith 2015). Higher-than-normal precipitation years in the winter were associated with limited EW production but related to increased LW production in natural stands of JPRF, likely due to timing of cell formation. Alternatively, reduction in summer precipitation in Fort St. James climate were shown to coincide with reduced radial growth (RW, LW) and increased cell wall thickness in planted and natural stands of JPRF during what should be optimal growth periods. Similar relationships were found between autumn precipitation and radial growth with reductions in autumn precipitation related to production of smaller, higher density cells. Percent carbon accumulation in JPRF was also affected by spring precipitation. Reduction in spring precipitation were also shown to coincide with reduced carbon accumulation in a planted stand of JPRF. Reductions in late spring precipitation, that could reduce snow depth and allow for an early bud burst, were also shown to coincide with increased percent carbon accumulation in a natural stand of JPRF.

Further, recent reductions in Fort St. James precipitation appear to have increased the strength of relationships between precipitation and radial growth variability in planted and natural stands of JPRF. Although tree growth in cool-moist areas is normally temperature limited, rising temperatures coupled with adequate moisture in PG appear to be promoting increased RW but reduced LW, likely due to timing differences. Differences in radial growth variation between JPRF and PG may also be due to reduced accuracy with increased distance to climate station and proximity of sampled stands to one another; JPRF stands may present a more accurate regional representation because of their closer proximity to one another than PG stands.

This thesis also determined that planted stand growth had increased sensitivity to climate variation than natural stands which may be attributed to differences in age and size of tree. Greater amounts of juvenile wood in planted stands may have increased their vulnerability to precipitation variation. Lack of rooting depth and substantial buildup of carbohydrate reserves in planted stands may also make them susceptible to rising temperatures and low precipitation periods. However, relationships between climate and natural stand chronologies and percent carbon truncated to the last 30 years of growth in this study suggest that warming of recent decades is having an amplified effect on natural stand tree growth; these relationships were not found between climate and percent carbon in natural stand data from PG. These results may indicate preliminary effects of long-term warming coupled with reductions in precipitation that have been predicted to negatively affect wood growth (Williamson et al. 2009; Adams 2014; Wood et al. 2016).

Chapter 3 of this thesis also explored relationships between individual and regional-level percent carbon and relationships between percent carbon and wood cell properties of cell wall thickness and density. Results demonstrated that individual stand percent carbon values were significantly different from each other, which may be attributed to differences in site-specific characteristics of warmer-south facing slopes and potentially higher soil-moisture regimes. Previous research has shown reduced percent carbon content in unfavorable climate conditions (Guehl 1985; McMahon et al. 2010; Hember et al. 2012) and increased carbon sequestration under favourable conditions (Li et al. 2015). Regional-level natural and planted stands percent carbon was not found to differ. Based on wood cell structural properties alone, planted stands with higher proportions of juvenile wood were expected to have lower percent carbon contents (Bao et al.2001; Elias and Potvin 2003; Thomas and Malczewski 2007; Lachenbruch and Mcculloh 2014; Weber et al. 2018). Although there are general trends presented in Chapter 3 that suggest there is a lower percent carbon in juvenile wood versus mature wood, the high variability in juvenile wood and small sample size limit confidence in this finding. However, relationships found between percent carbon and RW, EW, LW and maximum cell wall thickness and density values in natural stands of JPRF suggest that increases in lignin and cellulose (as represented by a thicker cell wall and denser wood) correspond to greater proportions of percent carbon. This may suggest that RW, EW, LW, cell wall thickness, and density are good indicators of sequestered carbon; mean and minimum values do not appear to be good indicators of percent carbon. These relationships may improve carbon approximations that derive carbon content with standard measurements of DBH and tree height and often under or over-estimate carbon (Somogyi et al. 2007; Kearsley et al. 2013; Ali et al. 2016; Weber et al. 2018).

4.2 CONSIDERATIONS FOR FUTURE RESEARCH

Future research into relationships between climate and radial growth properties (RW, EW, LW), wood cell properties (MCWT, MRD, MD), and carbon could investigate additional climate variables, such as snow depth and minimum and maximum temperature and precipitation to improve models of radial growth and percent carbon based on climate. Investigation into variables in addition to climate, such as crown cover, could also improve estimations of variations in radial growth and percent carbon in natural and planted stands as stands of different ages often have differences in crown cover. Previous research has shown that increased crown cover can intercept large portions of precipitation falling as snow and reduce melting and evaporation of accumulated snow by blocking irradiation (Burenina 2014; Dickerson-Lange et al. 2017). Future work could also focus on developing a standardized percent carbon measurement sampling protocol for comparison with density and cell wall thickness measurements to increase understanding of relationships found in this study. Finally, ensuring adequate volume is collected for annual percent carbon measurements per stand versus 5-year averages could allow for greater resolution and increased sample size in planted stands, which is lacking in this work.

4.3 IMPLICATIONS FOR THE BRITISH COLUMBIA FORESTRY INDUSTRY

Examination of the general relationships between climate and radial growth and wood cell variables allows for preliminary conclusions regarding wood quality in natural and planted stands of JPRF and PG. It was demonstrated that rising temperatures in Fort St. James and PG were negatively correlated with radial growth (RW, LW) and related to production of cells that were thicker and smaller in natural and planted stands. Projected increases in temperature may allow for growth of wood tissues with narrow annual rings and higher density that are ideal for solid wood production. It was also demonstrated that differences occurred in relationships between radial growth and precipitation variation in JPRF and PG. Lower average precipitation, recent reductions in precipitation, and rising temperatures of JPRF coincided with reduced radial growth (RW, LW) and production of cells that were smaller, narrower and thicker. Although production of LW-like cells is ideal for solid wood products, reduction in the size of the annual ring reduces volume of product gained. Stands growing in cool-moist areas, such as areas surrounding PG, were able to increase radial growth (RW (planted), LW (natural)) during the summer with precipitation in this area during summer appears to be adequate to mitigate rising temperatures; however, LW in planted stands was shown to be reduced with rising temperatures suggesting growth is connected with cell formation. It could be expected that trees in PG that experience rising temperature coupled with adequate precipitation will produce wider rings, with potentially lower cell wall thickness, that are more suited for pulp production. Finally, it was demonstrated that the last 30 years of radial growth in natural stand of JPRF and PG have increased sensitivity to climate variation than full-length chronologies. Relationships between climate and planted stands and truncated natural stands in this study suggest that projections of substantial warming and increased water stress in BC will significantly affect radial growth in both natural and planted stands of hybrid white spruce (Lo et al. 2010; Jiang et al. 2016).

4.4 REFERENCES

Ali A, Yan ER, Chen HYH, Chang SX, Zhao YT, Yang XD, Xu MS. 2016. Stand structural diversity rather than species diversity enhances aboveground carbon storage in secondary subtropical forests in Eastern China. Biogeosciences, 13(16): 4627–4635. https://doi.org/10.5194/bg-13-4627-2016

Bao FC, Jiang ZH, Jiang XM, Lu XX, Luo XQ, Zhang SY. 2001. Differences in wood properties between juvenile wood and mature wood in 10 species grown in China, 35.

Burenina TA, Shishikin AS, Onuchin AA. 2014. Snow cover on logged sites in fir-Siberian pine forests of the Yenisey Ridge. Contemporary Problems of Ecology, 7(7): 778–787. https://doi.org/10.1134/S1995425514070038

Charney ND, Babst F, Poulter B, Record S, Trouet VM, Frank D, Enquist BJ, Evans MEK. 2016. Observed forest sensitivity to climate implies large changes in 21st century North American forest growth. Ecology Letters, 19(9): 1119–1128. https://doi.org/10.1111/ele.12650

Dickerson-Lange SE, Gersonde RF, Hubbart JA, Link TE, Nolin AW, Perry GH, Roth TR, Wayand NE, Lundquist JD. 2017. Snow disappearance timing is dominated by forest effects on snow accumulation in warm winter climates of the Pacific Northwest, United States. Hydrological Processes. 31(10): 1846–1862. https://doi.org/10.1002/hyp.11144

Elias M and Potvin C. 2003. Assessing inter- and intra-specific variation in trunk carbon concentration for 32 neotropical tree species. Canadian Journal of Forest Research. 33(6): 1039–1045. https://doi.org/10.1139/x03-018

Hember RA, Kurz WA, Metsaranta JM, Black T, Guy RD, Coops NC. 2012. Accelerating regrowth of temperate-maritime forests due to environmental change. Global Change Biology. 18(6): 2026–2040. https://doi.org/10.1111/j.1365-2486.2012.02669.x

Kearsley E, De Haulleville T, Hufkens,K. Kidimbu A, Toirambe B, Baert, G, Huygens D, Kebede Y, Defourny P, Bogaert J, Beckman H, Steppe K, Boeckx P, Verbeeck H. 2013. Conventional tree height-diameter relationships significantly overestimate aboveground carbon stocks in the Central Congo Basin. Nature Communications. 4. https://doi.org/10.1038/ncomms3269

Lachenbruch B and Mcculloh KA. 2014. Tansley review Traits , properties, and performance : how mechanical functions in a cell, tissue, or whole. New Phytologist. 204(4): 747–764.

Li T, Ren B, Wang D, Liu G. 2015. Spatial variation in the storages and age-related dynamics of forest carbon sequestration in different climate zones-evidence from black locust plantations on the loess plateau of China. PLoS ONE, 10(3). https://doi.org/10.1371/journal.pone.0121862

Lo YH, Blanco JA, Seely B, Welham C, Kimmins JP. 2010. Relationships between climate and tree radial growth in interior British Columbia, Canada. Forest Ecology and Management. 259(5): 932–942. https://doi.org/10.1016/j.foreco.2009.11.033

McMahon MS, Parker GG, Miller DR. 2010. Evidence for a recent increase in forest growth is questionable. Proceedings of the National Academy of Sciences. 107(8): 3611–3615. https://doi.org/10.1073/pnas.1002725107

Somogyi Z, Cienciala E, Mäkipää R, Muukkonen P, Lehtonen A, Weiss P. 2007. Indirect methods of large-scale forest biomass estimation. European Journal of Forest Research, 126(2): 197–207. https://doi.org/10.1007/s10342-006-0125-7

Thomas SC and Malczewski G. 2007. Wood carbon content of tree species in eastern China: Interspecific variability and the importance of the volatile fraction. Journal of Environmental Management. 85(3): 659–662. https://doi.org/10.1016/j.jenvman.2006.04.022

Weber JC, Sotelo Montes C, Abasse T, Sanquetta CR, Silva, DA, Mayer S, Muniz GIB, Garcia, RA. 2018. Variation in growth, wood density and carbon concentration in five tree and shrub species in Niger. New Forests. 49(1): 35–51. https://doi.org/10.1007/s11056-017-9603-7

Wood LJ and Smith DJ. 2012. Climate and glacier mass balance trends from AD 1780 to present in the Columbia Mountains, British Columbia, Canada. The Holocene. 23(5): 739–748. https://doi.org/10.1177/0959683612465450

Wood LJ, Smith DJ, Hartley ID. 2016. Predicting softwood quality attributes from climate data in interior British Columbia, Canada. Forest Ecology and Management. 361: 81–89. https://doi.org/10.1016/j.foreco.2015.11.004

Appendix I: SilviScan

1. INTRODUCTION

SilviScan analysis consists of three primary components based on three principles: image analysis (optical microscopy), X-ray attenuation (densitometry) and X-ray diffraction (diffractometry). Image analysis is performed on polished transverse surface of the pith-to-bark strips to provide fibre cross- sectional dimensions, as well as annual ring orientation. Densitometry and diffractometry are performed on the longitudinal surface of the strips to provide microdensity and microfibril angle (MFA). Annual ring orientation information from image analysis is used to correct for annual ring orientation by aligning ring direction with X-ray beam.

A total of 89 hybrid white spruce samples were received for SilviScan analysis from University of Northern British Columbia in Vancouver (coordinator: Lisa Wood/Anastasia Ivanusic) on July 20, 2017. Physical quality of the samples was inspected upon arrival. The SilviScan analysis provides image analysis, pith-to-bark profiles of density, and microfibril angle (MFA) at 5-mm resolution.

2. SAMPLE CONDITIONS

Out of 89 samples, 85 were in the form of increment cores of 12 mm in diameter wrapped with writing papers for protection during shipping, and 4 were in the form of a pie shape (Figures 1 and 2). A sample list was later received via Email. Original plan was to send 90 samples, for some reason, one sample was missing in the shipment. The customer decided not to send this missing sample over for analysis. All of the samples were suitable for SilviScan analysis. Special efforts were made to keep pith and bark on SilviScan samples, however, it is not possible for some samples to retain pith and/or bark due to the sample conditions, e.g. off-center, curvy (warp), bark-missing, breakage, etc. Breakage and crushes occurred on a few samples on the bark side, possibly caused by coring process in which excessive force was applied when engaging borer into tree trunk. Some samples lost bark at arrival (Figure 2). More information about SilviScan sample conditions can be found in the enclosed comments sheet “1708-UNBC-LW.Sample List and Comments.xlsx”.

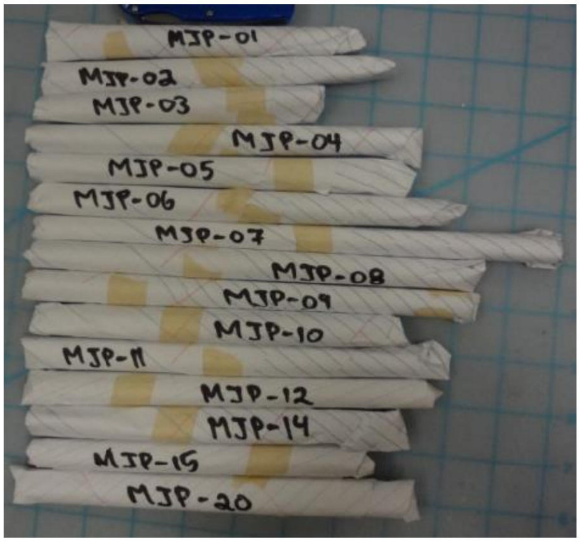

Figure 1 Increment cores wrapped with writing paper.

Figure 2 Increment cores and pie-shaped cookies received for SilviScan analysis.

3. METHODS

3.1 Sample preparation

Pie shaped cookies were first reduced to 12x12 mm (tangentially x longitudinally) pith-to-bark blocks. These blocks and core samples were sorted and conditioned at 40% relative humidity and 20°C temperature (SilviScan standard conditions) until equilibrium was reached (~8% moisture content, dry basis). They were then extracted with acetone to remove resins which may interfere with density measurements. The samples were soaked in acetone for 12 hours, and extracted for 8 hours at 70^{O}C in a modified Soxhlet extraction system. After extraction, the samples were air-dried, and conditioned at 40% relative humidity and 20°C (SilviScan standard conditions) until equilibrium was reached (~8% MC, dry basis). They were then cut into strips of 2 x 7 mm (tangentially x longitudinally) using twin- blade saws. One cross-section of each strip was polished to obtain smooth surface for image analysis with SilviScan's polishing unit equipped with various grits of sandpaper (i.e., 400-grit to 1200-grit). Each strip was scanned for radial and tangential fibre dimensions using optical microscopy, wood density using x-ray densitometry, and microfibril angle (MFA) using x-ray diffractometry. Fibre dimensions and wood density were determined at a 25-µm resolution whereas MFA was determined at a 5-mm resolution.

3.2 Cell scanner (image analysis) procedure

The following procedure is routinely used by SilviScan to determine fibre cross-sectional dimensions. Wood strips are scanned using an optical microscope equipped with a high resolution video camera. The frame size of the microscope is 1.8 X 1.8 mm. An autofocus algorithm maintains sharp, consistent focus on the polished transverse wood surface throughout the scan. High-contrast images of fibre cross-sections are obtained by using transmitted light which travels along the fibre walls. The length of the wood strip is measured as the distance from the pith to bark by locating the bark and pith ends in the microscope frames.

Images are automatically acquired across the entire sample length at a step slightly smaller than the width of the microscope frame size. Each image and its positional information are recorded during the scan and post-scan analysis is performed to extract property profiles from a succession of images onto a standardized distance scale along the sample axis.

Once acquired, each successive image is binarized and processed to identify radial and tangential cell wall boundaries. Figure 3 shows an example of radial and tangential walls extracted from an original image.

Radial walls Original image Tangential walls

Further image analysis is performed to determine the median value of radial and tangential fibre diameters, as well as to estimate fibre perimeters and cell populations within the 25-µm radial intervals. The orientation of each annual ring (isopycnic angle) is estimated and serves as the reference for densitometry and diffractometry analyses.

3.3 X-ray densitometry procedure

Densitometric measurement is based on Beer's Law which states that the intensity of an x-ray beam that passes through a sample falls off exponentially with sample thickness, and that extent of attenuation is related to the density of the sample (Eq. 1):

$I = I_0 e^{-\alpha_m DT}$ (1) where I_0 is the intensity of incident x-ray beam, I is the intensity of transmitted x-ray beam, D is the density of the sample, T is the thickness of the sample, i.e., the distance that x-ray travels, and α_m is the mass absorption coefficient.

In SilviScan, the amount of radiation that is transmitted through the wood strip is detected by a CCD (charge-coupled device) imaging camera that has a pixel size of 7 x 7 μm. Wood strip is mounted on a

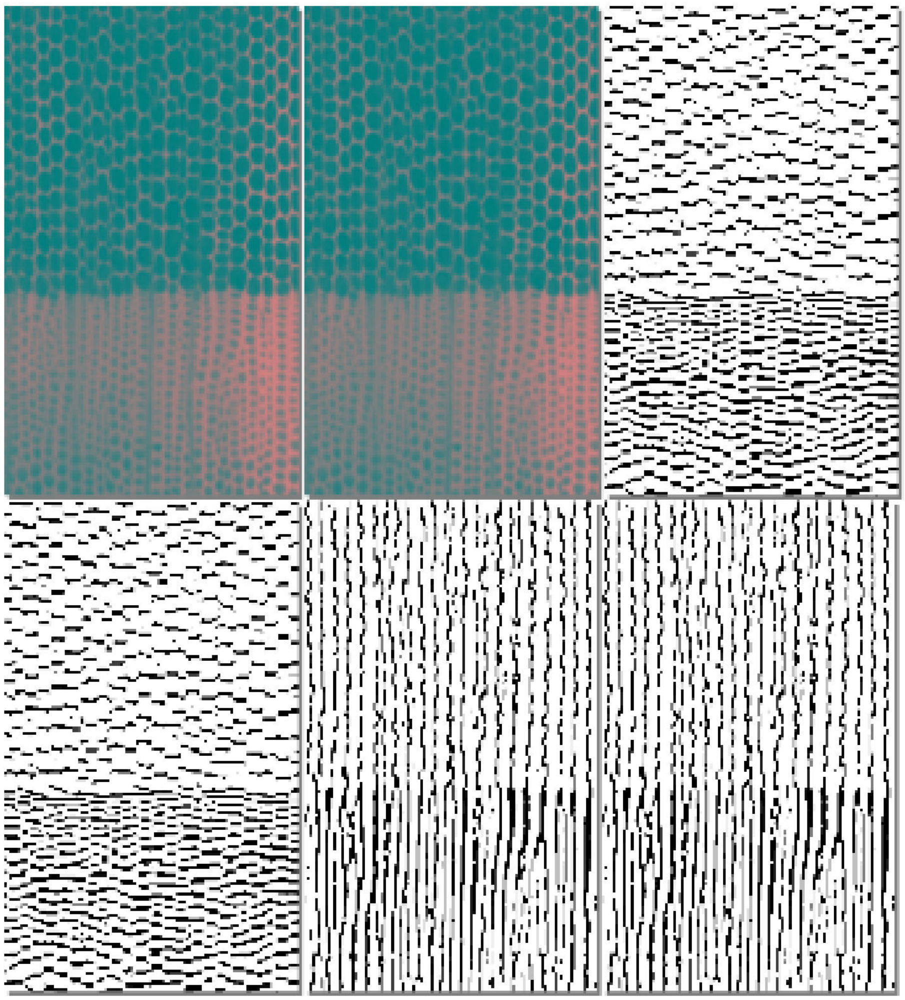

rotatable stage. When the strip is ready for scanning, a laser profilometer detects and measures the length of the strip by locating the bark and pith ends. Density images and positions are acquired automatically across the entire length of the strip. The beam size when exiting the collimator is 13 mm in diameter, and 11 mm in diameter when getting in contact with the strip. The frame size of the detector is 8.64 x 6.39 mm. The rotatable stage of the densitometer rotates the mounted strip according to the isopycnic angle of each growth ring estimated from the image analysis. The purpose is to make the x-ray beam parallel to the growth ring being measured to obtain a sharper definition of ring boundaries. When running at variable angle, the step size is controlled by the isopycnic angle which is less than 0.2 degrees in the window frame.

When the scan is completed, all the images are merged to form a grey scale density image (Figure 4). Post-scan analysis converts the density image into nominal density using the attenuation coefficient estimated from the cellulose acetate sheet during calibration of the densitometer. The nominal density profile is generated on a line 0.5 mm below the top surface (I.e., transverse surface) of the strip. This nominal density is then scaled to true density using the average density of the strip measured from its volume (micrometry) and mass. SilviScan measures density at 25 μm resolution in radial direction, allowing the easy detection of annual growth rings features. It is worth mentioning that the density measured by SilviScan is the density at 8% moisture content (dry basis). If needed, this density can be converted to basic or dry density using the swelling or shrinkage coefficient for the species. In the enclosed xlxs file, basic density (D_b) is calculated using following formula (Eq. 2) (Siau 1995):

$$D_b = \frac{1000 \times D_8}{1080 + 0.22 \times D_8} \quad (2)$$

Where D_8 is density at 8% moisture content (MC).

3.4 X-ray diffractometry procedure

SilviScan exploits the relationship between the variance of the (002) azimuthal diffraction profile of cellulose I and microfibril orientation distribution to estimate MFA (Eq. 3). The (002) diffraction patterns are obtained from the planes whose normal is perpendicular to the microfibril axis (Figure 5). The theory behind the measurement can be found in Evans (1999) and Evans et al. (1999). These papers showed that the variance (S^2) of the (002) azimuthal diffraction profile is related to the MFA (μ) and the variance (σ^2) of the microfibril orientation distribution:

$$S^2 \approx \frac{\mu^2}{2} + \sigma^2 \quad (3)$$

In SilviScan, a focused x-ray beam (0.2 mm) goes through the sample in the tangential direction. The scattered beam is detected and recorded by a CCD x-ray detector. Once acquired, the diffraction image is mapped onto a spherical coordinate system in which azimuthal angles become horizontal and radial lines become vertical. Then intensity profile is extracted for analysis by integrating over the radial limits of the 002 peaks. The total variance of the profile (Eq. 3) includes the average MFA and the dispersion of microfibril orientation. This last quantity has been estimated using MFA data obtained by optical microscopy.

As for density, samples were run in the diffractometer at variable angles to correct for annual growth ring orientation. MFA was acquired in integral mode (compared to point mode where MFA is acquired at a series of discrete points at any nominated segment) where MFA is averaged within segments along the sample. Each segment was 5 mm in this case (required step size).

3.5 Combined analysis

3.5.1 Modulus of elasticity

Density (D) from x-ray densitometry and the coefficient of variation of the intensity of the x-ray diffraction profile (I_{CV}) are combined to compute the fibre modulus of elasticity (MOE) (Evans 2005):

$$MOE = A(I_{cv}D)^{B} \quad (4)$$

The I_{cv} includes the scattering from S2 layer and the background scattering from other cell wall constituents such as the S1 and S3 layers, parenchyma, and amorphous cellulose and lignin present in the fibre wall. The model contains two statistically determined calibration constants (A and B), that have been shown to be insensitive to species, and relate to the sonic resonance method used for calibration (Evans 2005). This means the MOE calculated by SilviScan is the dynamic MOE. Sonic testing historically produces higher values of modulus of elasticity than static bending tests.

3.5.2 Other fibre properties

Fibre wall dimensions from image analysis and density are combined to compute fibre coarseness (C) (Eq.5), specific surface area (SSA) (Eq. 6), and fibre wall thickness (W) (Eq. 7), assuming a constant cell wall density (D_w) (1500 kg/m^3) (Evans et al. 1995):

$$C = R \times T \times D_w \quad (5) \qquad SSA = P / C \quad (6)$$

$$W = \frac{P}{8}\left(1 - \sqrt{1 - \frac{16C}{P^2 D_w}}\right) \quad (7)$$

Where R and T are the radial and tangential diameters of fibre, respectively, P is fibre perimeter, P=2(R+T). The specific surface area SSA reported by SilviScan does not include lumen. However, the specific surface area including the lumen can be calculated with the relation (Eq.8):

$$SSA_{withlumen} = (2P - 8W)/C \quad (8)$$

4.2 Pith-to-bark property profiles

4.2.1 Annual growth ring data

Two files contain ring information for each sample. One ending with "properties_ring_stats.csv" contains ring statistics (mean, standard deviation, quantile and etc.), ring positions and widths for each ring and for all the properties measured. Density in this file is basic density. The other ending with "ring_info.csv" contains ring number, ring width, ring area, and ring age. Figure 6 gives an example of the radial variations of annual growth ring width and density for sample # MJP-02.

Figure 6 Example of SilviScan annual growth ring width and density profiles for sample # MJP-02.

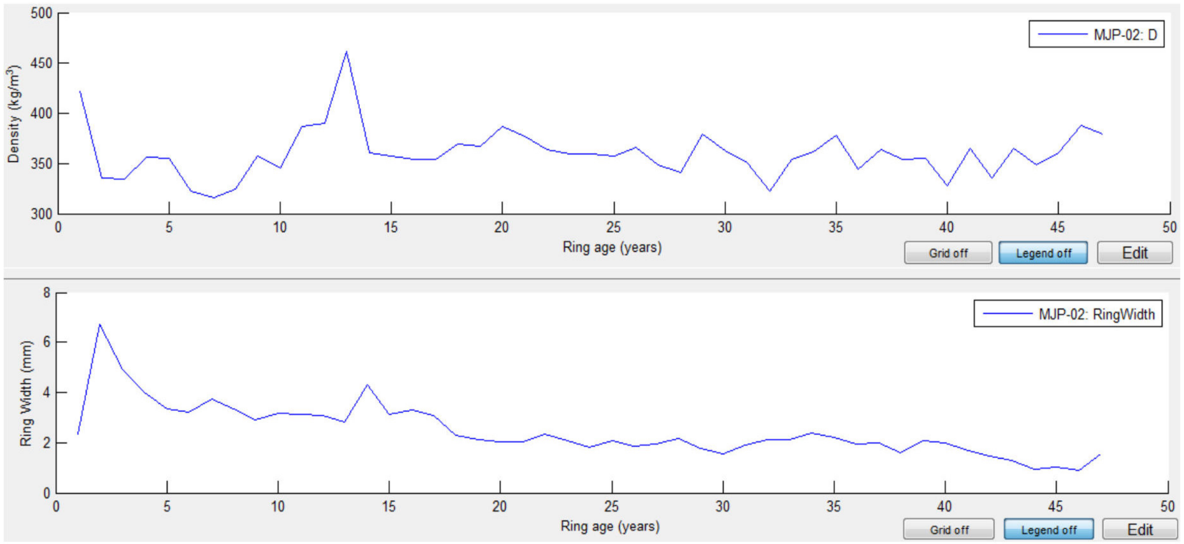

4.2.2 Raw data profiles

The raw data (i.e., data at 25-µm intervals) of wood and fibre properties for each sample are provided in a single csv file with file name ending with "properties.csv". For example, the file "MJP- 02_wood_010101_properties.csv" refers to the data for sample # MJP-02. A total of 89 csv files, one for each sample, are enclosed with this report. Figure 7 illustrates the pith-to-bark profiles for sample # MJP-02 as an example. Wood density in raw data is density at 8% moisture content.

Figure 7 Examples of pith-to-bark profiles for basic density, MOE and MFA, and wood coarseness (C) and specific surface area (SSA) for sample MJP-02. MFA and MOE were acquired at 5-mm resolution. Basic density was acquired at 25-µm resolution and images were acquired at 10-µm resolution. Density shown has been scaled to true density using the average density obtained gravimetrically at 8% moisture content and converted to basic density.

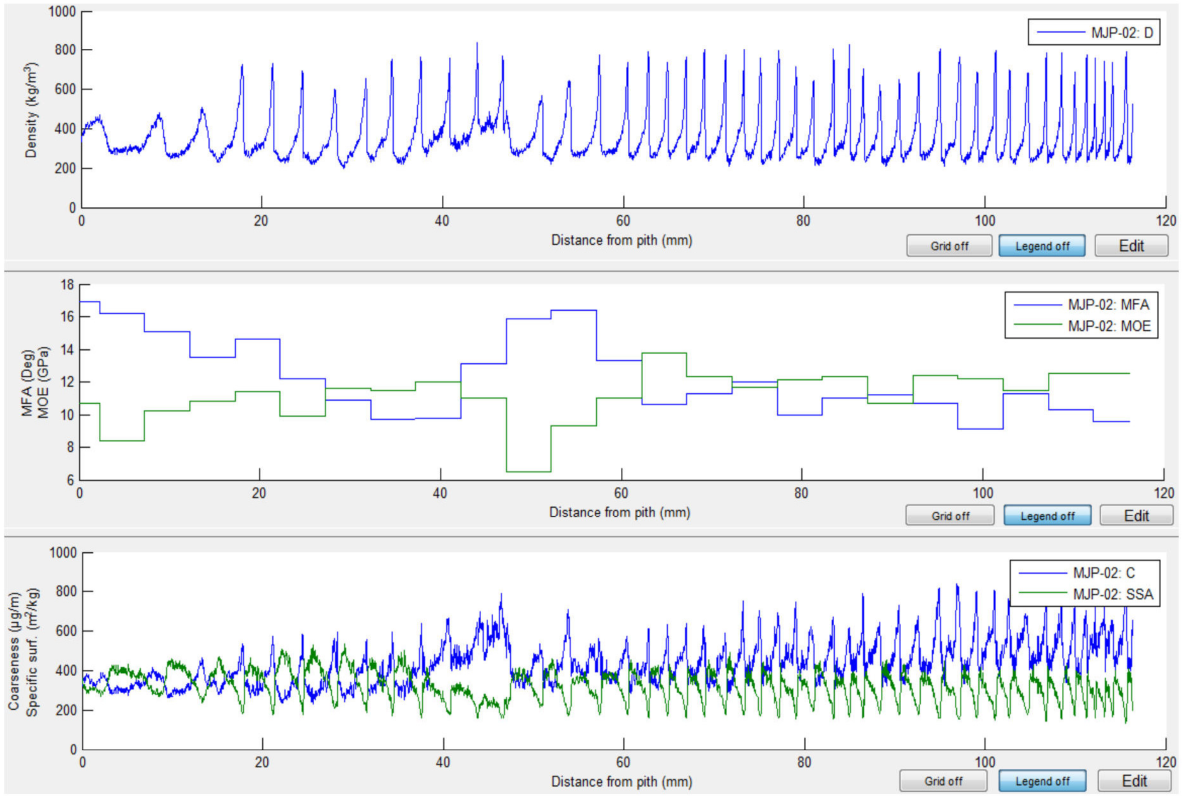

5. REFERENCES

Evans, R., G. Downes, D. Menz, and S. Stringer. 1995. Rapid measurement of variation in tracheid transverse dimensions in a radiata pine tree. Appita 48(2):134-138.

Evans, R. 1999. A variance approach to the x-ray diffractometric estimation of microfibril angle in wood. Appita Journal 52(4):283-294.

Evans, R., Hughes, M., and D. Menz. 1999. Microfibril angle variation by scanning x-ray diffractometry. Appita Journal. 52(5):363-367.

Evans, R. 2005. Wood stiffness by x-ray diffractometry. In: "Characterisation of the cellulosic cell wall", Chapter 11. Proceedings of the workshop 25-27 August 2003, Grand Lake, Colorado, USA. Sothern Research Station, University of Iowa and the Society of Wood Science and technology. D. Stokke and L. Groom, eds. Blackwell Publishing.

Siau, J. F. 1995. Wood: Influence of Moisture on Physical Properties. Department of Wood Science and Forest Products, Virginia Polytechnic Institute and State University. 227p.